universität wien

MASTERARBEIT / MASTER'S THESIS

Titel der Masterarbeit / Title of the Master's Thesis

„Development of an ECLIA based assay for MeCP2 protein"

verfasst von / submitted by

Anna Katharina Schönegger, BSc

angestrebter akademischer Grad / in partial fulfilment of the requirements for the degree of

Master of Science (MSc)

Wien, 2017 / Vienna, 2017

Studienkennzahl lt. Studienblatt / degree programme code as it appears on the student record sheet:	A 066 838
Studienrichtung lt. Studienblatt / degree programme as it appears on the student record sheet:	Masterstudium Ernährungswissenschaften
Betreut von / Supervisor:	Assoc. Prof. Priv.-Doz. Dr. Franco Laccone

Look up at the stars and not down at your feet. Try to make sense of what you see, and wonder about what makes the universe exist. Be curious. However difficult life may seem, there is always something you can do and succeed at. It matters that you don't just give up.

Stephen Hawkings

Acknowledgment

I would like to express my gratitude to my supervisor Dr. Hannes Steinkellner for his expert advice and support in planning this thesis, the laboratory work and his great assistance in the writing process.

Furthermore I wish to express my thankfulness to Prof. Dr. Laccone for giving me the opportunity to do my study in his highly committed research team as well as being on hand with help and counselling.

Last but not least, I would like to thank all my family members and friends, who supported me mentally, and financially during the last years. Thank you for being there when I needed you.

Abstract

Background: Rett syndrome is a severe neurodevelopmental disease, occurring in one out of every 10.000 female births. It is mainly caused by mutations in the *MeCP2* gene, leading to the corresponding protein's loss of function. Potential therapeutical approaches still require research. A possible protein replacement strategy, using the TAT-MeCP2 fusion protein is currently being investigated, thus bringing up the need for a diagnostic tool to assess the effect of this potential agent. Here we report on developing an electrochemiluminescence immunoassay (ECLIA) for quantifying endogenous MeCP2 as well as the TAT-MeCP2 fusion protein in cellular and animal models.

Methods: A carbon coated 96-well high-bind microplate associated with an $Ru(bpy)_3^{2+}$/TPA-ECL-system was used. Sample preparation followed nuclear extraction strategies of different human and animal cell lines as well as mouse tissues in order to determine MeCP2 concentrations. Herein, both mutant and wild-type samples were investigated.

Results: The ECLIA is characterized by a high sensitivity and specificity, showing a lower detection limit (LLOD) of 28.5pg/ml. In terms of accuracy, an intra-assay precision (CV≤1.21%) as well as inter-assay precision (CV≤12.5%) was successfully achieved. Marked differences in MeCP2 concentration were observed between wild-type fibroblasts and male Rett patients' fibroblasts. Comparing MeCP2 levels in wild-type as well as MeCP2-knock out mice brains, the latter did not show any MeCP2 signal. In contrast, MeCP2 concentrations could be measured over a broad range (1-20µg protein/well) in wild-type mice brains. Heterozygous mouse brains gave rise to intermediate MeCP2 values showing a 40% lower MeCP2 concentration than the wild-type mice brains.

Conclusion: The availability of this new tool for quantifying endogenous MeCP2 as well as TAT-MeCP2 fusion protein, serves as a promising diagnostic agent for further research in replacement strategies as well as other investigations in the course of treating Rett syndrome.

Zusammenfassung

Hintergrund: Das Rett Syndrom ist eine schwere, neurologische Entwicklungsstörung, die bei Mädchen mit einer Prävalenz von 1:10.000 auftritt. Als Ursache für diese Erkrankung wurde eine Mutation im MeCP2-Gen lokalisiert, die mit einem Funktionsverlust des dazugehörigen Proteins einhergeht. Die Entwicklung potentieller Therapieoptionen ist jedoch immer noch Gegenstand der Forschung. Derzeit wird die Idee einer Proteinersatztherapie mittels eines TAT-MeCP2-Fusionsproteins näher untersucht. Dies bedarf natürlich auch eines neuen diagnostischen Tools, um den Effekt dieser Behandlungsmethode quantitativ zu beurteilen. Darum setzten wir uns in dieser Arbeit die Entwicklung eines Elektrochemilumineszenz-Immunoassays (ECLIA) für die quantitative Bestimmung von endogenem MeCP2 als auch des TAT-MeCP2 Fusionsproteins im Zell- und Tiermodell, zum Ziel.

Methoden: Es wurde eine Carbon-beschichtete 96-well Mikroplatte eingesetzt, die mit einem Ru(bpy)32+/TPA-Elektrochemilumineszenz-System verknüpft wurde. Für die Quantifizierung von MeCP2 erfolgte die Probenaufbereitung mittels Kernextraktion. Es wurden sowohl Wildtyp-Mausgewebe und -zelllinien als auch jene mutierter Herkunft untersucht.

Ergebnisse: Der MeCP2-ECLIA zeichnete sich durch eine hohe Sensitivität und Spezifität aus. Die untere Bestimmungsgrenze (LLOD) lag dabei bei 28.5pg/ml. Auch hinsichtlich der Genauigkeit erfüllte der ECLIA mit eine Intra-Assay Präzision von CV≤1.21% sowie eine Inter-Assay Präzision von CV≤12.5% entsprechende Anforderungen. Ferner konnten mittels ELCIA in Wildtyp-Fibroblasten deutlich höhere MeCP2-Konzentrationen gemessen werden, als in den von männlichen Rett Syndrom Patienten stammenden Zellen. Bei den Messungen in Maushirnen wurden in den Hirnen von MeCP2-Knockout-Mäusen, im Gegensatz zu jenen von Wildtypen, keine Signale gemessen. Hirne von heterozygoten Mäusen zeigten um 40% verringerte MeCP2-Levels, verglichen mit den Wildtyp-Mäusen.

Schlussfolgerung: Die Verfügbarkeit eines solch neuen Tools für die Quantifizierung von endogenem als auch TAT-MeCP2-Fusionsproteins stellt ein vielversprechendes diagnostisches Agens, für zukünftige Forschung im Bereich der Proteinersatztherapie sowie anderer Therapieoptionen im Zuge des Rett Syndroms, dar.

Index

1. INTRODUCTION

1.1. The Rett syndrome

The Rett syndrome (RTT) is a severe neurodevelopmental disease, which manifests during early childhood and mostly affects females with a prevalence of 1:10 000 in the classic form [Fehr et al., 2011]. Hence, it counts among the most frequent reasons for complex disability in girls. The life expectation of patients developing RTT lies just between 15 and 20 years. Most deaths occur due to disease related disorders such as epilepsy, pneumonia, wasted condition, poor health and lacking autonomic control. Although one quarter succumb to RTT by unexpected sudden death [Julu and Witt Engerström, 2001; Smeets et al., 2011]. Despite remarkable progression in RTT research, there are a number of questions especially in understanding RTT's pathogenesis, implicating therapeutical targets, which have yet to be clarified.

1.1.1. Historical overview

Eponymous for this complex disability was the Austrian pediatric neurologist Andreas Rett. He was the first physician who published the characteristic features of the disease in 1966. In his report in the “Wiener Medizinische Wochenschrift” he described it as a neurodevelopmental disorder, affecting females. He characterised it as an early onset of developmental delay followed by a successive regression, loss of cognition and communication, limitation of motor skills, presence of stereotypic hand movements as well as breathing disturbances when awake. In course of detecting a possible metabolic marker for the disease, Rett observed increased blood levels of ammonia in these patients and associated this hyperammonemia with the cerebral atrophy [Percy, 2016; Rett, 1966, 1977]. However, this hypothesis was discounted by the Swedish neurologist Bengt Hagberg, who contemporaneously researched this unique syndrome. From a historical viewpoint, Hagberg was the second most important neurologist in the syndromes’ clarification, as he officially manifested the disease as “Rett syndrome” in the international medical world in 1983. Hagberg made remarkable contributions to the staging system and the initial criteria development for RTT as well as to the recognition of variant forms of the disease [Hagberg et al., 1983, 1986, 1994]. The third milestone in Rett syndrome history was the identification of the genetic background in 1999.

Here, Ruthie Amir (Zoghbi laboratory) found a mutation in the methyl-CpG-binding protein 2 *(MeCP2)* gene, located on the X chromosome [Amir et al., 1999]. From then on, RTT research took on greater significance in several laboratories around the world, focusing on the role of MeCP2 in brain development and possible therapeutic strategies for Rett syndrome patients' inter alia. [Percy, 2016].

1.1.2. The MeCP2 gene and protein

1.1.1.1. The gene

What we know today is that 80% of Rett syndrome patients show a dominantly acting mutation in the coding region of the X-linked *MeCP2* gene, revealing this as the main cause of RTT. Nowadays more than 600 of these genetic abnormalities are known, whereas most of them are recurrent point mutations, including the wide spread missense mutations R106W, R133C, T158M, R306C as well as the nonsense protein-truncating mutations R168X, R255X, R270X, R294X. The residual mutations arise due to C-terminal deletions and complex chromosomal rearrangements [Amir et al., 1999; Chahrour and Zoghbi, 2007; Gadalla et al., 2011, Smeets et al., 2011].

As a result of the genes' localisation (Xq28), it underlies X chromosome inactivation (XCI) in females [Adler et al., 1995]. This fact is of essential medical significance, implying that the severity of RTTs' clinical manifestations is subject to gender. Given homozygosity, males who inherited a single mutated *MeCP2* allele, are much more severely affected and commonly do not get older than two years. Females with a mutated *MeCP2* allele develop a mosaicism, consisting of mutated and normal MeCP2 alleles. This is a result of the gene dosage compensation occurring during embryogenesis, yielding cells either silencing the maternal or the paternal *MeCP2* gene. In contrast to the male type, not every cell expresses the mutant allele, meaning that a kind of a diluting effect weakens the pathology in females [Amir et al., 1999; Guy et al., 2011; Schule et al., 2008].

The consequence of these gender dependent clinical varieties is that males just come down with the phenotype of the "classical RTT" if the mutation appears as a somatic mosaic or in cases of an X-polysomy. The residual ones are rather categorized as MeCP2-related disorders (e.g. MeCP2 duplication syndrome), including severe congenital encephalopathy, complete

intellectual disability and multiple neurological symptoms [Leonard et al., 2001; Smeets et al., 2011].

Usually RTT is not a result of family history, as affected males and females are not able to reproduce. This assumes however, that the patients are symptomatic carriers, which is almost always the case. 95% of the RTT mutations arise de novo on the paternal X chromosome without a family history, consequently implicating a recurrence risk of less than 0.1%. Nevertheless, in exceptional circumstances women can also appear as asymptomatic carriers. This is due to a highly skewed XCI, in favour of the normal copy of MeCP2. These females phenotypically turn out as normal carrier mothers but can inherit an X chromosome with a mutant MeCP2 gene to her offspring. In such cases, the recurrence risk is obviously much higher, namely 50%, bearing the chance for an intra-uterine death or severe neonatal encephalopathy in boys [Chahrour and Zoghbi, 2007; Girard et al., 2011, Guy et al., 2011, Smeets et al., 2011].

At this point the consideration of an association between the clinical severity of RTT and the pattern of X chromosome inactivation in females arises. Actually, different patterns of XCI have been found in female RTT twins with different phenotypical characteristics [Ishii et al., 2001]. However, it is not the only hypothesis, as other possible factors influencing the genotype-phenotype correlation have also been identified. Researchers observed that even the location of the mutation has an impact on the clinical outcome, e.g. nonsense mutation affect the patients more severely than a C-terminal deletion. Although modifier genes that possibly influence MeCP2 are also up for discussion [Huppke et al.; 2000, Renieri et al., 2003, Smeets et al., 2005, 2011].

1.1.1.2. The protein

As the MeCP2 gene encodes for the nuclear protein MeCP2, the proteins function and localisation has to be clarified, to gain a better understanding of MeCP2s' role in the pathogenesis of RTT.

MeCP2 is ubiquitously expressed throughout human tissues with a notably high concentration in the brain or rather in neurons, indicating its essential function in those cells [Amir et al., 1999]. Interestingly, the MeCP2 concentrations stay quite low while embryogenesis and do not rise until the postnatal period of neuronal maturation [Shahbazian et al., 2002]. The authors Chahrour and Zoghbi state that "*the pattern of increasing expression in the cortex*

follows an inner-to-outer sequence akin to that of cortical development" [Chahrour and Zoghbi, 2007].

Generally, the MeCP2 gene consists of 4 exons. In consequence of alternative splicing of exon 2, two isoforms (e1 and e2) of MeCP2 exist, which are characterised by differences in their N-termini respectively in their translational start sites (Figure 1). Although MeCP2 e1 is the dominant one, the isoforms are functionally equal [Guy et al., 2011; Zahorakova, 2013].

As already defined in its name, the methyl-CpG-binding protein 2 belongs to the MBD (methylated DNA-binding domain) protein family. MeCP2 is characterised by two functional domains, pointing towards its role as a transcriptional repressor in methylated regions of the DNA. Thus, it presents a methyl-CpG-binding domain for one, with a strong affinity to 5-methyl-cytosine throughout the genome. On the other hand, it contains a transcriptional repressor domain which shows interactions with histone deacetylase and the Sin3A corepressor [Smeets et al., 2011]. Further, MeCP2 comprises two nuclear localization signals for its direction into the nucleus and a C terminal segment that binds to the nucleosome core as well as naked DNA and increases the proteins' stability [Chahrour and Zoghbi, 2007].

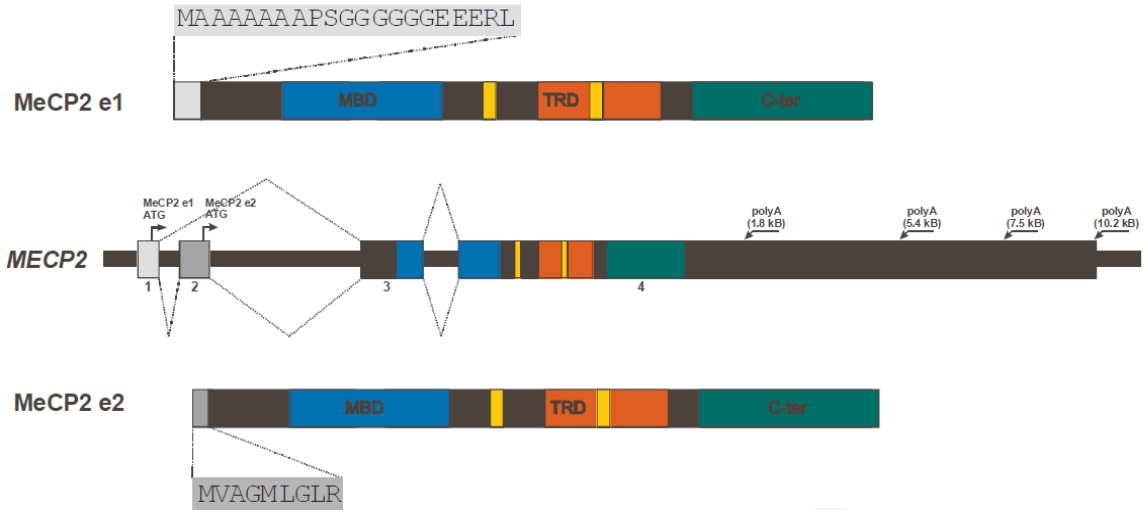

Figure 1: MeCP2 gene structure and the isoforms MeCP2 e1 and MeCP2 e2. Showing differences in their N-termini and translation start sites. MBD: methyl-CpG-binding domain, TRD: transcriptional repression domain, C-ter: C-terminal domain, yellow boxes: nuclear localization signals [Zahorakova, 2013].

MeCP2 acts as transcriptional repressor by causing a chromatin condensation through a deacetylation of histones. Thus, the promotor is hindered to bind on the transcription machinery and expression of downstream genes is stopped. In detail, MeCP2 specifically binds

with its MBD to methylated-CpG-dinucleotiods of eventual target genes. The TRD of the protein then recruits the corepressor protein Sin3A as well as the histone deacetylases (HDACs) 1 and 2, forming the Sin3A-HDAC transcription silencing complex. Besides Sin3A, it is assumed that other chromatin remodelling proteins (e.g. the corepressors c-Ski and N-CoR, histone methyltransferase Suv39H1, the transcription factor TFIIB) are involved in this repressing procedure too, but their exact functional consequence has yet to be clarified. However, the MeCPs' transcription repression can also occur HDAC independently. Therefore, the C-terminal segment directly interacts with the chromatin, causing its compaction.

These silencing modes usually take place in resting neurons. Whereas a neuronal activation implicates the phosphorylation of MeCP2, resulting in a disassociation from the promotor region and consequently a decomposition of the repressor complex. Thus, the target genes can be expressed unhampered (Figure 2). Additionally, recent research also indicates a function of MeCP2 in regulating RNA splicing via interaction with the RNA-binding protein Y box-binding protein 1 (YB1) and the formation of complexes with the RNA itself.

Altogether, facing its multiplex interactions with various proteins, RNA, DNA and chromatin, MeCP2 seems to be a multifunctional protein primary involved in chromatin remodelling and RNA splicing [Chahrour and Zoghbi, 2007; Nan et al., 1998, 2007; Young et al., 2005].

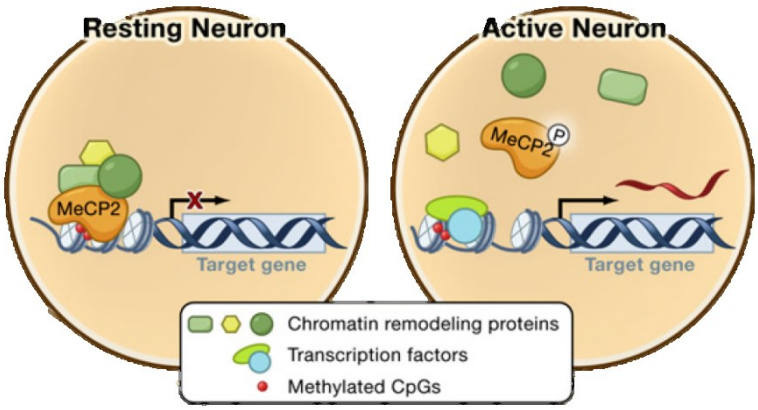

Figure 2: Model of MeCP2 action in resting and active neurons. Resting neuron shows the transcription repressor activity of MeCP2 (left). Active neuron pictures MeCPs' release from the promotor region, allowing unhampered gene expression (right) [Chahrour and Zoghbi, 2007].

1.1.3. Pathogenesis of RTT

Basically, MeCP2 is considered to act as transcription regulator of genes in specific brain regions during particular developmental stages rather than as a global repressor. In so far, a lack of MeCP2 function particularly causes damaging effects during central nervous system maturation. As a result a dysregulation in neurotransmitter systems (e.g. cholinergic, dopaminergic, glutaminergic, serotoninergic, GABAergic transmission) and trophic factors (e.g. brain-derived neurotrophic factor, nerve growth factor) emerges [Smeets et al., 2011; Tudor et al., 2002; Zahorakova, 2013].

In terms of understanding the pathogenesis of RTT, the essential issue which comes up, is the question of the MeCP2s' target genes. Several candidates have already been identified, even though their relevance for pathogenesis is considered controversial. Table 1 sums up research progress in finding supposed target genes of MeCP2 and their function. Among these, the brain-derived neurotrophic factor (BDNF) is said to be the clearest and best investigated one [Chahrour and Zoghbi, 2007]. The trophic factor is of essential importance in terms of neuronal plasticity, synapse formation, learning as well as memory. As BDNFs' physiological gene regulation relies on a normal MeCP2 function, it seems comprehensible that a lack of MeCP2 implicates several neuronal dysfunctions [Martinowich et al., 2003].

TARGET GENE	FUNCTION	REFERENCES
Bdnf	neuronal development and survival	Chen et al., Martinowich et al.
Xhairy2a	neuronal repressor	Stancheva et al.
DLX5/dlx5	neuronal transcription factor	Horike et al.
Sgk1	hormone signaling	Nuber et al.
Fkbp5	hormone signaling	Nuber et al.
Uqcrc1	mitochondrial respiratory chain	Kriaucionis et al.
ID1-3/Id1-3	neuronal transcription factors	Peddada et al.
FXYD1/Fxyd1	ion channel regulator	Deng et al.
IGFBP3/Igfbp3	hormone signaling	Itoh et al.
Crh	neuropeptide	McGill et al.
UBE3A	ubiquitin ligase	Samaco et al.
GABRB3	GABA-A receptor	Samaco et al.

Table 1: List of possible target genes of MeCP2 and their function [Chahrour and Zoghbi, 2007].

However, the precise pathophysiological mechanisms underlying RTT are mostly still unknown. According to current knowledge, a mutation in the MeCP2 gene causes a partial or complete loss of the proteins' transcription silencing function [Gabellini et al., 2004]. De facto

an inadequate overexpression of MeCP2 target genes arises, which implicates various neuronal abnormalities [Ellaway and Christodoulou, 2001]. However, overexpression of MeCP2 target genes is by far not the only mechanism in RTT pathogenesis. Interestingly, studies of MeCP2 knock-out mice did show e.g. that their BDNF levels are decreased up to 70%, compared to wild-type mice. Low BNDF levels are further reported with an earlier onset of RTT symptoms and a shortened life expectancy. Prima facie, this finding would argue against the hypothesis of overexpression. In fact this conclusion would have been made without considering the neuronal activity in RTT. As described above, an upregulation of the target genes expression is MeCP2-independent in activated neurons. This indicates that the BDNF concentration in the brain would be equal in wild-type and MeCP2 mutant mice, if all neurons are activated. Neuronal, especially cortical activity, is however innately diminished in MeCP2 mutants' brain, probably explaining the low BDNF levels found in the knock-out mice [Chang et al., 2006]. An imbalance between cortical excitation and inhibition is responsible for this reduced cortical activity in RTT, although the particular involvement of MeCP2 in this context again remains obscure [Dani et al., 2005]. Herein, BNDF should just serve as an example for the enormous complexity of RTT pathogenesis.

Although the pathogenetic mechanisms of the Rett syndrome including the neurophysiological consequences of MeCP2 malfunction have yet to be resolved , the leading pathogenetic hypothesis describes the RTT as *"a postnatal dysfunction of the integration, maturation and maintenance of neurons determining a dysfunction of the synapses"* [Laccone, 2006].

1.1.4. Clinical features of classical RTT

The main characteristic of classical RTT is a neurodevelopmental regression, usually occurring between 1 and 4 years of age, that severely affects motor, cognitive and communication skills. In the course of this, microcephaly, growth retardation, weight loss, autonomic perturbations such as breathing abnormalities, ataxia, apraxia, abnormal muscle tone, stereotyped hand movements, autistic and seizure disorders as well as absence of speech make an appearance. Predominately, the disease affects the central nervous system, causing the six cardinal features of RTT (Table 2). However, this is not the only system to be involved. In fact, RTT is a multisystem problem including growth, nutrition, the gastrointestinal tract and pubertal development [Chahrour and Zoghbi, 2007; Julu et al., 2008; Percy, 2016; Smeets et al., 2011].

BRAIN AREA	ABNORMALITIES	CLINICAL OBSERVATIONS
Cortex	Decreased dendritic arborisation and smaller than normal brain size	Severe intellectual disability
Cortex	Epilepsy	Seizures
Brainstem	Monoaminergic dysfunction	Dystonia, no coordination of motor activities, orthopaedic deformities and muscle wasting with contractures
Brainstem	Monoaminergic dysfunction	Dyspraxia, agitation and sleep disturbances
Brainstem	Immaturity with incompetence of inhibitory neuronal networks	Abnormal breathing rhythms and lack of integrative inhibitors are likely causes of sudden deaths
	Dysautonomia	Cold and blue extremities and neonatal level of cardiac vagal tone against normal sympathetic tone, leading to a unique sympathovagal imbalance

Table 2: Six cardinal features of brain immaturity in RTT [Julu et al., 2008].

1.1.4.1. The staging system of classical RTT

Not all of the typical RTT features are initially distinct, but rather appear in the form of a cascade, showing a pattern of progression of diseases. Therefore, Hagberg and others developed a staging system (Figure 3), enabling a differentiation between the non-specific symptoms of the disease in early life and the more specific characteristics later on [Chahrour and Zoghbi, 2007; Hagberg, 2002; Smeets et al., 2011].

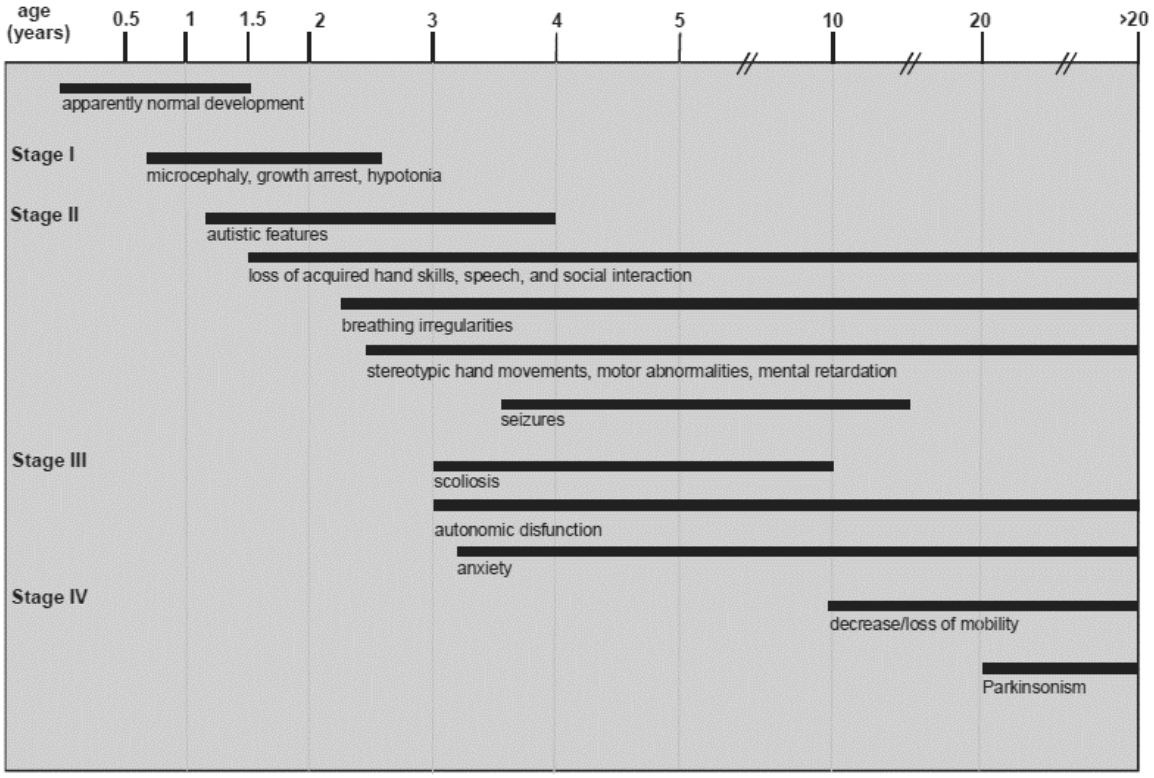

Figure 3: Onset and progression of RTT [Zahorakova, 2013 modified to Chahrour and Zoghbi, 2007].

Stage 1: Early-onset stagnation (onset: 6-18 months of age)

The onset of the clinical symptoms of RTT is characterized by a delay in developmental progress. Commonly, the baby learns to sit up right, but neither to crawl nor to stand up. Bottom-shuffling is an often seen type of movement. Language skills come up too, but babbling and new words remain deficient. Nevertheless, in this stage the developmental pattern is still not significantly abnormal and it is often just the mother, who notices a change in her baby's interactive behaviour (e.g. restlessness, little demand of attention). This phase usually lasts for weeks or months [Hagberg, 2002; Smeets et al., 2011].

Stage 2: Developmental regression (onset: 1-4 years of age)

Herein, a rapid and specific regression of acquired skills and communication occurs. Fine motor skills (e.g. hand use), babbling, words and active playing are lost. Hand movements according to age, such as grasping and reaching out for objects and toys cease. Coincidently, mental deficiencies appear and brainstem immaturity manifests, showing diminished interpersonal contact and apathy to the surrounding environment. The child seems to be "in another world", although eye contact is usually preserved. Automatisms such as senseless hair-pulling, head-tapping, mouthing, unremarked painting and facial grimacing are displayed. Further, seizures, breathing problems (e.g. hyperventilation, aerophagia), spitting, crying at night, infections and fever are consistently present. This specified decline can either emerge gradually or suddenly. The latter case is often accompanied by pseudo-toxic symptoms, such as high-pitched crying, fever and apathy. After this acute episode with a need of hospitalization, the child shows an awfully altered personality. Generally, the 2nd stage of RTT again lasts for weeks or months [Hagberg, 2002; Smeets et al., 2011].

Stage 3: Pseudostationary period (onset: after passing stage 2)

This stage is also known as "wake up period" and represents kind of a stabilization phase. The RTT children seems more alert, joyful and sociable. Herein, some communicative restitution occurs and recovered learning abilities concerning new things, situations and persons are reported. However, neuromotor regression takes its course. Ataxic as well as apraxic hand movements and breathing anomalies become more prominent. Stereotypic twisting of fingers, wringing, hand washing, rubbing, patting and clapping are manifested (Figure 4). These specific and repetitive hand movements are probably the most characterizing

feature of the disease. It has often been reported, that these movements alter with the child's emotion and are even associated with breathing patterns.

Figure 4: Stereotypic hand movements in RTT [1].

Additionally, patients suffer from strongly marked hyperventilation, apneustic and feeble breathing as well as Valsalva-maneuver type of breathing. This clinical stage is also characterized by neurogenic scoliosis based on dystonic asymmetrical posture, deformation of ankles to shortening of the Achilles tendons as well as cold feet and lower limbs due to a hypoperfusion, resulting of reduced autonomic control. Night laughing, awakeness at night, sleeping at daytime and clinical epilepsy are common too. Anyhow, the patients are able to express their needs through a remarkable eye-pointing form of communication and preserved ambulant ability is apparent. In contrast to stage 1 and 2, the pseudostationary period can last for years to decades [Hagberg, 2002; Smeets et al., 2011].

Stage 4: Late motor deterioration (onset: when stage 3 ambulation ceases)

The later motor deterioration phase is divided into two substages, 4a and 4b. Generally, wheelchair-dependency is indicated in both substages. Patients, who were previous walkers pass over from stage 3 to 4a, where they cease walking and become non-ambulant. Others, who were never ambulant, displaying severe RTT cases, directly pass over to stage 4b. Herein, severe disability arises, including advanced neurological impairment, wasting, distal distortion and quadriplegia. The patients often stay in this phase for decades. Albeit visual contact and communication survives until the end [Hagberg, 2002; Smeets et al., 2011].

1.1.4.2. Outline of some selected features

Seizure

Over 90% of RTT patients do get epileptic fits during their lifetime [Steffenburg et al., 2001]. Interestingly, early seizures show a significantly more frequent occurrence in individuals with missense mutation in the MBD of MeCP2. Whereas, BDNF seems to function as a protective agent. Although the general prevalence of epileptic discharges does not differ from other severely mentally affecting disorders, the mean onset age is significantly later in RTT compared to others (4 years vs. 8 months) [Nectoux et al., 2008]. Only half of the cases can be

controlled by medication. Unresponsive ones are most notably those with an obvious deceleration of head growth. However, the severity of epilepsy decreases with advancing age and many girls turn seizure-free after the age of 20 [Smeets et al., 2011; Steffenburg et al., 2001]. The differential diagnosis between true cortical epileptic fits and symptoms based on brainstem immaturity, such as blinking of the eyes, facial twitching, episodic laughing, staring, vacant spells and hypocapneic attacks involving tetany, is of significant importance. In the latter cases, anti-epilectic medication is neither indicated nor helpful. On this account, neurophysiological monitoring (e.g. EEG) of cortical and brainstem functions is essential to verify their existence [Cooper et al., 1998; Hagberg, 2002; Julu et al., 2001].

Autonomic Manifestations

In course of autonomic manifestations, the brainstem irregularities mentioned before are even causative for multiple cardiorespiratory perturbations. Herein, the term "brainstem storm" is used to describe the pathological spontaneous brainstem activation associated with abnormal breathing behaviour. In fact, sympathovagal imbalance and incompetence of inhibitory neuronal networks, as a consequence of brainstem abnormalities lead to a defective control mechanism of carbon dioxide exhalation. As a result, respiratory alkalosis and acidosis emerges. Here, Julu et al. differentiates three cardiorespiratory phenotypes:

1. *Forceful breather*: chronic respiratory alkalosis (↓ pCO_2)
2. *Feeble breather*: chronic respiratory acidosis (↑ pCO_2, due to weak respiration)
3. *Apneustic breather*: CO_2 accumulation (due to delayed and inadequate expirations)

This sympathovagal imbalance, which is characterized by an insufficient parasympathic control and sympathic overactivity, further causes prolonged QT times and a reduced heart rate variability. Especially the combination of breathing perturbations and prolonged QT times, is a significant risk factor for the development of cardiac arrhythmia [Julu et al., 2001, 2008].

Gastrointestinal features

Basically, the RTT affected are excited for preparing food and eating. The act of feeding is characterized by a particular phase of vigilance. However, even gastrointestinal functions do not escape the disease. Herein, symptomatology is seen through the whole gastrointestinal tract, mostly attributed to abnormalities in the autonomic nervous system. Reduced gastrointestinal motility and deranged mobility of the upper gastrointestinal tract implicate

problematic and delayed issues. As a result, almost all RTT girls suffer from gastroesophageal reflux and obstipation. Control of primary mouth functions (e.g. swallowing, chewing) is often very difficult. Further, delayed gastric emptying as well as gallbladder dysfunction are present. Another characteristic feature is an extreme bloating of the abdomen, caused by air swallowing – a unique feature in RTT. These manifestations actually diminish general comfort and are in need of a particular attention regarding the girls' annoyance, unhappiness and awakeness at night as the patient is not able to express her pain in words. In more than a third of RTT individuals gastrostomy tubes have to be used additionally or exclusively for feeding [Hagberg, 2002; Smeets et al., 2011; Percy, 2016].

Deformities

Insufficient mobility and trunk hypotonia are the main causes for back deformities such as neurogenic scoliosis and kyphosis. Progression is subject to ambulation, muscle wasting and asymmetry in muscle tone. However its rapidness and severity is often unforeseeable. Sever double curve deformations (Figure 5), exceeding 25° are frequently seen in non-ambulatory girls. Surgical correction with spinal fusion is indicated from 40° upwards. On the contrary, ambulatory ones rather show manifestations of the more benign kyphosis. This often arises due to tiptoe walking, a phenomena commonly observed in RTT patients. By bending forward on stiff legs, the gait facilitates them to stabilise and balance.

Figure 5: Far advanced kyphoscoliosis of a 15-year-old RTT patient. Showing a thoracic 120° curve [Soultanis, 2007].

Besides scoliosis and kyphosis, foot respectively joint deformities are even prominent. Equinus and equinovalgus/varus positions are generated through the reasons mentioned before as well as through an extrapyramidal syndrome, leading to a shortening of Achilles tendons. Inherently, young children are not severely affected by these deformities and have available walking skills. However, their gait is determined by ataxia and apraxia, leading to specific locomotor patterns. Most RTT affected do have one prominent leg, with which they start and direct every step. The other one just serves as a balance assistance. As the latter is often twisted to the side, the children tend to walk in circles [Hagberg, 2002; Smeets et al., 2011].

1.1.4.3. Atypical RTT

Besides the depicted classical RTT, phenotypic deviations exist. These atypical forms vary in the onset age, sequences of clinical profile as well as in the severity and presence of expected features. The majority of atypical RTT cases, namely 80%, represent the “forme frust variant”. It is a significantly milder manifestation of RTT and characterized by a later onset of the disease and a prolonged clinical course. Communication and motor skills are frequently preserved, just minimal stereotypic hand movements are obvious as well as mild neurodevelopmental regression [Hagberg, 2002; Chahrour and Zoghbi, 2007].

To add to the complexity, a small number of cases show specifically defined variant forms of RTT, such as the “preserved speech variant”, the “congenital variant” and the “early seizure variant” [Hanefeld, 1985; Rolando, 1985; Zappella, 1992]. These forms show distinct clinical features, however several of the typical criteria for classical RTT are missing (e.g. clear period of regression, intense eye-gaze). Further, except for the preserved speech variant, mutation in MeCP2 has rarely been found in these individuals. To a greater degree, the clinical features are associated with mutations in the FOXG1 (congenital variant) and the CDKL5 (early seizure variant) genes [Ariani et al., 2008; Bahi-Buisson et al., 2008]. Hence, a diagnosis of RTT in such cases is discussed inconsistently.

1.1.5. Diagnosis

As previously described, MeCP2 mutations do occur in the majority of RTT patients, but not in every individual. Further, the genotype does not compulsorily correlate with the phenotype, respectively the mutation pattern does not necessarily represent the severity of the disease. Conversely, there are some individuals, who show MeCP2 mutations but lack in presenting its clinical features (e.g. period of regression). Instead other neurodevelopmental disorders such as autism, Angelman syndrome-like presentations or non-specific intellectual disability are apparent. As a result *“MeCP2 mutations are neither necessary nor sufficient to make the diagnosis of RTT, concluding that RTT remains a clinical diagnosis”* [Neul et al., 2010]. In course of this, RettSearch reviewed the following diagnostic criteria for RTT in 2010 (Table 3).

Consider RTT diagnosis when postnatal deceleration of head growth is observed

Required for typical or classic RTT 1. A period of regression followed by recovery or stabilization 2. All main and all exclusive criteria **3.** Supportive criteria are not required, although often present in typical RTT
Required for atypical or variant RTT 1. A period of regression followed by recovery or stabilization 2. At least 2 out of the 4 main criteria 3. 5 out of 11 supportive criteria
Main Criteria 1. Partial or complete loss of acquired purposeful hand skills. 2. Partial or complete loss of acquired spoken language 3. Gait abnormalities: Impaired (dyspraxic) or absence of ability. 4. Stereotypic hand movements such as hand wringing/squeezing, clapping/tapping, mouthing and washing/rubbing automatisms
Exclusion Criteria for typical RTT 1. Brain injury secondary to trauma (peri- or postnatally), neurometabolic disease, or severe infection that causes neurological problems 2. Grossly abnormal psychomotor development in first 6 months of life
Supportive Criteria for atypical RTT 1. Breathing disturbances when awake 2. Bruxism when awake 3. Impaired sleep pattern 4. Abnormal muscle tone 5. Peripheral vasomotor disturbances 6. Scoliosis/kyphosis 7. Growth retardation 8. Small cold hands and feet 9. Inappropriate laughing/screaming spells 10. Diminished response to pain 11. Intense eye communication - “eye pointing”

Table 3: Diagnostic criteria of RTT [Neul et al., 2010].

Regarding the variant RTT forms, mentioned in 1.1.4.3., RettSearch states their diagnosis only under the premise that the criteria for an atypical RTT are met (Table 4) [Neul et al., 2010].

To clear up the matter of this obscure RTT nomenclature, RettSearch recommends to categorize all individuals with clinical disorders and MeCP2 mutations as “MeCP2-related disorders”. These include both RTT and other neurological disorders associated with MeCP2 mutations. Patients showing the typical clinical features for RTT should be termed as either typical or atypical RTT, together with the characterization of their genetic mutation. Vice versa, MeCP2 mutants without the typical clinic features of RTT should be called by their respective underlying clinical condition together with the mention of their MeCP2 mutation. This also pertains for MeCP2 duplications [Neul et al., 2010].

Variant forms of RTT

1. Meets criteria for atypical RTT
2. Assess for presence of clinical features of defined variant forms

Preserved Speech Variant (Zappella Variant)
Clinical features: 1. Regression at 1-3 y, prolonged plateau phase 2. Milder reduction of hand skills: better retained hand use 3. Recovery of language after regression : mean age of recovery: 5y, single words or phrases 4. Milder intellectual disability: IQ up to 50 5. Autistic behaviours common 6. Decreased frequency of typical RTT features: rare epilepsy, rare autonomic dysfunction, milder scoliosis and kyphosis, normal head circumference, normal height and weight in most
Genetics: Mutations in MeCP2 found in the majority of cases
Early Seizure Variant (Hanefeld Variant)
Clinical features: 1. Early onset of seizures: before 5 month of life, infantile spasms, refractory myoclonic epilepsy, seizure onset before regression 2. Decreased frequency of typical RTT features
Genetics: Mutations in MeCP2 rarely found, analysis for mutation in CDKL5 should be performed
Congenital Variant (Rolando Variant)
Clinical features: 1. Grossly abnormal initial development: severe psychomotor delay, inability to walk 2. Severe postnatal microcephaly before 4 months 3. Regression in first 5 months 4. Lack of typical intense RTT eye gaze 5. Typical RTT autonomic abnormalities present: small cold hands and feet, peripheral vasomotor disturbances, breathing abnormalities while awake 6. Specific movement abnormalities: tongue stereotypes, jerky movements in the limbs
Genetics: Mutation in MeCP2 rarely found, analysis for mutations in FOXG1 should be performed

Table 4: Diagnostic criteria of variant forms of RTT [Neul et al., 2010].

Generally, the differential diagnosis in RTT is often a difficult and prolonged process, especially in young infants [Smeets et al., 2011]. Today, the average age at diagnosis is about 2.7 years [Tarquinio et al., 2015]. In addition to the discrimination of various RTT forms also other neuronal disease with similar phenotypes have to be excluded. Hereby, Angelman syndrome is assumed to be the most difficult differential diagnosis given its developmental delay, stereotyped movements, epilepsy and others [Smeets et al., 2011; William et al., 2010].

1.1.6. Therapeutic strategies and their challenges

To date, rehabilitation programs serve as cornerstones in RTTs' clinical management. Hereby early intervention and life-long medical care are essential with regard to the patients' health status and longevity. Although specific approaches for various RTT symptoms such as epilepsy or cardiorespiratory perturbations have successfully been established, finding effective pharmacological treatment, interfering with neurotransmitter systems, gene expression or altering DNA methylation, still requires research [Smeets et al., 2011].

However, in recent valid cellular and animal models combined with a better understanding of MeCP2 function has paved the way for identifying and developing several therapeutic strategies. The approaches are divided in two main categories (Figure 6) [Katz et al., 2016]:

1. Strategies, targeting the primary underlying cause of the disease (MeCP2 dysfunction)
2. Strategies, targeting downstream cellular processes (pharmacological approaches)

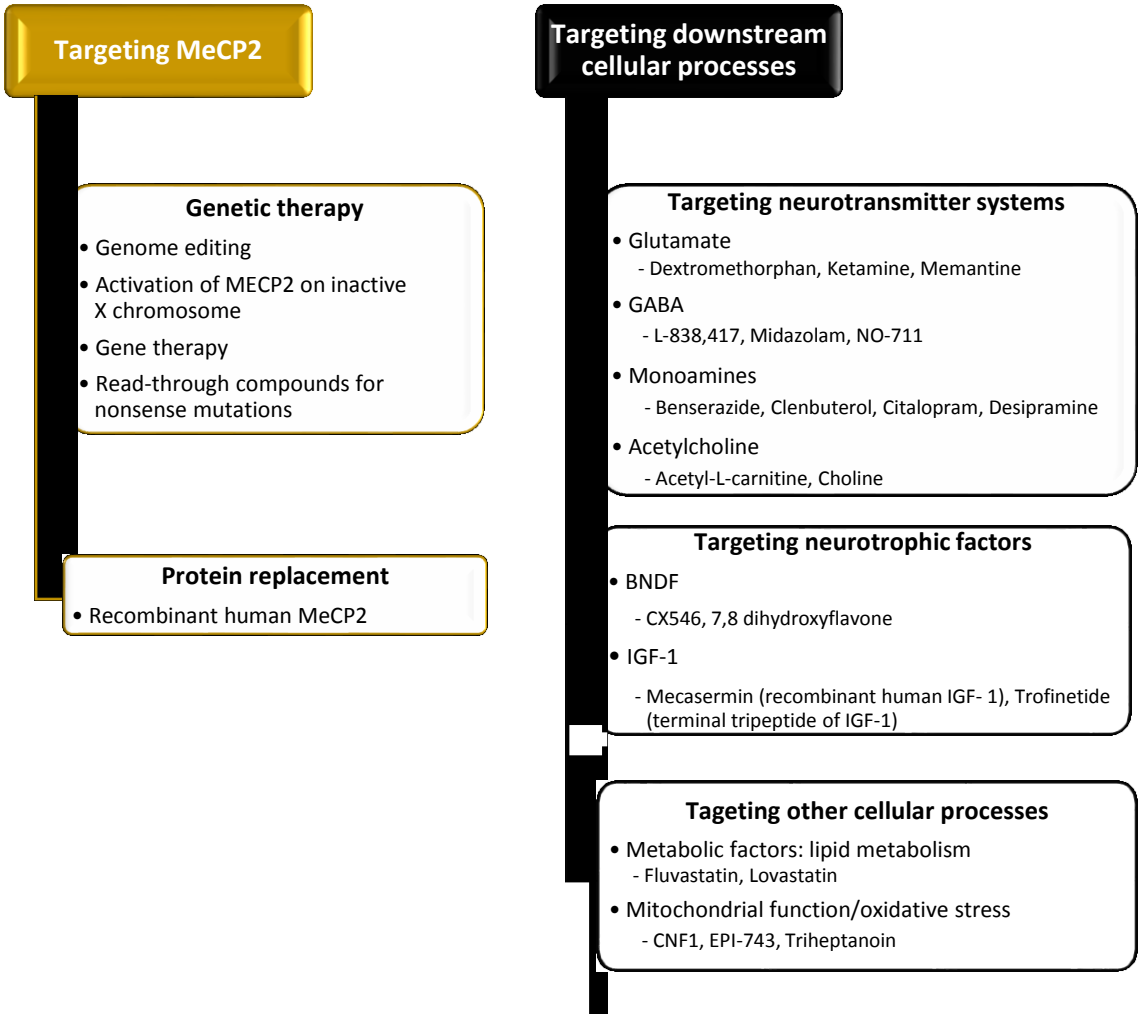

Figure 6: Therapeutic strategies of RTT [modified according to Leonard et al., 2016].

1.1.5.1. Strategies targeting MeCP2

More precisely, the former category comprises interventions that address MeCP2 at the level of the gene, RNA or protein in order to reconstitute functional MeCP2 within the nervous system [Leonard et al., 2016]. Following the example of the reversibility of the MeCP2-knockout phenotype in MeCP2-STOP mice [Guy et al., 2007], these strategies target the transmission to humans for the purpose of restoring existing dysfunctions in RTT as well as preventing its onset [Gadalla et al., 2011]. In fact, such molecular manipulations share two essential obstacles. On the one hand, the physiological range of cellular MeCP2 concentration is quite narrow. Not only diminished but also increased MeCP2 levels may cause neurological symptoms seen in patients suffering from Xq28 duplications as well as in mice overexpressing the protein. However, creating overexpression-related pathology by reversing MeCP2 function is likely to happen and must be avoided [Luikenhuis et al., 2004; Van Esch et al., 2005]. On the other hand, these strategies rely on novel designed molecules, implicating issues such as an effective brain delivery, safety and regulatory coherence [Leonard et al., 2016].

a) Genetic therapy

Reactivation of the normal allele

In terms of interventions at genetic level, one hypothesis for promoting MeCP2 in cells expressing the mutant allele, is the reactivation of the inactive X chromosome. Thus expression of the cells' normal allele would be ensured. However, this theory would exclusively work under the premise of a specifically MeCP2 locus targeted reactivation. Since an entire X chromosome reactivation would override the initial purpose of XCI, videlicet a gene dosage compensation. As a result gene overexpression at various loci would occur [Gadalla et al., 2001].

Gene therapy

The other possibility would involve the delivery of a working gene copy of MeCP2 to affected cells. Ideally, this would lead to an appropriate increase of functional MeCP2 expression, curing clinical features of RTT. However, several difficulties arise ranging from finding an appropriate vector and transducing sufficient cells to avoiding transgene repression as well as overexpression of exogenous MeCP2 [Gadalla et al., 2011].

Besides lentiviruses and retroviruses, adeno-associated viruses (AAV) represent a promising agent in regard to vectors [Gadalla et al., 2011]. Especially the AAV9 serotype is of particular interest in RTT research as it has the ability to cross the blood-brain barrier, efficiently infect neurons, mediate long-term transgene expression and refrain randomly integration into host chromosomes [Arruda et al., 2005; Duan et al., 1998; Jiang et al., 2006; Herzog et al., 1997]. Apart from choosing an appropriate vector, therapeutic dosage is of great significance. Finding the balance between transducing enough cells for coverage and avoiding harmful multiplicity of infection resulting in MeCP2 overexpression, is actually challenging. Assuming that the requirements for an exemplary transduction (one viral particle per cell combined with a MeCP2 expression from a single extra copy of the gene) are met, the challenges in avoiding overexpression are still not overcome. Due to the genetic mosaicism in females, described in 1.1.1.1., the delivery of MeCP2-expressing constructs to those cells expressing the normal and not the mutant allele could again lead to an overexpression. Counteracting this eventuality, "*the construct has to be designed either in a way that pre-existing expression of MeCP2 leads to the transgene not being expressed or in a way that an included agent suppresses endogenous MeCP2 expression while leaving the transgene to do its work"* [Gadalla et al., 2011]. Although potential molecular strategies for implementing this assumptions have already been discovered, research is still in progress [Gadalla et al., 2011; Zhou et al., 2006].

Read through compounds for nonsense mutations

Around 40% of MeCP2 mutations in patients suffering from classical RTT are nonsense mutations, which are associated with premature stop codons [Philippe et al., 2006]. Consequentially, the third mentionable strategy, is addressing MeCP2 at the level of RNA respectively translation by developing compounds to enable ribosomal read-through of nonsense mutations [Leonard et al., 2016]. On that account, aminoglycoside antibiotics (e.g. gentamycin) are a promising pharmacological agent in promoting the production of full-length functional proteins. Their working mechanisms for bypassing the premature stop codon is an insertion of another amino acid that causes a missense mutation [Martin et al., 1989]. From the theoretical point of view this could mean the supply of functional MeCP2 from the allele which is endogenously active, preserving native regulatory mechanisms and excluding any possible form of toxicity caused by overexpression. [Katz et al., 2016].

b) Protein replacement

An additional potential strategy for titrating appropriate MeCP2 concentrations is displayed by a protein replacement. Challenges appearing in this context include *"securing that regular post-translational modifications are present, homogenous and ongoing delivery of the appropriate levels across the blood–brain barrier as well as an adequate cell penetration and localization of the supplied MeCP2 to the nucleus"* [Katz et al., 2016].

This research approach was also investigated by Laccone et al., in terms of developing specific MeCP2 encoding constructs that are biologically active and manage to get into the cells of the nervous system. [Laccone, 2007]. In terms of delivery, they used the idea of Schwarze et al., who stated the possibility of transporting biologically active macromolecules into living cells by the use of a TAT (transcriptional transactivator protein of human immunodeficiency virus-1)-domain. In their mice model, Schwarze et al. achieved ubiquitous tissue distribution of the recombinant TAT-fusion protein after its intraperitoneal injection [Schwarze et al., 1999]. Therapeutical benefits resulting from the application of such protein transduction molecules range from controllable dosage application and high delivery efficiency to the exclusion of immunological reactions against viral proteins (seen in gene therapy). Hence, Laccone et al. successfully designed and patented a recombinant TAT-MeCP2 fusion protein for substitutional therapy options in treating RTT [Laccone, 2007].

1.1.5.2. Strategies targeting downstream mechanisms in the pathogenic process

These strategies sum up pharmacological approaches, which rather affect symptoms of the disease than targeting its underlying aetiology. However, as the precise function of MeCP2 is obscure, it is difficult to discriminate between primary clinical features directly resulting from MeCP2 dysfunction and secondary ones with less value as therapeutic agents. Moreover, the missing pathophysiological knowledge entails a limitation for these drugs benefits just to a subset of symptoms. Nevertheless, currently developed pharmaceuticals are of hugely importance in alleviating the patients' discomforts and improving their life quality. Generally, they are categorized in agents addressing neurotransmitter systems disrupted in RTT (e.g. glutamate, GABA, monoamines, acetylcholine), agents targeting neurotrophic factors (e.g. BDNF, IGF1) as well as agents for other cellular processes perturbed in RTT (e.g. cell metabolism and homeostasis) [Gadalla et al., 2011; Leonard et al., 2016].

Picking trophic factors and their targeting drugs out of this large variety of candidates, they mainly function as promotors of brain growth and development. Herein, especially the modulation of the BDNFs' pathway is of therapeutical priority [Leonard et al., 2016]. As mentioned above, deviations in BNDF concentrations are consistently associated with the RTT brain, and targeting their signalling has already resulted in improvements of RTT symptoms [Chang et al., 2006]. For example, Ogier et al. investigated the effects of BNDF enhancement in MeCP2 knock out mice on respiratory function. Herein, the mice were successfully treated with ampakine CX546 (a positive modulator of AMPA and known booster of BDNF levels), resulting in a restoration of normal breathing patterns and respiratory minute volume. This research paved a promising way for respiratory abnormalities in RTT [Ogier et al., 2007].

1.2. Aim of the study

This issue is linked to the protein replacement strategy of our working group, outlined in 1.1.5.1. As reported there, Laccone et al. were the first to develop a patented method for production of efficient MeCP2 fusion proteins with the possible potential to circumvent blood-brain barrier and to reverse deficiency of MeCP2 protein in neurons. This intervention brought up the need of a suitable assay to measure this TAT-MeCP2 fusion protein for the diagnostic in cellular and animal models.

Therefore, the main aim of this study was the development and verification of an electrochemiluminescence based-immunoassay (ECLIA) for the quantification of endogenous MeCP2 as well as TAT-MeCP2 fusion protein. This assay was chosen due to its benefits as a simple and highly quantitative method able to measure much lower protein levels than classical western blotting. Besides meeting the requirement of determining protein levels in cell lines as well as animal tissues, we put emphasis on a high sensitivity and specificity of this high-throughput assay to enable high accuracy and low detection limits, being essential for diagnostic implementation. Additionally, we focused on a comparison with a commercially available MeCP2-ELISA, in regards of the already mentioned aspects as well as economic arguments.

2. MATERIALS & METHODS

2.1. Materials

2.1.1. Antibodies

Product name	Product number	Source
Monoclonal Anti-MeCP2, produced in mouse, clone 1B11, purified immunoglobulin	SAB1404063-100UG	Sigma-Aldrich®
Monoclonal Anti-MeCP2, produced in mouse, clone 4B6, purified immunoglobulin	WH0004204M1-100UG	Sigma-Aldrich®
Monoclonal Anti-MeCP2, produced in mouse, clone Mec-168, purified immunoglobulin	M6818-100UL	Sigma-Aldrich®
Monoclonal Anti-MeCP2, produced in mouse, clone Men-8, purified immunoglobulin	M7443-200UL	Sigma-Aldrich®
MeCP2 (D4F3) XP® Rabbit mAb	3456S	Cell Signaling Technology Inc.®
Polyclonal Anti-MeCP2, produced in rabbit	custom-designed	Eurogentec S.A.®
Polyclonal Anti-MeCP2, produced in rabbit	07-013	Merck KGaA®
SULFO-TAG™ Labeled Anti-Rabbit Antibody (goat)	W0015528S	Meso Scale Diagnostics®
Anti-Rabbit IgG (whole molecule) - Peroxidase antibody produced in goat	A0545	Sigma-Aldrich®
Anti-Mouse IgG (whole molecule) - Peroxidase antibody produced in goat	A4416	Sigma-Aldrich®

2.1.2. Proteins

Product name	Product number	Source
Human MeCP2 full length protein	ab125491	Abcam plc. ®
MeCP2 (Human) Recombinant Protein (P01)	H00004204-P01	Abnova Corporation®
Methyl CpG Binding Protein 2 (MeCP2) Human Recombinant	PRO-212	ProSpec-Tany TechnoGene Ltd.®
Standard of the ELISA Kit for Methyl CpG Binding Protein 2 (MeCP2)	SEC616Mu	Cloud-Clone-Corp.®
Recombinant transactivator of transcription (TAT)-MeCP2 fusion protein	lab-designed	lab-designed

2.1.3. Common laboratory chemicals

Product name	Product number	Source
1,4-Dithiothreitol (DTT)	D9779	Sigma-Aldrich®
2-Mercaptoethanol	M3148-25M	Sigma-Aldrich®
2-Propanol	278475	Sigma-Aldrich®
Ammonium persulfate (APS)	A3678	Merck KGaA®
Bio-Rad Protein Assay Dye Reagent Concentrate	500-0006	Bio-Rad Laboratories Inc. ®
Blocker Casein in PBS	37582	Thermo Fisher Scientific Inc. ®
Bovine Serum Albumin (BSA)	A9647	Sigma-Aldrich®
Bromphenol blue	B0126	Sigma-Aldrich®
EDTA	EDS	Sigma-Aldrich®
EGTA	3054.1	Carl Roth GmbH + Co.KG®
Fixmilch Instant (sofortlösliches Magermilchpulver)	115710-10	Maresi Austria GmbH®
Glycerol	G2025	Sigma-Aldrich®
Glycine	S0046	Sigma-Aldrich®
HEPES	H3375	Sigma-Aldrich®
IGEPAL® CA-360	I3021	Sigma-Aldrich®
Magnesium chloride hexahydrate ($MgCl*6H_20$)	M2670	Sigma-Aldrich®
Methanol	T909.1	Carl Roth GmbH + Co.KG®
MSD Blocker A	R93BA-4	Meso Scale Diagnostics®
PageRuler™ Prestained Protein Ladder	26616	Thermo Fisher Scientific Inc. ®
Protease Inhibitor Cocktail (100X)	8340	Sigma-Aldrich®
Protease Inhibitor Cocktail (25X)	11873580001	Roche Dignostics GmbH®
PMSF	93482	Sigma-Aldrich®
Ponceau-S	1142750010	Merck KGaA®
Potassium chloride (KCl)	1049361000	Merck KGaA®
Potassium phosphate monobasic (KH_2PO_4)	1048771000	Merck KGaA®
ProSieve™ 50 Gel	50618	Lonza®
Read Buffer T (4x) with surfactant	R92TC-3	Meso Scale Diagnostics®
Sodium chloride (NaCl)	S3014	Sigma-Aldrich®
Sodium deoxycholate	D6750	Sigma-Aldrich®
Sodium dodecyl sulfate (SDS)	428023	Merck KGaA®
Sodium fluoride (NaF)	S7920	Sigma-Aldrich®
Sodium orthovanadate	S6508	Sigma-Aldrich®

Sodium phosphate dibasic dihydrate ($Na_2HPO_4*2H_2O$)	1065801000	Merck KGaA®
Sterile Water	W3500	Sigma-Aldrich®
TEMED	1107320100	Merck KGaA®
Tricine	T0377	Sigma-Aldrich®
Triton X-100	T-8787	Sigma-Aldrich®
Trizma® base	T6066	Sigma-Aldrich®
Tween® 20	P9416	Sigma-Aldrich®

2.1.4. Cell Culture Materials

Product name	**Product number**	**Source**
Cellstar® cell culture flasks, 250ml, 75cm^2	82050-856	Greiner Bio-One®
DMEM (1X) [+] 4.5g/L D-Glucose [+] L-Glutamine [+] Pyruvate	41966-029	gibco® by Life Technologies™
DMEM (1X) [+] 4.5g/L D-Glucose [+] L-Glutamine [-] Pyruvate	41695-039	gibco® by Life Technologies™
Fetal Bovine Serum (1)	F9665	Sigma-Aldrich®
Fetal Bovine Serum (2)	F4135	Sigma-Aldrich®
Forskolin	A2165	AppliChem GmbH®
D-(+)-Glucose solution	G8769	Sigma-Aldrich®
Dulbecco's PBS (sterile)	D8537-500ML	Sigma-Aldrich®
Penicillin-Streptomycin	15140122	gibco® by Life Technologies™
0.25% Trypsin EDTA (1X)	25200-056	gibco® by Life Technologies™

2.1.5. Kits

Product name	**Product number**	**Source**
ELISA Kit for Methyl CpG Binding Protein 2 (MECP2)	SEC616Mu	Cloud-Clone-Corp.®
ChemiGlow™ West Chemiluminescence Substrat Kit (Stable Peroxide Buffer & Luminol/Enhacer Solution)	60-12597-00	ProteinSimple®

2.1.6. Common laboratory solutions

Solution	Volume	Composition
Blot Buffer	1l	100ml Tris-Glycin Buffer (10X) 200ml Methanol 200µl 10% SDS → *fill up with ddH_20, store at 4°C*
DTT (0.1M)	1ml	15.425mg DTT → *fill up with sterile water, store at -20°C*
Electrophoresis Buffer	1l	100ml Tris-Tricine Buffer (10X) 10ml 10% SDS → *fill up with ddH_20, store at 4°C*
Extraction Buffer, ph=7.9	50ml	1ml HEPES (1M) 15.25mg $MgCl*6H_2O$ 1.23g NaCl 20µl EDTA (0.5M) 12.5ml Glycerol → *fill up with ddH_20 adjust pH, store at 4°C*
Hypotonic Lysis Buffer, pH=7.9	50ml	0.5ml HEPES (1M) 15.25mg $MgCl*6H_2O$ 27.28mg KCl → *fill up with ddH_20, adjust pH, store at 4°C*
MeCP2 Lysis Buffer	9.4ml	**w/o inhibitors:** 1ml 10X TBS (pH=7.4) 1ml 10% Triton X-100 20µl 0.5M EDTA 40µl 0.25M EGTA 500µl 1% SDS 200µl 5% Na-deoxycholate 10% IGEPAL® CA-360 → *fill up with ddH_20, adjust pH, store at 4°C*
	1ml	**ready to use:** 960µl MeCP2 Lysis Buffer w/o inhibtors 10µl 0.5M NaF 10µl 0.1M Na-orthovanadate 10µl (0.1M) PMSF 10µl PI8340 100X

PBS Buffer (1x), pH=7.4	1l	137mM NaCl 2.7mM KCl 5.4mM Na_2HPO_4*2 H_2O 1.5mM KH_2PO_4 → *fill up with ddH_20, adjust pH, autoclave, store at 4°C*
Read Buffer T (4x) with surfactant	50ml	12.5ml Read Buffer T (4x) with surfactant → *fill up with ddH_20*
Sample Buffer (6x), non-reducing	20ml	7ml Tris-HCl 6ml Glycerol 2g SDS 2.4mg Bromphenol blue → *fill up with ddH_20, store at -20°C*
Separating Gel (12%)	15.108ml	4.9ml ddH_20 4.8ml ProSieve™ 50 Gel Solution 5ml 1.5M Tris/HCl 200µl 10% SDS 200µl 10% APS 8µl TEMED
Stacking Gel (5%)	5.005ml	3.75ml ddH_20 0.5ml ProSieve™ 50 Gel Solution 0.65ml 1M Tris/HCl 50µl 10% SDS 50µl 10% APS 5µl TEMED
TBS Buffer (10X), pH=7.6	1l	24.2g Trizma® base 80.0g NaCl → *fill up with ddH_20, adjust pH, autoclave, store at RT*
Tris-Glycine Buffer (10X)	1l	30g Trizma® base 144g Glycine → *fill up with ddH_20, autoclave, store at 4°C*
Tris-HCl, pH=6.8	1l	121.14g Trizma® base → *fill up with 800ml ddH_20, adjust pH by 10% HCl , fill up with ddH_20, autoclave, store at RT*
Tris-Tricine Buffer (10X)	1l	121g Trizma® base 179g Tricine → *fill up with ddH_20, autoclave, store at 4°C*

2.1.7. Other Materials

Product name	Product number	Source
Multi-Array® 96-well Plate	L15XB-3/L11BX-3	Meso Scale Diagnostics®
Laboratory Shaker, rocking motion (low speed)	3014	GFL®
Microplate Shaker (high speed)	PMS-1000i	Grant Instruments®
Microplate 96-well	655161	Greiner Bio-One®
Nitrocellulose Membranes 0.2µm	162-0112	Bio-Rad Laboratories Inc. ®

2.1.8. Measuring instruments

Product name	Product number	Source
MSD SECTOR® Imager 2400	I30AA-0	Meso Scale Diagnostics®
Peqlab® Fusion Fx7 chemiluminescence imaging system	51115451	VWR International GmbH®
Microplate Reader, Perkin Elmer Wallac 1420 Victor2 Multilabel Counter	PE-WV22	Marshall Scientific LLC.®

2.2. Methods

2.2.1. Immunoassays

As the principle methods of this master thesis are immunoassays, in particular electrochemiluminescence immunoassays (ECLIAs), their concepts should be described shortly. Generally, immunoassays encompass all bioanalytical methods, whose fundamental principle is the quantification of an analyte through reaction of an antigen with an antibody, forming an immunocomplex, as well as the ability to produce a measurable signal in response to the binding. This antigen-antibody binding is characterised by its high specificity and bond strength, making these assays together with their high-throughput and high sensitivity an often used and widely spread detection procedure in pharmaceutical analysis and medical research. The particular immunoassays distinguish themselves in several aspects with the detection system leading the way. Usually specific, detectable labels - which vary from enzymes and radioactive isotopes to fluorogenic reporters and electrochemiluminescent tags- are linked to one of the immunoanalytical reagents (antibody or antigen), producing respective and measurable signals in form of colour intensity, radiation or light. Furthermore the assays principles can be direct or indirect as well as competitive and non-competitive [Darwish, 2006]. As we especially focused on an electrochemiluminescence detection system in developing our assay, its principle should be explained in more detail.

2.2.1.1. Electrochemiluminescence immunoassay (ECLIA)

Rubrene, 9,10-diphenylanthracene (DPA) represents the first molecule on which electrochemiluminescence was first noticed in the 1960's – describing a phenomena where applying voltage to an electrode leads to the generation of compounds that undergo electron transfer reactions resulting in the emission of light. Such compounds - called luminophores – soon represented a breakthrough in biochemical analytics as their application as tags for diverse molecules and therefore the utilization in immunoassays significantly increased the sensitivity of these techniques, allowing measurements at sub-picomolar concentrations [Pyati et al., 2007]. Nowadays, a widespread complex with electrochemiluminescence characteristics is tris-2,20-bipyridylruthenium(II) ($Ru(bpy)_3^{2+}$), which was first observed in an aqueous solution by Rubinstein in 1981. Since then a lot of research work was carried out to improve the application of the Ru-chelate in immunoassays. About 10 years after Rubinstein's work Leland achieved a milestone in the enhancement of the assays detection sensitivity by

adding tripropylamine (TPA) to the electrolyte solution, acting as a powerful reducing agent after electrochemical oxidation, resulting in a significantly broader detection range (<0.2pmol) [Namba et al., 1999].

For our research work we also used a $Ru(bpy)_3^{2+}$/TPA-ECL-system, choosing Meso Scale Diagnostics® to serve with their technology (Figure 16). Starting at the very beginning, we employed Multi-Array™ high-bind, 96-well, single-spot microplates with carbon electrodes in the bottom. These microplates are featured by a 10-fold higher binding capacity than achieved by commercial polystyrene surfaces and the applying of voltage to their electrons to smooth the way to electrochemiluminescence [Meso Scale Discovery®, 2013-2014]. For the actual immunoassay we chose a non-competitive sandwich-system in the form of "capture antibody – antigen – primary detection antibody – labeled secondary detection antibody", as described above. Our capture antibodies to be tested were all monoclonal ones, targeted against the MeCP2 protein and produced in a mouse, which bound unspecifically on the carbon surface after a coating step during an over-night incubation (Figure 13).

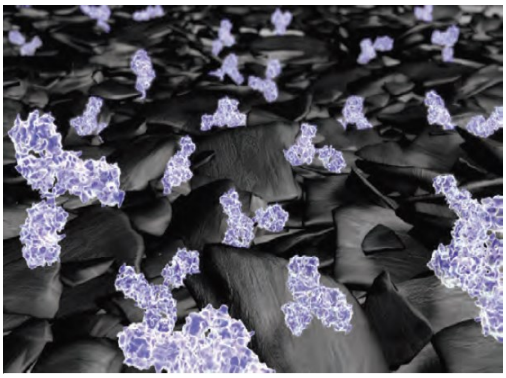

Figure 13: Capture antibodies coated on the carbon surface [Meso Scale Discovery®, 2011-2013]

Coating with monoclonal antibodies boots achieves the purpose of a precise qualification as well as quantification of marginal varieties of antigens as they bind monospecifically toward one single epitope [Thermo Scientific™, 2011]. For primary detection to the contrary, we just tested polyclonal antibodies as we did not consider it necessary – in a cost and time predicted assessment – to embed our antigen between two monoclonal antibodies. In addition, our research group already designed a specific polyclonal anti-MeCP2 antibody - produced in a rabbit - with an accurate way of working before. Lastly, we chose the SULFO-TAG™ labeled anti-rabbit antibody, produced in a goat (Meso Scale Diagnostics®) to serve as a secondary detection antibody for our ECLIA-system. As mentioned at the outset, Meso Scale Diagnostics® thereby uses a tris-2,20-bipyridylruthenium(II)-tag or more specifically its ester (meaning ruthenium(III)-tris-bipyridine-(4-methylsulfonate) NHS ester) for labelling (Figure 14). To accomplish the system and generating an appropriate signal there was a need of the Read

Buffer T (4x) with surfactant (Meso Scale Diagnostics®), which is a Tris-based buffer implicating tripropylamine (TPA) as co-reactant (Figure 15).

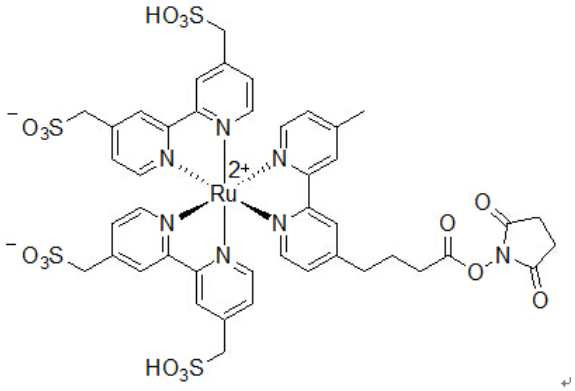

Figure 14: Ruthenium(III)-tris-bipyridine-(4-methylsulfonate) NHS ester [3]

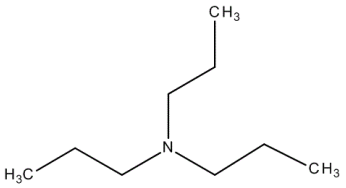

Figure 15: Tripropylamine [4]

Generation of electrochemiluminescence then resulted in the following (Figure 16): If voltage is applied at the microplates surface during the measurement by our MSD SECTOR® Imager 2400, $Ru(bpy)_3^{2+}$ and TPA are oxidized on the carbon electrons, forming the cations $Ru(bpy)_3^{3+}$ and TPA^+•. Subsequently through a spontaneous proton loss, the latter is transformed to the radical TPA •, forming a strong reducing agent. This molecule in turn reacts, respectively reduces $Ru(bpy)_3^{3+}$ to $Ru(bpy)_3^{2+}$• , generating the energetic excited state of the molecule. The ensuing energetic decay of this excited state to the ground state, leads to the emission of a photon (620nm), resulting in a measurable light known as electrochemiluminescence [Namba et al., 1999]. A special charge-coupled device (CCD) camera in the MSD SECTOR® Imager 2400 makes the transformation of light into an appropriate numerous signal possible. Herein, the measured light intensity is relative to the quantity of antigen in the sample.

Figure 16: MSD® ECLIA technology [5]

Our basic protocol for performing an ECLIA was the following:

1. Coating of the Multi-Array™ high-bind 96-well single-spot microplate
   - *Capture antibody: monoclonal, anti-MeCP2, produced in a mouse*
   - *Dilution in: 1x PBS (pH=7.4), varying concentration*
   - *Coating Volume: 25µl/well, solution coating method with dead volume*
   - *Incubation: sealing the plate and incubate overnight (4°C)*
2. Preparation of diverse solutions
   - *Washing solution: 1x PBS (pH=7.4) + 0.05% Tween 20*
   - *Blocking solution: 3% MSD Blocker A Kit in 1x PBS (pH=7.4)*
3. Blocking of unspecific surface-binding sites
   - *Remove liquid of the wells (absorbent paper)*
   - *Pipetting Volume: 125µl/well of the blocking solution, solution coating method with dead volume, multichannel-pipette*
   - *Incubation: sealing the plate and incubate for 1.5 hours on an appropriate shaker*
4. Preparation of the standard solution and samples
   - *Standard stock solution: MeCP2 recombinant protein [200ng/ml]*
   - *Serial dilution (1:3) of the standard stock solution with 1x PBS (pH= 7.4)*
   - *Sample types: cell lines & mouse tissues*
   - *Sample preparation: varying lysis protocols including nuclear and total protein extraction methods (2.2.3.)*
5. Washing step
   - *Remove liquid of the wells (absorbent paper)*
   - *Washing Volume: 150µl/well of the washing solution, solution coating method with dead volume, multichannel-pipette*
   - *Frequency: 3 times*
6. Adding sample and standard solution
   - *Coating Volume: 27µl/well, spot coating method, changing pipette tips after every well*
   - *Incubation: sealing the plate and incubate for 2 hours on an appropriate shaker*

7. Washing step
    - *Remove liquid of the wells (absorbent paper)*
    - *Washing Volume: 150µl/well of the washing solution, solution coating method with dead volume, multichannel-pipette*
    - *Frequency: 3 times*
8. Adding primary detection reagent
    - *Primary Detection Antibody: polyclonal, anti-MeCP2, produced in a rabbit*
    - *Dilution in: 1% blocking solution in 1x PBS (pH=7.4), varying concentration*
    - *Coating Volume: 25µl/well, solution coating method with dead volume, multichannel-pipette*
    - *Incubation: sealing the plate and incubate for 1 hours on an appropriate shaker*
9. Washing step
    - *Remove liquid of the wells (absorbent paper)*
    - *Washing Volume: 150µl/well of the washing solution, solution coating method with dead volume, multichannel-pipette*
    - *Frequency: 3 times*
10. Adding secondary detection reagent
    - *Secondary Detection Antibody: SULFO-TAG™ labelled anti-rabbit antibody, produced in a goat*
    - *Dilution in: 1% blocking solution in 1x PBS (pH=7.4), varying concentration*
    - *Coating Volume: 25µl/well, solution coating method with dead volume, multichannel-pipette*
    - *Incubation: sealing the plate and incubate for 1 hours on an appropriate shaker (avoiding sun exposure)*
11. Washing step
    - *Remove liquid of the wells (absorbent paper)*
    - *Washing Volume: 150µl/well of the washing solution, solution coating method with dead volume, multichannel-pipette*
    - *Frequency: 3 times*
12. Adding Read Buffer T (4x) with surfactant (MSD®)
    - *Dilution in: ddH_2O*

- *Coating Volume: 150µl/well, solution coating method with dead volume, multichannel-pipette*

13. Measuring
    - *Quick analysis using the MSD SECTOR® Imager 2400*

2.2.1.2. Western Blot (WB)

The second immunoassay used, was the Western Blotting technique. As distinguished from Elisa here the immobilisation of the antigen takes place on a membrane, instead of a microplate surface. This method was first described in 1979 by Towbin et al., making immunoblotting one of the most commonly used techniques in molecular biology disciplines [Towbin et al., 1979].

Our basic protocol for performing a Western Blot was the following:

1. Preparation of the Tris/Tricine-SDS-polyacrylamide gel:
    - Separating gel (12%):
        - *4.9ml ddH_20*
        - *4.8ml ProSieve™ 50 Gel*
        - *5ml 1.5M Tris/HCl (pH=8.8)*
        - *200µl 10% SDS*
        - *200µl 10% APS*
        - *8µl TEMED*
    - *Mixing the reagents quickly, pipetting the fluid separating gel in the cavity of the appliance to below the comb edge, filling up with isopropyl alcohol (25%), letting the gel polymerize for 30 minutes, decanting the isopropyl alcohol supernatant and rinsing with ddH_20*
    - Stacking gel (5%):
        - *3.75ml ddH_20*
        - *0.5ml ProSieve™ 50 Gel*
        - *0.65ml 1M Tris/HCl (pH=6.8)*
        - *50µl 10% SDS*
        - *50µl 10% APS*
        - *5µl TEMED*

- *Mixing the reagents quickly, pipetting the fluid stacking gel on the already polymerized separating gel, inserting the comb, letting the gel polymerize for 30 minutes, storing the Tris/Tricine-SDS-polyacrylamide gel at 4°C under moist conditions*

2. Sample preparation
   - *Adding sample buffer (6X) plus 5% ß-mercaptoethanol to a calculated amount of protein lysate*
   - *Filling up with ddH_20 (total volume: ~15µl)*
   - *Heating samples for 5 minutes at 95°C*
3. Electrophoresis
   - *Putting the gel in the electrophoresis equipment*
   - *Filling up with electrophoresis buffer*
   - *Removing the comb and rinsing the wells with electrophoresis buffer*
   - *Loading the samples and the marker into the wells slowly*
   - *Running the gel for 50 minutes at 180 volt*
   - *Removing the gel out of the electrophoresis equipment*
4. Protein Transfer
   - *Cutting away the stacking gel*
   - *Opening the blotting cassette in a tray filled with blot buffer*
   - *Incorporating the residual gel into a sandwich, consisting of blotting cassette (anode-facing side) - prewetted sponge – prewetted blot paper – gel – prewetted membrane – prewetted blot paper – prewetted sponge – blotting cassette (cathode- facing side)*
   - *Making sure that the sandwich is tightly packed and no air bubbles arose*
   - *Placing the closed blotting cassette together with a cooling unit in the electrophoresis equipment*
   - *Filling up with blot buffer*
   - *Running the gel for 35 minutes at 0.5 ampere*
   - *Removing the blotted membrane out of the blotting cassette*
5. Confirmation of protein transfer to the membrane
   - *Staining the membrane with Ponceau S (red)*

- *Cutting the membrane in appropriate parts, according to the stained proteins of interest*
- *Rinsing the membrane with 1x PBS several times to remove the staining afterwards*

6. Blocking of unspecific binding sites
   - *Blocking solution: 5% dry milk powder in 0.1% Tween in 1x TBS*
   - *Incubation time: 1 hour on an appropriate shaker*
7. Antibody detection
   - Incubating with the primary detection antibody
     - *Antibody: mono- or polyclonal, anti-MeCP2, produced in a mouse or a rabbit*
     - *Dilution in: 5% dry milk powder in 0.1% Tween in 1x TBS; 1:15000 (monoclonal anti-MeCP2, clone Mec-168 of Sigma-Aldrich®) or 1:10000 (polyclonal anti-MeCP2 of Eurogentec S.A.®)*
     - *Incubation time: overnight under cooled (4°C) and rotating conditions*
   - Washing step
     - *3 times for 5 minutes with 0.1% Tween in 1x TBS on an appropriate shaker*
   - Incubating with the labelled secondary detection antibody
     - *Antibody: anti-rabbit or anti-mouse, produced in goat, peroxidase labelled*
     - *Dilution in: 5% dry milk powder in 0.1% Tween in 1x TBS, 1:15000*
     - *Incubation time: 1 hour on an appropriate shaker*
   - Washing step
     - *3 times for 5 minutes with 0.1% Tween in 1x TBS on an appropriate shaker*
8. Measuring
   - *Incubating the membrane with ~1ml of the ChemiGlow™ West Chemiluminescence Substrat Kit (1:1) for 5 minutes*
   - *Foil-coating the membrane*
   - *Analysing quickly using Peqlab® Fusion Fx7 imaging system*

2.2.2. Protein determination according to Bradford

For protein determination, which is an essential requirement in preparing accurate cell as well as tissue lysates, we used the Bio-Rad protein assay. This assay is based on Bradford's method to measure the concentration of solubilized proteins, which the author established in 1976 [Bradford, 1976]. Its principle is based on the supplementing, respectively the binding, of an acidic dye, namely Coomassie® Brilliant blue G-250, to the proteins of the solution to be determined. Here, the dye agent predominantly binds to the basic and aromatic amino acid residues, such as arginine. Depending on the proteins presence and concentration, a correspondingly strong colour change of the dye agent occurs from brown to blue, simultaneously implicating a shift in absorbance maximum from 465nm (without any protein) to 595nm. The absorbance intensity is then measured with a photometer at 595nm, reflecting a correlation with the protein concentration. For generating the appropriate standard curve, bovine serum albumin is used as a stock solution and serially diluted with distilled water [Bio-Rad, 1994].

Our basic protocol for performing a Bio-Rad protein assay was the following:

1. Preparation of the standard stock solution: BSA [0.1mg/ml]
   - *Starting concentration: 1mg/ml BSA*
   - *Dilution: 1:10 with distilled water*
2. Serial dilution (1:10) of the standard stock solution

Protein concentration [µg/ml]	*BCA (0.1mg/ml)*	*Distilled water*
0	*0 µl*	*800 µl*
2	*20 µl*	*780 µl*
4	*40 µl*	*760 µl*
6	*60 µl*	*740 µl*
8	*80 µl*	*720 µl*
10	*100 µl*	*700 µl*
12	*120 µl*	*680 µl*
14	*140 µl*	*660 µl*

3. Sample preparation
   - *Filling up 2-10µl protein or cell lysate with distilled water to a volume of 800µl*
4. Adding Bio-Rad reagent
   - *Adding 200µl Bio-Rad reagent to each sample with a dispenser (as simultaneously as possible)*
   - *Vortexing*

- *Incubating for 20 minutes at room temperature*
- *Vortexing*

5. Measuring
   - *Pipetting 200µl of each sample in a 96-well microplate (in duplicates)*
   - *Measuring absorbance at 595nm with a photometric plate reader (Microplate Reader, Perkin Elmer Wallac 1420 Victor2 Multilabel Counter)*

2.2.3. Preparation of cell and tissue lysates

2.2.3.1. Cell lysates

a) Cell culture and harvesting of cell pellets

For our research, we cultivated the following five cell lines:

1. Cofib: wild-type fibroblasts #21708A
2. Rettfib: male Rett patients' fibroblasts
3. HepG2: human hepatocellular carcinoma cell line
4. HSC: human Schwann cells

Therefore, we needed to prepare two varying cell growth culture media, based on Dulbecco's modified eagle's medium (DMEM).

Medium 1 (used for Cofib, Rettfib, HepG2)	Medium 2 (used for HSC)
450ml DMEM (#41966)	440ml DMEM (#41965)
50ml FBS 1 (10%)	50ml FBS 2 (10%)
5ml PenStrep (5%)	10ml Glucose (0.2%)
	5ml PenStrep (5%)
	2µM Forskolin

For an appropriate growth, the adherent cells were cultivated in sterile culture flasks with a surface area of 75cm^2 and incubated in a sterile incubator at 37°C and 5% CO_2. Regular splitting occurred when the flasks surface was at least 80% confluent.

Our basic protocol for splitting diverse cell lines was the following:

1. Aspirating the media from the flask (carefully, using a Pasteur pipette)
2. Washing step
   - *With ~10ml 1x DPBS (sterile)*
   - *Aspirating the washing solution afterwards (carefully, using a Pasteur pipette)*
3. Detaching the cells from the flasks surface
   - *Adding ~2ml trypsin (0.05%)*
   - *Making sure all cells are entirely covered*
   - *Incubating the flask in the sterile incubator at 37°C and 5% CO_2 for 2-6 minutes*
   - *Checking appropriate trypsinization microscopically*
4. Inactivating trypsin with the appropriate FBS containing medium
   - *Resuspending the cell-trypsin-solution with ~12ml of the appropriate cell culture medium*
5. Dividing the cell suspension
   - *Choosing a suitable splitting ratio according to the cells growing speed*
   - *Pipetting the calculated volume of cell suspension into new flasks*
   - *Filling up with the appropriate cell culture medium to a volume of ~12ml in each flask*
6. Placing flasks in the incubator again

The main aim of our cell culturing process was to have an abundant cell harvesting to form respective packed cell pellets, which served as the starting basis in the course of preparing different cell lysates.

Our basic protocol for harvesting diverse cell lines was the following:

1. Aspirating the media from the flask (carefully, using a Pasteur pipette)
2. Washing step
   - *With ~10ml 1x PBS (sterile)*
   - *Aspirating the washing solution afterwards (carefully, using a Pasteur pipette)*
3. Detaching the cells from the flasks surface
   - *Adding ~2ml trypsin (0.05%)*
   - *Making sure all cells are entirely covered*

- *Incubating the flask in the sterile incubator at 37°C and 5% CO_2 for 2-6 minutes*
- *Checking appropriate trypsinization microscopically*

4. Inactivating trypsin with the appropriate FBS containing medium
   - *Resuspending the cell-trypsin-solution with ~12ml of the appropriate cell culture medium*
5. Centrifuging the cell suspension
   - *At 1000g and 4°C for 5 minutes in a 10ml falcon*
6. Aspirating the supernatant media save for the pellet (carefully, using a Pasteur pipette)
7. Washing step (2x)
   - *Resuspending the pellet with ~10ml (1st time) or ~2ml (2nd time) of cooled 1x PBS*
   - *Centrifuging the cell suspension at 1000g and 4°C for 5 minutes in a 10ml falcon (1st time) or a 2ml Eppendorf tube (2nd time)*
   - *Aspirating the supernatant 1x PBS save for the pellet (carefully, using a Pasteur pipette)*
8. Freezing the Eppendorf tubes at -20°C

b) Different lysis protocols

In the final procedure of establishing cell lysates we tested three different protocols, including total protein extraction (Protocol for cell lysis using MeCP2 Complete Lysis buffer, Protocol for cell lysates of LifeSpan BioScience®) as well as nuclear protein extraction (Nuclear protein extraction without the use of detergent from adherent cells of Sigma-Aldrich®) methods.

Our protocols for a total protein extraction of cell lines were the following:

➔ **Protocol for cell lysis using MeCP2 complete lysis buffer**

1. Preparing MeCP2 complete lysis buffer ready to use (1ml)
   - *Adding the following reagents to the already prepared MeCP2 lysis buffer w/o inhibitors (960µl)*
     - *10µl 0.5M NaF*
     - *10µl 0.1M Na-orthovanadate*
     - *10µl 0.1M PMSF*
     - *10µl PIC 100x*
2. Resuspending the cell pellets in MeCP2 complete lysis buffer ready to use
   - *40µl MeCP2 complete lysis buffer ready to use per pellet*

3. Incubating for 30 minutes on ice
4. Removing cellular debris
   - *Centrifuging at 10000g and 4°C for 10 minutes*
5. Collecting the supernatant

➔ **Protocol for cell lysates [LifeSpan BioScience®, 2016]**

1. Resuspending the cell pellets in 1x PBS
   - *100µl 1x PBS per pellet*
2. Lysing the cells
   - *4 times á 5 seconds by ultrasonication*
   - *3 times by freezing to -20°C and thawing to room temperature subsequently*
3. Removing cellular debris
   - *Centrifuging at 1500g and 4°C for 10 minutes*
4. Collecting the supernatant

<u>Our protocol for a nuclear protein extraction of cell lines was the following:</u>

➔ **Nuclear protein extraction without the use of detergent from adherent cells [Sigma-Aldrich®, 2016]**

1. Preparing hypotonic lysis buffer ready to use (1428µl)
   - *Adding the following reagents to the already prepared hypotonic lysis buffer (1400µl)*
     - *14µl 0.1M DTT*
     - *14µl PIC 100x*
2. Resuspending the cell pellets in hypotonic lysis buffer ready to use
   - *100µl hypotonic lysis buffer ready to use per 4 pellets*
3. Incubating the suspension, allowing the cells to swell
   - *At room temperature for 15 minutes*
4. Centrifuging the suspension and decanting the supernatant
   - At 420g and 4°C for 5 minutes
5. Resuspending the cell pellet in the hypotonic lysis buffer ready to use conscientiously
   - 200µl hypotonic lysis buffer ready to use per pellet
6. Centrifuging the suspension and decanting the supernatant (cytoplasmic fraction)

- At 10500g and 4°C for 20 minutes

7. Preparing the extraction buffer ready to use (150µl)
   - *Adding the following reagents to the already prepared extraction buffer (147µl)*
     - *1.5µl 0.1M DTT*
     - *1.5µl PIC 100x*
8. Resuspending the nuclei pellet in the extraction buffer ready to use conscientiously
   - *70µl extraction buffer ready to use per pellet*
9. Shaking gently
   - *At 0°C and 400rpm for 30 minutes*
10. Centrifuging the suspension and transferring the supernatant into a chilled tube (nuclear fraction)
    - *At 16500g and 4°C for 5 minutes*

All similar cell lysates were pooled together and stored at -80°C.

2.2.3.2. Tissue lysates (mouse)

a) Organ harvesting

For preparing various tissue lysates we killed our mice (wildtype, heterozygous, MeCP2-knock out) via neck fracture and subsequently harvested the required organs quickly. The organs were then washed in 1X PBS, transferred in Eppendorf tubes, rapidly frozen by use of liquid nitrogen and stored at -80°C.

b) Different lysis protocols

Again we performed a total protein extraction (Protocol for tissue homogenates, LifeSpan BioScience®) as well as a nuclear protein extraction (Nuclear protein extraction without the use of detergent from tissues, Sigma-Aldrich®) to lyse mice tissues.

Our protocols for a total protein extraction of mouse tissue were the following:

➔ **Protocol for tissue homogenates [LifeSpan BioScience®, 2016]**

1. Weighing the frozen tissue
2. Pulverizing the frozen tissue
   - *By use of a pastille in liquid nitrogen*
3. Resuspending the pulverized tissue
   - *With 10ml 1X PBS per gram tissue*

- *By use of a glass homogenizer on ice*

5. Lysing the cells
   - *4 times á 5 seconds by ultrasonication*
   - *3 times by freezing to -20°C and thawing to room temperature subsequently*
6. Removing cellular debris
   - *Centrifuging at 5000g and 4°C for 5 minutes*
7. Collecting the supernatant

Our protocols for a nuclear protein extraction of mouse tissue were the following:

➔ **Nuclear protein extraction without the use of detergent from tissues [Sigma-Aldrich®, 2016]**

1. Preparing hypotonic lysis buffer ready to use (1428µl)
   - *Adding the following reagents to the already prepared hypotonic lysis buffer (1400µl)*
     - *14µl 0.1M DTT*
     - *14µl Protease Inhibitor Cocktail*
2. Weighing the frozen tissue
3. Pulverizing the frozen tissue
   - *By use of a pastille in liquid nitrogen*
4. Resuspending the pulverized tissue
   - *With 1ml hypotonic lysis buffer ready to use per 100mg tissue*
   - *By use of a glass homogenizer on ice*
5. Centrifuging the suspension and decanting the supernatant (cytoplasmic fraction)
   - At 10500g and 4°C for 20 minutes
6. Preparing the extraction buffer ready to use (150µl)
   - *Adding the following reagents to the already prepared extraction buffer (147µl)*
     - *1.5µl 0.1M DTT*
     - *1.5µl PIC 100x*
7. Resuspending the nuclei pellet in the extraction buffer ready to use conscientiously
   - *140µl extraction buffer ready to use per pellet*
8. Shaking gently
   - *At 0°C and 400rpm for 30 minutes*

9. Centrifuging the suspension and transferring the supernatant into a chilled tube (nuclear fraction)
    - *At 16500g and 4°C for 5 minutes*

All tissue lysates were stored at -80°C.

3. RESULTS

3.1. Development of an ECLIA based assay for MeCP2

3.1.1. Basic system development and determination of the standard curve

3.1.1.1. Antibodies

a) Capture and Primary Detection Antibody

In the development of an ECLIA, finding the appropriate antibodies and their concentration is often a long-winded process. It is influenced by several variables such as the plate type used. To start at the basis of our research, we chose a 96-well high-bind plate to work with. High-bind plates are characterized through their hydrophilic surface, determining the capacity of coated capture reagent. They usually have a higher binding capacity than hydrophobic surfaces. Accordingly, Meso Scale Discovery® recommends coating these plates at a certain concentration within the binding capacity, which should be 5 times higher than for hydrophobic surfaces. For a high-bind, 96-well, single-spot plate the binding capacity for their reference capture reagent IgG (150.000Da) was about 5.0 pmol/well. For other proteins they recommend to align the molecular weight relative to IgG. In our case, for MeCP2 with a molecular weight of ~ 75.000 Da, the binding capacity to examine would be half of IgG, assuming that the molar concentration is equivalent. Of course, this measurement may vary for diverse proteins, but can serve as an useful orientation. Another point that factors into the selection of the right capture antibody concentration is the coating technique. As we chose the solution coating method, the recommended coating concentrations range from 1µg/ml to 20µg/ml, whereas the coating volume should be between 25µl/well and 40µl/well. Keeping these guidelines in mind, we conducted a titration of different coating concentrations for various contemplable capture antibodies, using 1x PBS (pH=7.4) as coating buffer. [Meso Scale Discovery®, 2013-2014.]

Concerning the primary detection antibody, similar basic conditions applied, as a solution coating technique was used again. Also for our primary detection antibodies we used 1x PBS (pH=7.4) as buffer, but in terms of avoiding high background signals, we added 1% of blocking solution MSD Blocker A Kit (Meso Scale Diagnostics®).

The following table gives an overview of the tested capture and primary detection antibodies as well as of their tested dilution ranges:

Antibody purpose	Name	Dilution
capture	monoclonal, anti-MeCP2, clone Mec-168, produced in mouse (Sigma-Aldrich®)	1:500 – 1:10 000
capture	monoclonal, anti-MeCP2, clone 4B6, produced in mouse (Sigma-Aldrich®)	1:250 – 1:4000
capture	monoclonal, anti-MeCP2, clone Men-8, produced in mouse (Sigma-Aldrich®)	1:500 – 1:4000
capture	monoclonal, anti-MeCP2, clone 1B11, produced in mouse (Sigma-Aldrich®)	1:500 – 1:4000
capture	MeCP2 (D4F3) XP® rabbit mAb (Cell Signaling Technology Inc.®)	1:500 – 1:4000
detection (primary)	polyclonal, anti-MeCP2, produced in rabbit (Eurogentec S.A.®)	1:2000 – 1:20 000
detection (primary)	polyclonal, anti-MeCP2, produced in rabbit (Merck KGaA®)	1:2000 – 1:20 000

As we combined some of these titration experiments, we performed two-dimensional serial dilutions at first and started our antibody-test-series with the chessboard titration below.

1. Experimental set-up:

Capture antibody	monoclonal, anti-MeCP2, clone Mec-168, produced in mouse (Sigma-Aldrich®): 1:500, 1:1000, 1:2000, 1:4000
Protein	MeCP2 (Human) recombinant protein (Abnova Corporation®): 200ng/ml, 25ng/ml, 0ng/ml in MeCP2 lysis buffer ready to use
Detection antibodies	polyclonal, anti-MeCP2, produced in rabbit (Eurogentec S.A.®): 1:2000, 1:20 000
	polyclonal, anti-MeCP2, produced in rabbit (Merck KGaA®): 1:2000, 1:20 000
SULFO-TAG™ antibody	SULFO-TAG™ labeled anti-rabbit antibody (Meso Scale Diagnostics®): 1:500

Pattern of the chessboard titration:

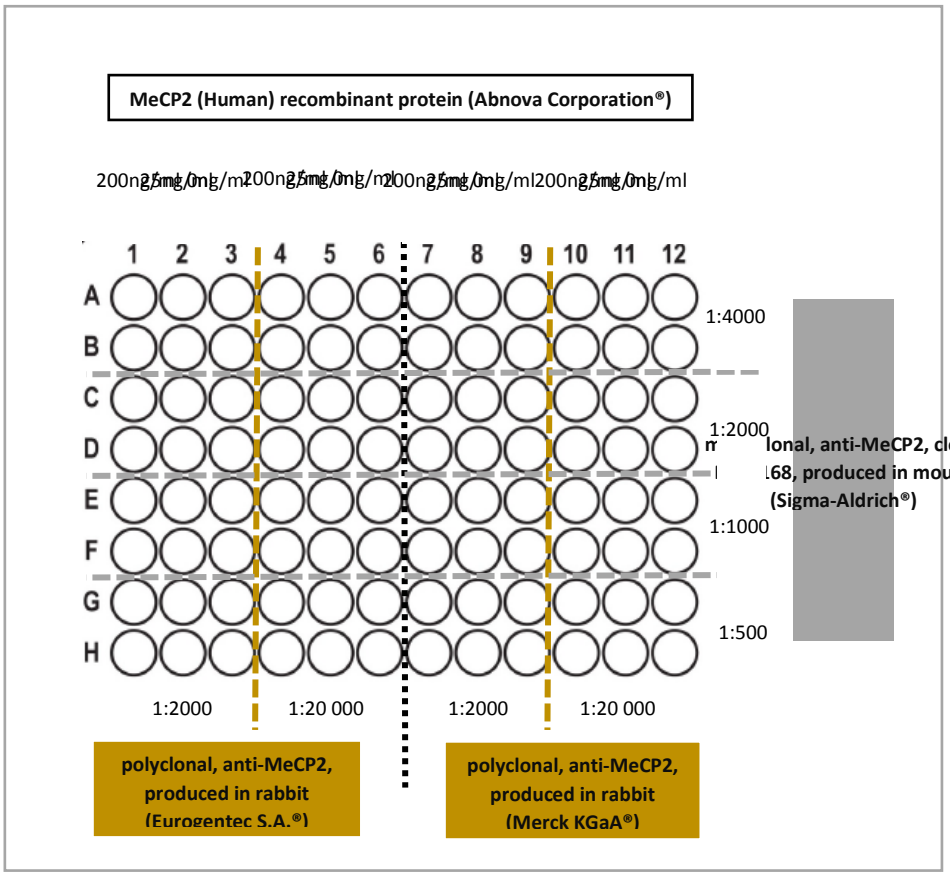

According to the signal strengths, we chose the detection antibody of Eurogentec S.A.® used on the left half of the plate.

Based on this data we calculated the signal-to-noise ratios (SNR) for the columns 1-6 (Figure 19). As the highest SNR was observed for the combination CAB (1:4000) and Eurogentec S.A.®-DAB (1:2000) at 200ng/ml, indicating the highest specificity of the tested pairs of antibodies, we used this opportunity to further increase the dilution of the capture antibody as well as decrease the interval between the detection antibody dilutions in the subsequent ECLIA.

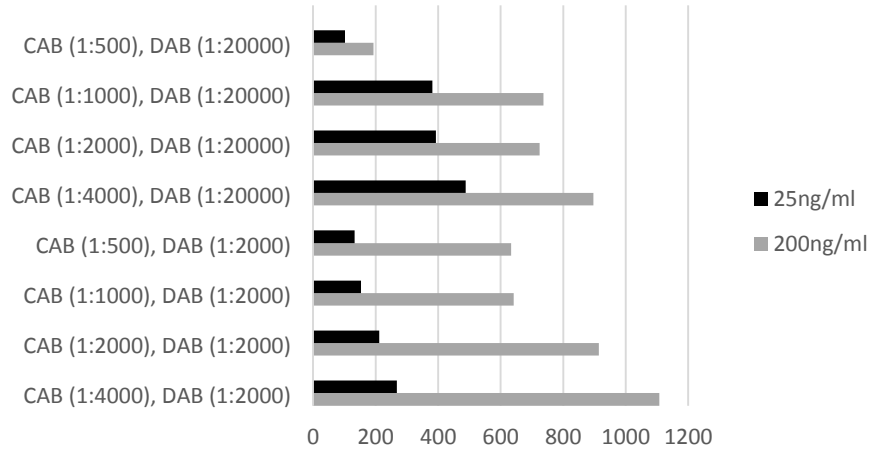

Figure 19: Signal-to-noise ratios using different combinations of capture and primary detection antibody concentrations. Calculating SNR as ratio between the signal at 25ng MeCP2 per ml or 200ng MeCP2 per ml and the blank value. Presented data are the mean of duplicates (n=2).

2. Experimental set-up:

Capture antibody	monoclonal, anti-MeCP2, clone Mec-168, produced in mouse (Sigma-Aldrich®): 1:4000, 1:6000, 1:8000, 1:10 000
Protein	MeCP2 (Human) recombinant protein (Abnova Corporation®): 200ng/ml, 25ng/ml, 0ng/ml in MeCP2 lysis buffer ready to use
Detection antibodies	polyclonal, anti-MeCP2, produced in rabbit (Eurogentec S.A.®): 1:2000, 1:5000, 1:10 000, 1:20 000
SULFO-TAG™ antibody	SULFO-TAG™ labeled anti-rabbit antibody (Meso Scale Diagnostics®): 1:500

Pattern of the chessboard titration:

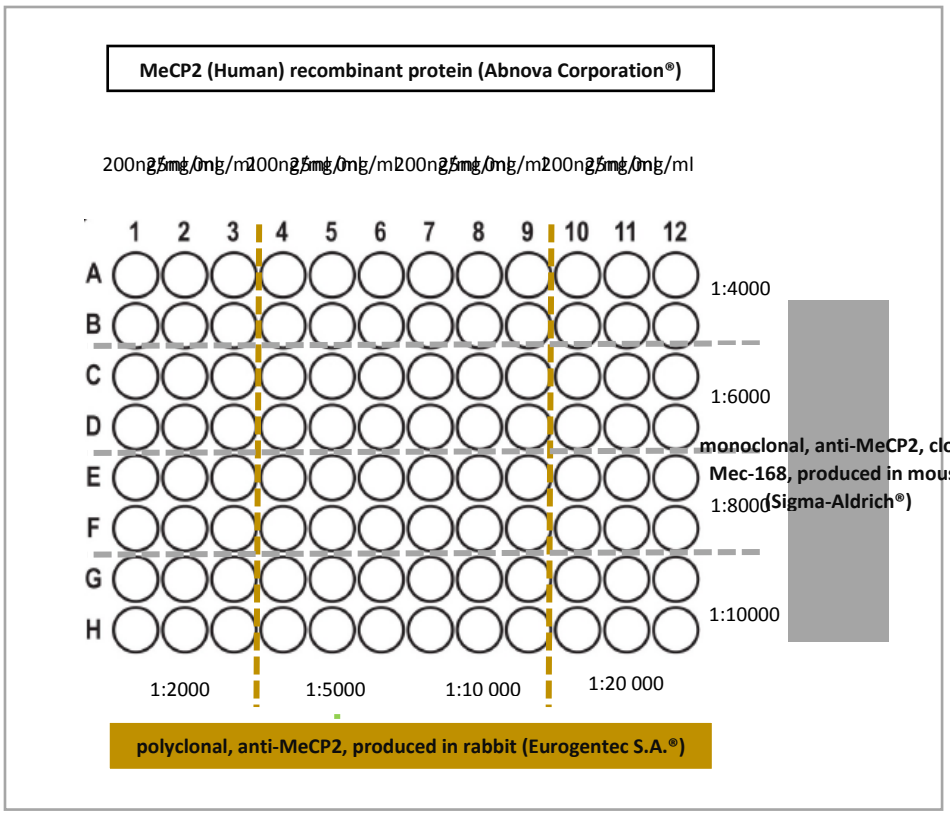

Herein, the highest specificity was achieved with the 1:6000 capture and 1:5000 detection antibody dilutions (Figure 20). From now on, we fixed the 1:6000 diluted of Eurogentec S.A.® polyclonal antibody to serve as primary detection reagent in our system. Before we finalized this decision for the capture antibody, we compared further monoclonal antibodies from different cell clones (4B6, Men-8, 1B11) with our initial one (Mec-168) to identify the highest possible SNR.

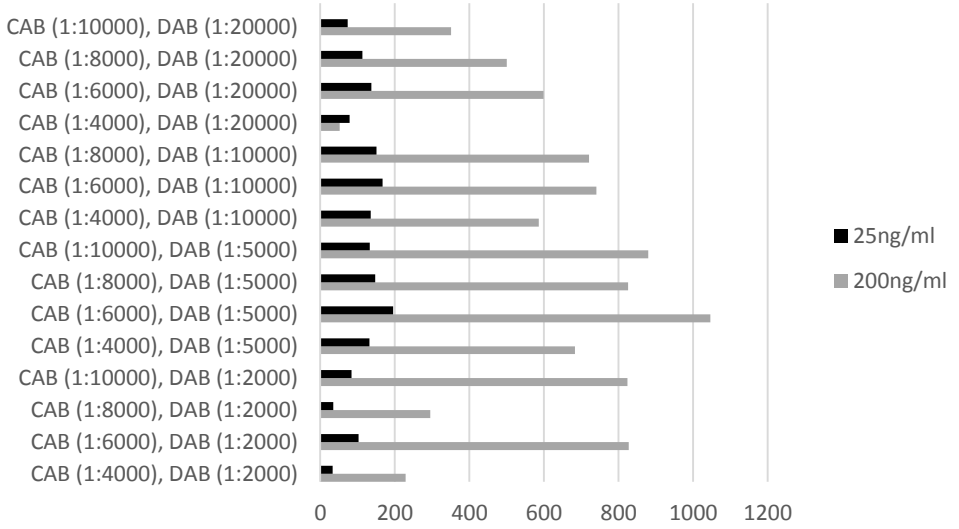

Figure 20: Signal-to-noise ratios using different combinations of capture and primary detection antibody concentrations. Calculating SNR as ratio between the signal at 25ng MeCP2 per ml or 200ng MeCP2 per ml and the blank value. Presented data are the mean of duplicates (n=2).

3. Experimental set-up:

Capture antibody	monoclonal, anti-MeCP2, clone Mec-168, produced in mouse (Sigma-Aldrich®): 1:6000 a) monoclonal, anti-MeCP2, clone 4B6, produced in mouse (Sigma-Aldrich®): 1:250, 1:500, 1:750 b) monoclonal, anti-MeCP2, clone Men-8, produced in mouse (Sigma-Aldrich®): 1:500, 1:1000, 1:2000, 1:4000 c) monoclonal, anti-MeCP2, clone 1B11, produced in mouse (Sigma-Aldrich®): 1:500, 1:1000, 1:2000, 1:4000
Protein	MeCP2 (Human) recombinant protein (Abnova Corporation®): 200ng/ml, 25ng/ml, 10ng/ml, 1.25ng/ml, 0.156ng/ml, 0ng/ml in MeCP2 lysis buffer ready to use
Detection antibodies	polyclonal, anti-MeCP2, produced in rabbit (Eurogentec S.A.®): 1:6000
SULFO-TAG™ antibody	SULFO-TAG™ labeled anti-rabbit antibody (Meso Scale Diagnostics®): 1:500

As depicted in Figure 21 a-c, the specificity of the antibodies produced in 4B6, Men-8 and 1B11 was nowhere near that produced in Mec-168, showing a significantly higher SNR.

To complete these experiments we defined the monoclonal anti-MeCP2, clone Mec-168, produced in mouse (Sigma-Aldrich®) and diluted 1:6000 to serve as capture reagent for our ECLIA.

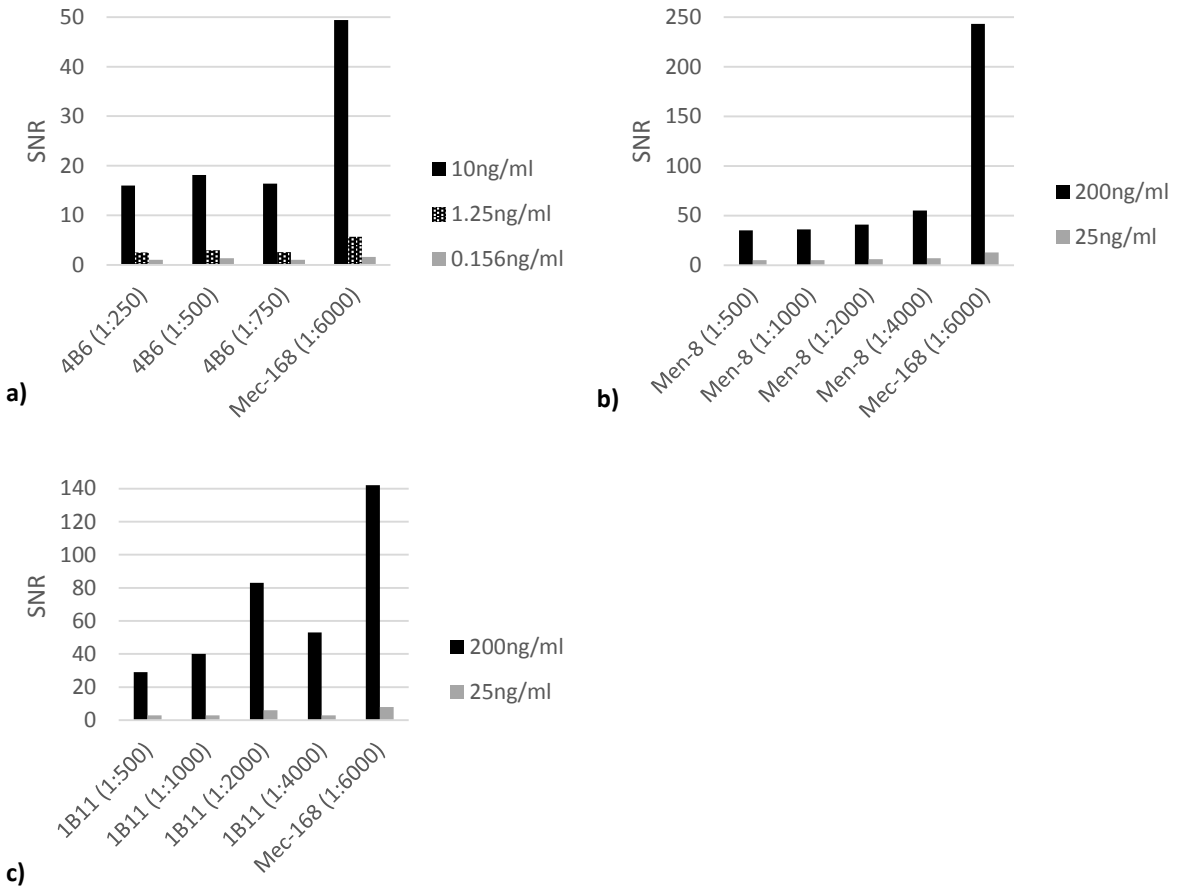

Figure 21: Signal-to-noise ratios comparing monoclonal capture antibodies from different cell clones (4B6, Men-8, 1B11, Mec-168). a): SNR of clone 4B6 vs. clone Mec-168. b): SNR of clone Men-8 vs. clone Mec-168. c): SNR of clone 1B11 vs. clone Mec-168. Using various, recommended antibody dilution ranges (4B6: 1:250-1:6000; Men-8: 1:500-1:600; 1B11:1:500-1:6000) and different MeCP2 concentrations (0.156ng/ml, 1.25ng/ml, 10ng/ml, 25ng/ml, 200ng/ml). Calculating SNR as ratio between the signal at each concentration and the blank value. Presented data are the mean of duplicates (n=2).

b) Secondary Detection Antibody

The last antibody to test was the electrochemiluminescent label conjugated secondary detection antibody of Meso Scale Diagnostics® (SULFO-TAG™ labeled anti-rabbit antibody, produced in goat). As recommended by the manufacturer, we started diluting the antibody in a 1:500 scheme. In the course of this experiment, we hypothesized again a possible specificity improvement for our system due to a lower antibody concentration. The used buffer was similar to that of the primary detection antibody (1% of blocking solution MSD Blocker A Kit in PBS).

4. Experimental set-up:

Capture antibody	monoclonal, anti-MeCP2, clone Mec-168, produced in mouse (Sigma-Aldrich®): 1:6000
Protein	MeCP2 (Human) recombinant protein (Abnova Corporation®): 200ng/ml, 25ng/ml, 0ng/ml in MeCP2 lysis buffer ready to use
Detection antibodies	polyclonal, anti-MeCP2, produced in rabbit (Eurogentec S.A.®): 1:6000
SULFO-TAG™ antibody	SULFO-TAG™ labeled anti-rabbit antibody (Meso Scale Diagnostics®): 1:500, 1:750, 1:1000

Herein, the signal strength was the highest for the 1:500 dilution but the 1:750 dilution performed better in regard to specificity (Figure 22). As a result, we steered a middle course and chose a 1:666.67 dilution to provide an easier pipetting volume.

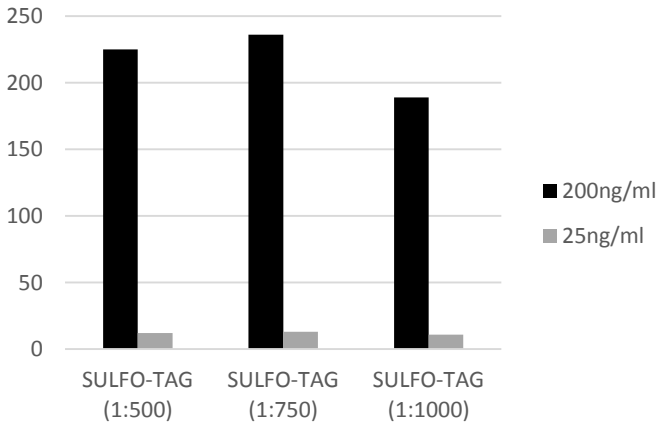

Figure 22: Signal-to-noise ratios using different MSD® SULFO-TAG™ dilutions (1:500, 1:750, 1:1000). Calculating SNR as ratio between the signal at 25ng MeCP2 per ml or 200ng MeCP2 per ml and the blank value. Presented data are the mean of duplicates (n=2).

3.1.1.2. Protein

In the course of finding the appropriate protein, serving as calibrator for our standard curve, we tested and compared several MeCP2-variants, including the standard of a commercial MeCP2-Elisa Kit and our own recombinant transactivator of transcription (TAT)-MeCP2 fusion protein. The following table gives an overview of the different tested proteins as well as their dilution ranges:

Protein	Concentration	Serial dilution range
MeCP2 (Human) recombinant protein (Abnova Corporation®)	0.09µg/µl	0.00025 - 270 ng/ml
Human MeCP2 full length protein (Abcam plc.®)	1mg/ml	0.15625 – 270 ng/ml
Methyl CpG Binding Protein 2 (MeCP2) Human Recombinant (Prospec-Tany Technogene Ltd.®)	0.45mg/ml	0.15625 – 200 ng/ml
Standard of the ELISA Kit for Methyl CpG Binding Protein 2 (Cloud-Clone-Corp.®)	20ng/ml	0.15625 – 10ng/ml
Recombinant transactivator of transcription (TAT)-MeCP2 fusion protein (lab-designed)	1.22µg/µl	0.078 – 100ng/ml

Herein, the several experimental set-ups only varied with regard to the antigens and their concentrations.

5. Experimental set-ups:

Capture antibody	monoclonal, anti-MeCP2, clone Mec-168, produced in mouse (Sigma-Aldrich®): 1:6000
Detection antibodies	polyclonal, anti-MeCP2, produced in rabbit (Eurogentec S.A.®): 1:6000
SULFO-TAG™ antibody	SULFO-TAG™ labeled anti-rabbit antibody (Meso Scale Diagnostics®): 1:666.67

First, we compared the *MeCP2 (Human) recombinant protein (Abnova Corporation®)* with the *Human MeCP2 full length protein (Abcam plc.®)* in a three-fold serial dilution, starting at 270ng/ml plus blank value (Figure 23). As the Abcam plc.® protein showed a significantly lower detection range (Calc. Low = 3.01ng/ml, Calc. High = 270ng/ml) than the Abnova Corporation® protein (Calc. Low = 0.553ng/ml, Calc. High = 270ng/ml), we conducted the same experiment again, replacing the Abcam plc.® protein by the *Methyl CpG Binding Protein 2 (MeCP2) Human Recombinant (ProSpec-Tany TechnoGene Ltd.®)* (Figure 24). Here, we started the serial dilution at 200ng/ml and got similar results as the experiment before (ProSpec®-Tany TechnoGene Ltd.®protein: Calc. Low = 1.6ng/ml, Calc. High = 200ng/ml; Abnova Corporation® protein: Calc. Low = 0.464ng/ml, Calc. High = 200ng/ml). Starting at a concentration of 10ng/ml, the two-fold diluted standard of the commercial *ELISA Kit for Methyl CpG Binding Protein 2 (Cloud-Clone-Corp.®)* completely failed to fit our system, as not even a rise in concentration was

observable (Figure 25). However, our lab-designed *recombinant transactivator of transcription (TAT)-MeCP2 fusion protein* worked properly well, actually showing a slightly broader detection range than the Abnova Corporation® protein (TAT-MeCP2: Calc. Low = 0.285ng/ml, Calc. High = 200ng/ml; Abnova Corporation® protein: Calc. Low = 0.371ng/ml, Calc. High = 200ng/ml) in a three-fold serial dilution, starting at 200ng/ml (Figure 26). Due to these findings, we determined the fusion protein to serve as calibrator in our system. Both the recombinant human MeCP2 and TAT-MeCP2 could be measured over a wide range (~0.03 - 200 ng/ml) with high accuracy (R^2=0.99).

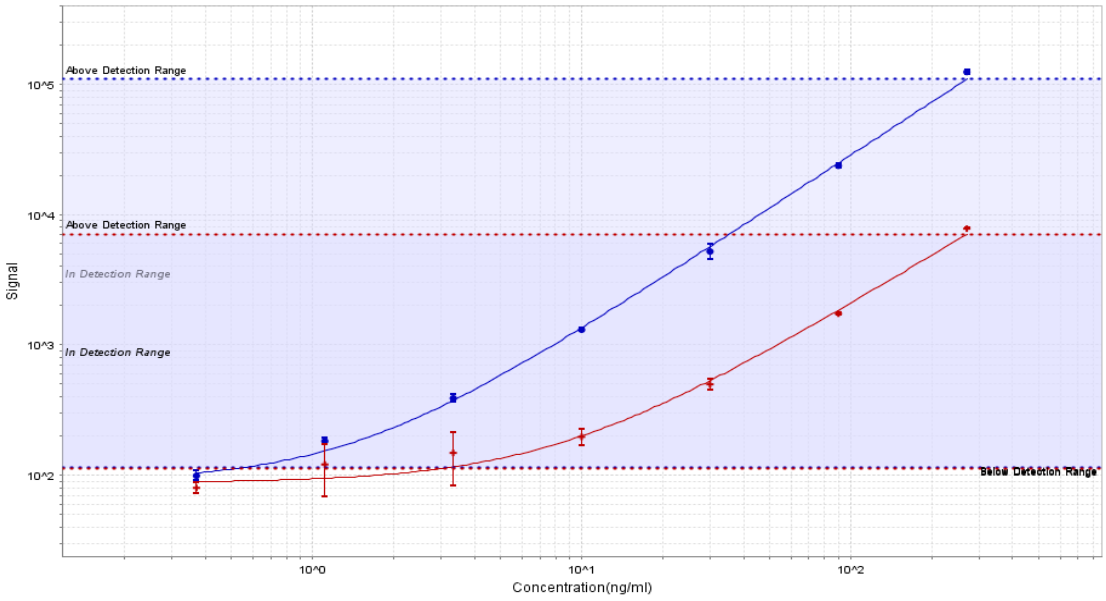

Figure 23: Standard curve of MeCP2 (human) recombinant protein (Abnova Corporation®) (blue) and human MeCP2 full length protein (Abcam plc.®) (red). Error bars show standard error at each dilution (n=2) and were partly smaller than the symbols. 5-Parameter-Logistic curves in a range from 0.6 ng/ml and 3.1 ng/ml respectively to 270 ng/ml were generated using Discovery Workbench 4.0 software from Meso Scale Discovery.

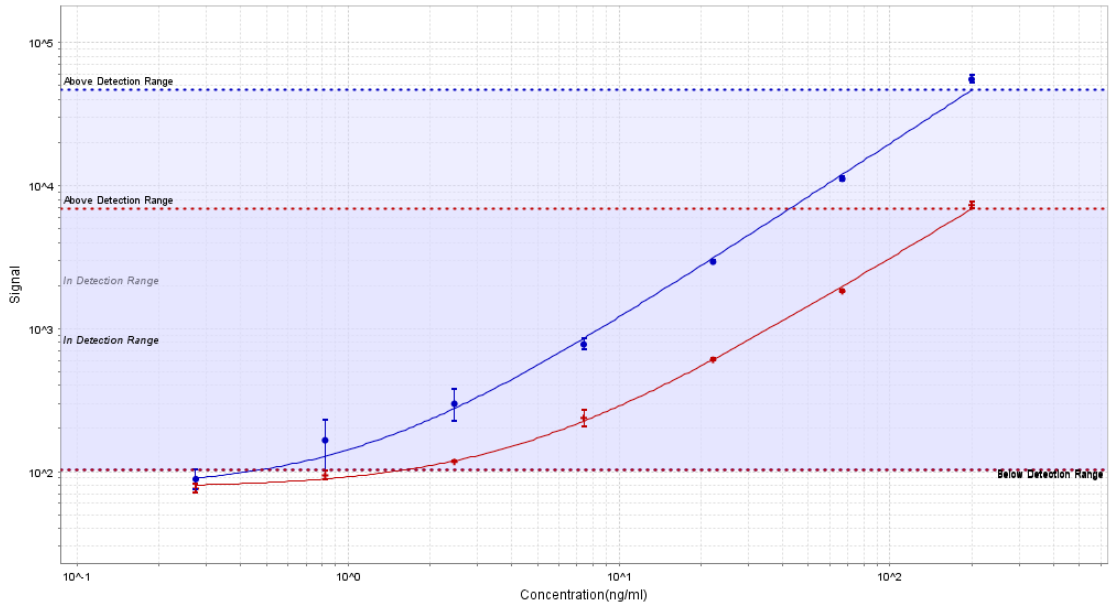

Figure 24: Standard curve of MeCP2 (human) recombinant protein (Abnova Corporation®) (blue) and Methyl CpG Binding Protein 2 (MeCP2) human recombinant (ProSpec-Tany TechnoGene Ltd.®) (red). Error bars show standard error at each dilution (n=2) and were partly smaller than the symbols. 5-Parameter-Logistic curves in a range from 0.5 ng/ml and 1.6 ng/ml respectively to 200 ng/ml were generated using Discovery Workbench 4.0 software from Meso Scale Discovery.

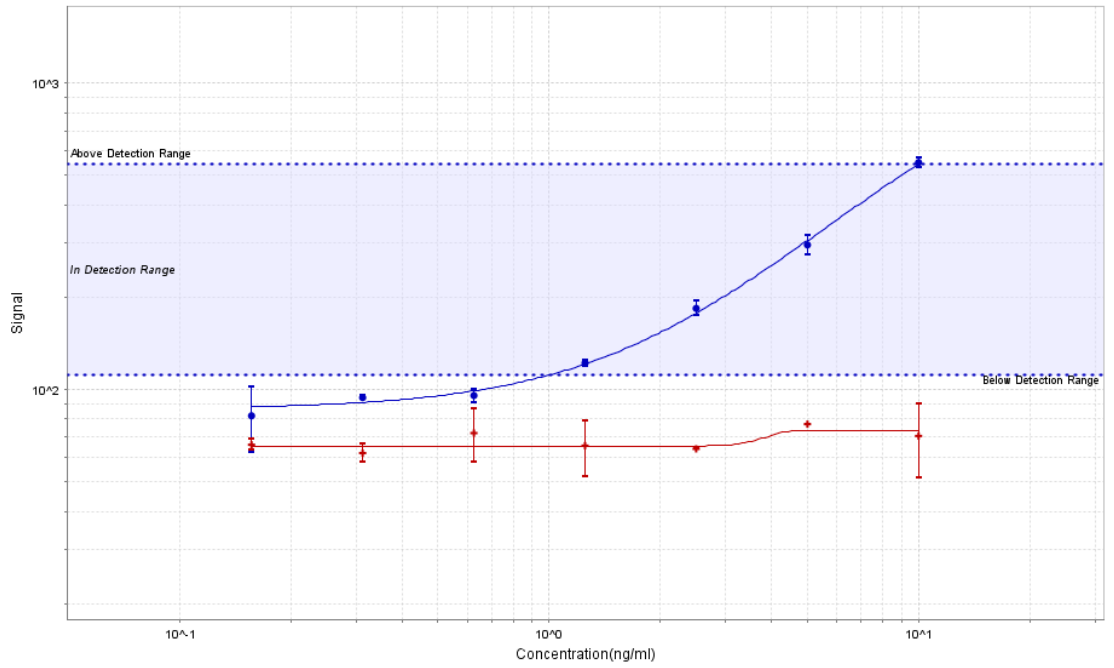

Figure 25: Standard curve of MeCP2 (human) recombinant protein (Abnova Corporation®) (blue) and the standard of the ELISA Kit for Methyl CpG Binding Protein 2 (Cloud-Clone-Corp.®) (red). Error bars show standard error at each dilution (n=2) and were partly smaller than the symbols. 5-Parameter-Logistic curves in a range from 0.99 ng/ml to 10 ng/ml (Abnova Corporation®) were generated using Discovery Workbench 4.0 software from Meso Scale Discovery.

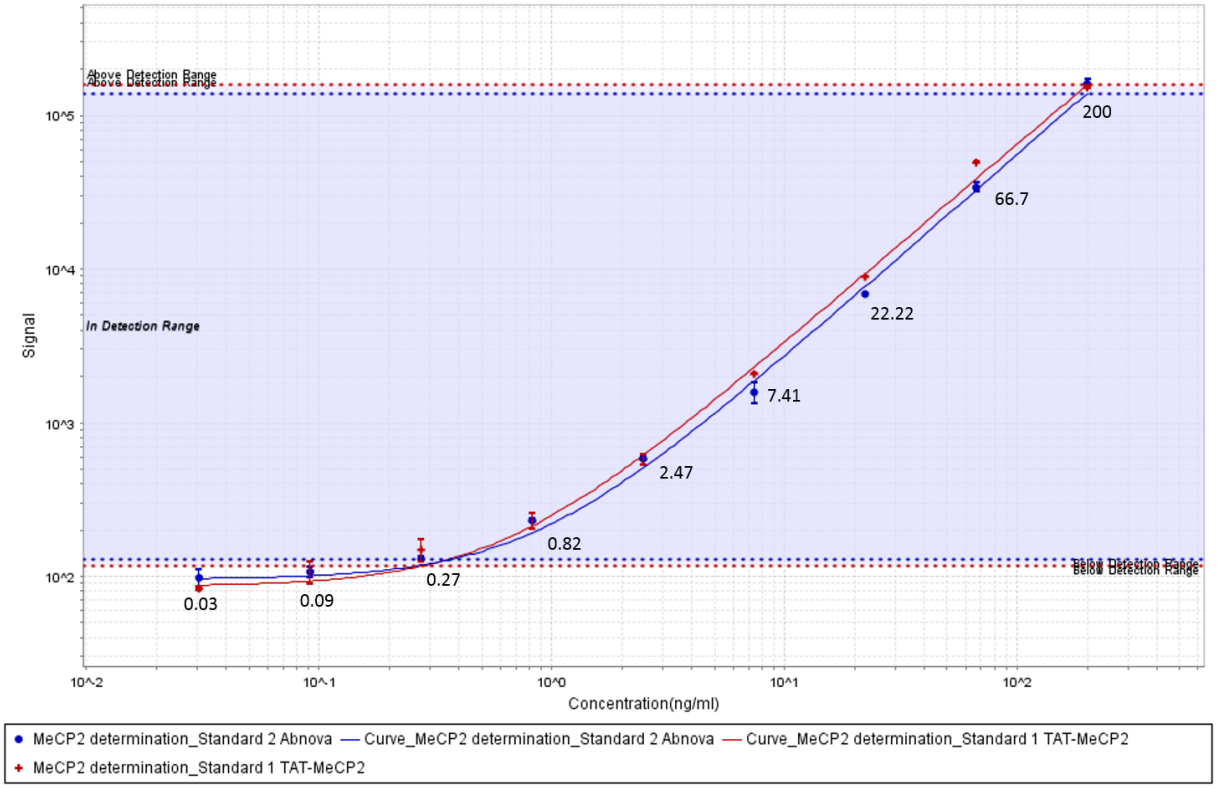

Figure 26: Standard curve of MeCP2 (human) recombinant protein (Abnova Corporation®) (blue) and recombinant transactivator of transcription (TAT)-MeCP2 fusion protein (lab-designed) (red). Error bars show standard error at each dilution (n=2) and were partly smaller than the symbols. 5-Parameter-Logistic curves in a range from 0.03 ng/ml to 200 ng/ml were generated using Discovery Workbench 4.0 software from Meso Scale Discovery.

3.1.2. Optimisation procedures

To further optimise our system we focused on three parameters possibly influencing the absolute signal, namely the shaking intensity of the 96-well plate during incubation time, the incubation time itself - especially that of the antigen - as well as the ideal blocking solution.

3.1.2.1. Shaking Intensity

Starting with the intensity with which the plates were shaken during the respective incubation times, it is known that letting the plate shake while the specific bindings occur brings two big advantages. On the one hand, shaking ensures that the dissolved analytes and antibodies are replenished to the surface of the capture antibody during the incubation time. On the other hand, shaking leads to an increase of diffusion rates resulting in better binding kinetics and therefore reducing the period of time in which the binding equilibrium is reached. That is why the shaking speed can have a significant impact on the absolute signals of the assay. To guarantee optimal reproducibility together with minimal variability, it is necessary to meet constant shaking requirements. Meso Scale Discovery® recommended in their guidelines a shaking intensity between 300rpm and 1000rpm [Meso Scale Discovery®, 2013-2014].

Subsequently, we performed an ECLIA where we increased our shaking speed from 50rpm to 850rpm and replaced the conventional, rocking motion, low-speed laboratory shaker (GFL®) with a high speed microplate shaker (Grant Instruments®).

6. Experimental set-up:

Standard	Protein	Standard serial dilution (n=8)	Shaker (intensity)
1	Human MeCP2 full length protein (Abcam plc.®)	two-fold, starting at 10ng/ml plus blank value	rocking motion, low-speed laboratory shaker (GFL®): 50rpm
2	Human MeCP2 full length protein (Abcam plc.®)	two-fold, starting at 10ng/ml plus blank value	high speed microplate shaker (Grant Instruments®): 850rpm

Other assay conditions remained as usual [CAB: monoclonal, anti-MeCP2, clone Mec-168, produced in mouse (Sigma-Aldrich®): 1:6000; DAB: polyclonal, anti-MeCP2, produced in rabbit (Eurogentec S.A.®): 1:6000; SULFO-TAG™ labeled anti-rabbit antibody (Meso Scale Diagnostics®): 1:666.67].

We concluded that increased shaking speed has an impact on the signal strength and the detection range, wherefore this new setting was incorporated in our protocol from now on

(Figure 27 a&b). Obviously, even the 850rpm result fails to meet the criteria for an optimal standard-curve, which we attributed to the antigen (Abcam plc.®) itself. As we saw in the calibrator-experiments before (3.1.1.2.), the *Human MeCP2 full length protein (Abcam plc.®)* did not pass with distinction.

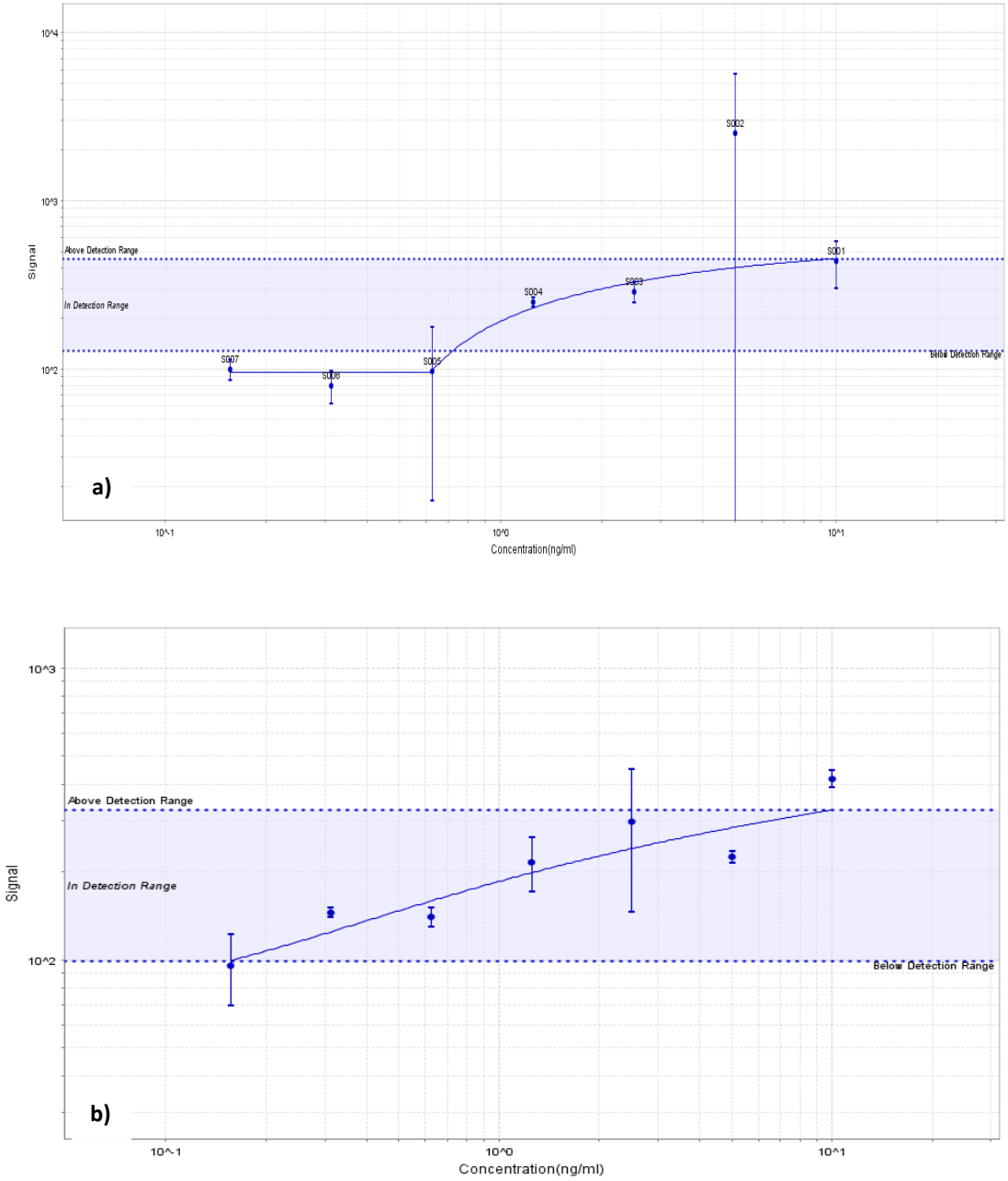

Figure 27: Standard curve of Human MeCP2 full length protein (Abcam plc.®). a): Using a conventional, rocking motion, low-speed laboratory shaker (GFL®) for incubation, shaking with 50rpm. Figure b): Using a high speed microplate shaker (Grant Instruments®) for incubation, shaking with 850rpm. Error bars show standard error at each dilution (n=2). 5-Parameter-Logistic curves in a range from 0.07 ng/ml and 0.15 ng/ml respectively to 10 ng/ml were generated using Discovery Workbench 4.0 software from Meso Scale Discovery.

3.1.2.2. Incubation Time

During our optimisation processes we focused as well on the optimum incubation time for the antigen. Generally, we intentionally chose the typical incubation format for sandwich immunoassays, where the sample or calibrator is not mixed with the detection antibody as it is the case in the simultaneous incubation format. Thus the chosen incubation format gave us a hand in preventing a possible hook-effect a priori [Meso Scale Discovery®, 2013-2014.]. Now, in the early stages of our developmental procedure, we started with a typical antigen-incubation-time of 2 hours. To test if we could further optimize our signals, we prolonged this step up to 6 hours. As we combined this trial with the investigation of the ideal SULFO-TAG™-antibody concentrations (3.1.1.1.), different dilutions of the SULFO-TAG™-antibody (1:500, 1:750, 1:1000) were used. At the first step we tested if a difference in signal levels is detectable between 2 hours and 4 hours of incubation time.

7. Experimental set-up:

Plate	Protein	Protein concentrations	Incubation time	Sulfo-tag™-ab dilution
1	MeCP2 (Human) recombinant protein (Abnova Corporation®)	200ng/ml, 25ng/ml, 0ng/ml	2 hours	1:500, 1:750
2	MeCP2 (Human) recombinant protein (Abnova Corporation®)	200ng/ml, 25ng/ml, 0ng/ml	4 hours	1:500, 1:750

De novo, the residual assay conditions remained as usual [CAB: monoclonal, anti-MeCP2, clone Mec-168, produced in mouse (Sigma-Aldrich®): 1:6000; DAB: polyclonal, anti-MeCP2, produced in rabbit (Eurogentec S.A.®): 1:6000; SULFO-TAG™ labeled anti-rabbit antibody (Meso Scale Diagnostics®): 1:666.67].

As the doubled incubation time of 4 hours showed significantly higher signals and higher signal-to-noise ratios at both protein concentrations, independent of the different SULFO-TAG™-AB dilutions (Figure 28 a-d), we extended this step up to 6 hours next.

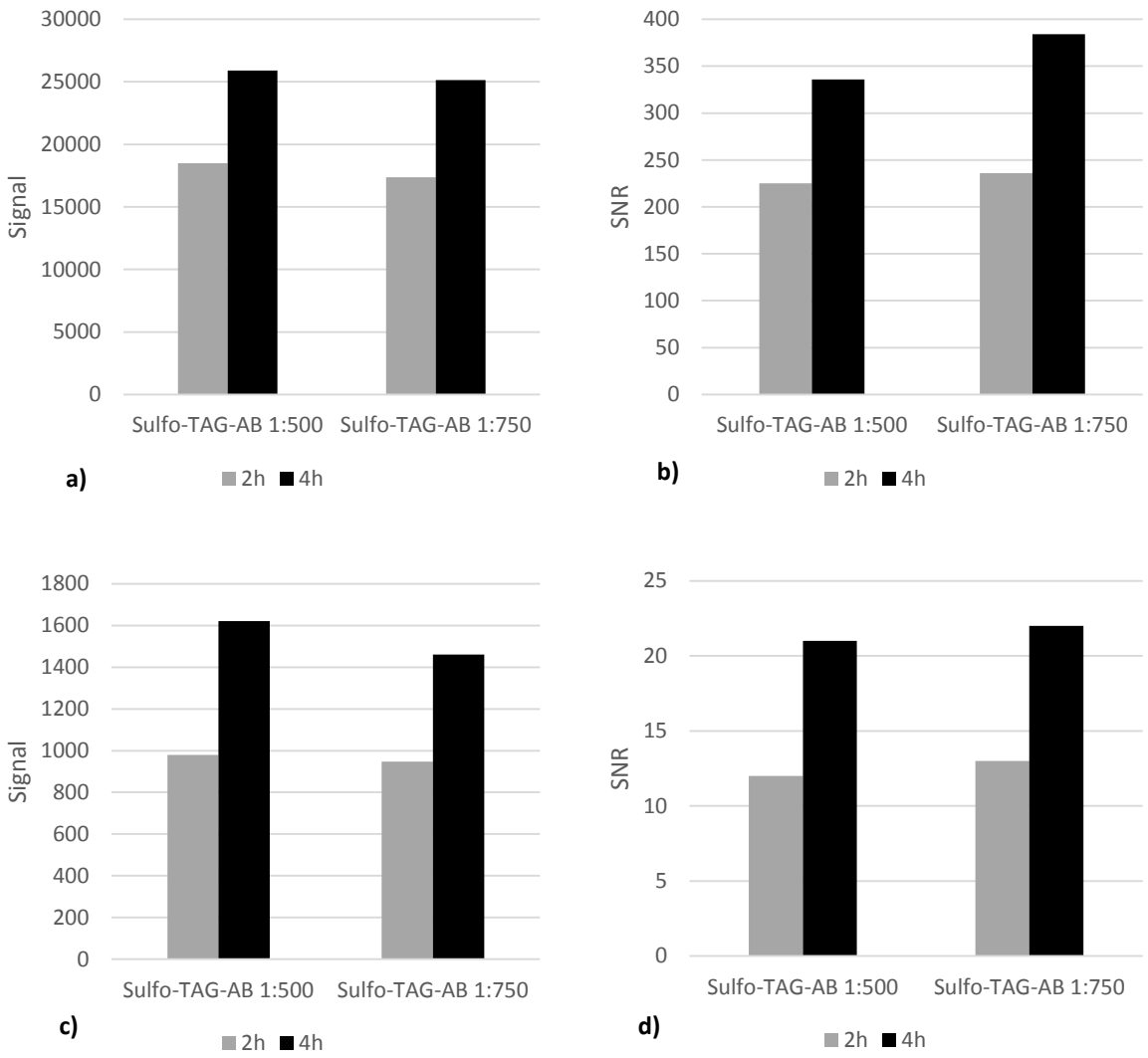

Figure 28: Signals and signal-to-noise ratios comparing 2 and 4 hours of antigen incubation time. a): Signals at 200 ng MeCP2/ml, comparing 2 and 4 hours of antigen incubation time with two different SULFO-TAG™-AB dilutions (1:500, 1:750). b): Corresponding signal-to-noise ratios at 200 ngMeCP2/ml, comparing 2 and 4 hours of antigen IT with two different SULFO-TAG™-AB dilutions (1:500, 1:750). c): Signals at 25 ngMeCP2/ml, comparing 2 and 4 hours of antigen IT with two different SULFO-TAG™-AB dilutions (1:500, 1:750). d): Corresponding signal-to-noise ratios at 25 ngMeCP2/ml, comparing 2 and 4 hours of antigen IT with two different SULFO-TAG™-AB dilutions (1:500, 1:750). Calculating SNR as ratio between the signal at each concentration and the blank value. All presented data are the mean of duplicates (n=2).

8. Experimental set-up:

Plate	Protein	Protein concentrations	Incubation time	Sulfo-tag™-ab dilution
1	MeCP2 (Human) recombinant protein (Abnova Corporation®)	200ng/ml, 25ng/ml, 0ng/ml	4 hours	1:750, 1:1000
2	MeCP2 (Human) recombinant protein (Abnova Corporation®)	200ng/ml, 25ng/ml, 0ng/ml	6 hours	1:750, 1:1000

Consequently, an additional signal as well as signal-to-noise ratio improvement could be reported, indicating a higher specificity of the 6h-variant (Figure 29 a-d). However, considering the practical feasibility of the assay within a normal working day, we chose the 4h-modification.

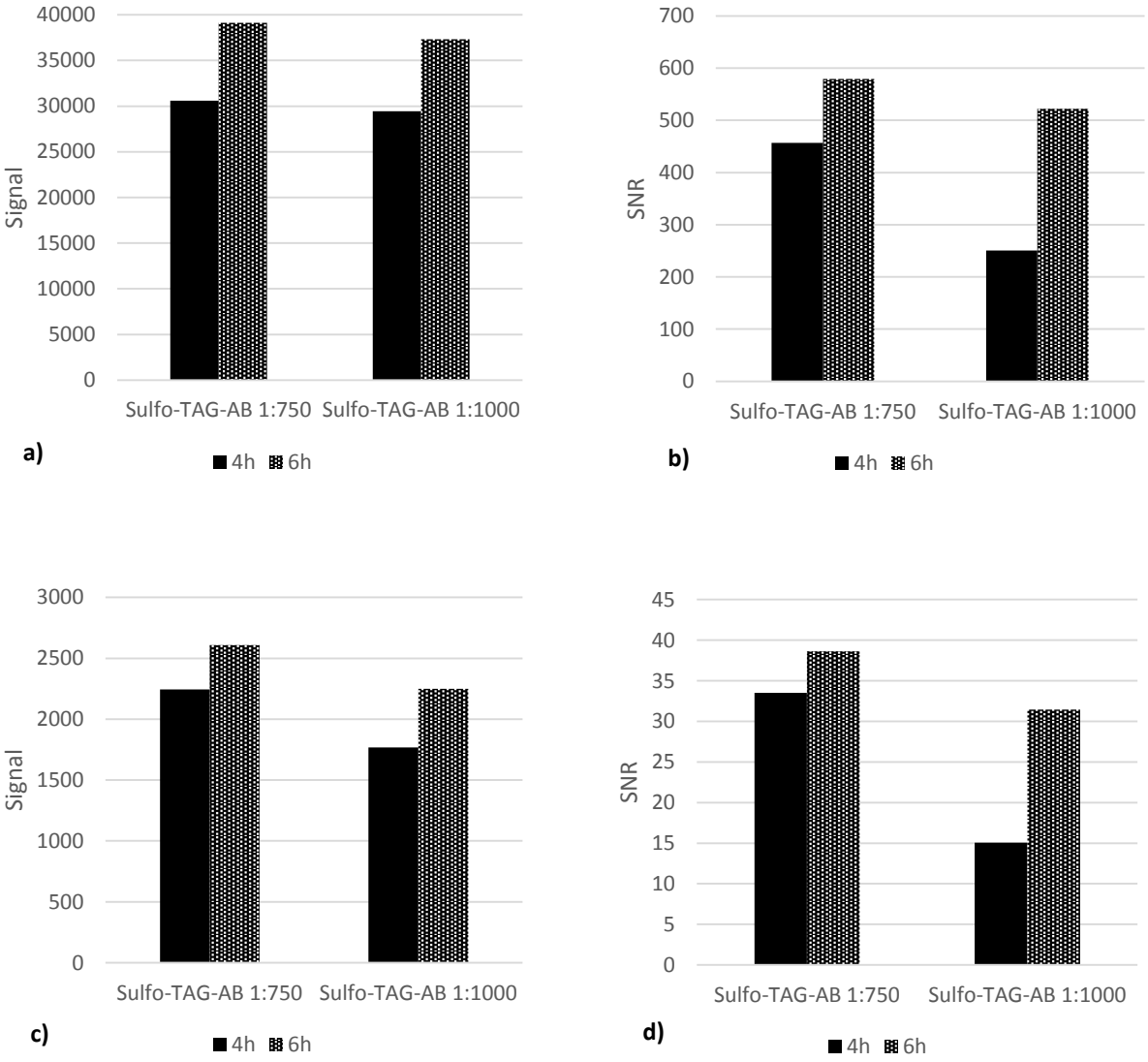

Figure 29: Signals and signal-to-noise ratios comparing 4 and 6 hours of antigen incubation time. a): Signals at 200 ngMeCP2/ml, comparing 4 and 6 hours of antigen IT with two different SULFO-TAG™-AB dilutions (1:750, 1:1000). b): Corresponding signal-to-noise ratios at 200 ngMeCP2/ml, comparing 4 and 6 hours of antigen IT with two different SULFO-TAG-™AB dilutions (1:750, 1:1000). c): Signals at 25 ngMeCP2/ml, comparing 4 and 6 hours of antigen IT with two different SULFO-TAG™-AB dilutions (1:750, 1:1000). d): Corresponding signal-to-noise ratios at 25 ngMeCP2/ml, comparing 4 and 6 hours of antigen IT with two different SULFO-TAG™-AB dilutions (1:750, 1:1000). Calculating SNR as ratio between the signal at each concentration and the blank value. All presented data are the mean of duplicates (n=2).

3.1.2.3. Blocking solutions

From day one of our research work, we used the *MSD Blocker A Kit (Meso Scale Diagnostics®)* to gain control of the non-specific protein-surface bindings. From the relatively low background signals, we concluded that this method did work well. Nevertheless, we tried out alternative blocking solutions on a final note to possibly find an even more effective option. Therefore we tested different protein blockers like dry milk-powder (Fixmilch Instant of Maresi Austria GmbH®) and casein (Blocker Casein of Thermo Fisher Scientific Inc. ®) as well as just a less expensive bovine serum albumin (BSA of Signa-Aldrich®) version. To ensure that all the remaining conditions of the ECLIA were kept constant, we used our previously defined standard curve from 3.1.1. for both of the following experiments.

9. Experimental set-up:

Standard	Protein	Standard serial dilution (n=8)	Blocking solution	Detection ab dilution (1:6000)	Sulfo-tag™-ab dilution (1:666.67)
1	TAT-MeCP2	three-fold, starting at 200ng/ml plus blank value	3% MSD Blocker A Kit (Meso Scale Diagnostics®) in PBS	1% MSD Blocker A Kit (Meso Scale Diagnostics®) in PBS	1% MSD Blocker A Kit (Meso Scale Diagnostics®) in PBS
2	TAT-MeCP2	three-fold, starting at 200ng/ml plus blank value	1% Blocker Casein (Thermo Fisher Scientific Inc. ®) in PBS	0.1% Blocker Casein (Thermo Fisher Scientific Inc. ®) in PBS	0.1% Blocker Casein (Thermo Fisher Scientific Inc. ®) in PBS
3	TAT-MeCP2	three-fold, starting at 200ng/ml plus blank value	1% Fixmilch Instant (Maresi Austria GmbH®) in PBS	0.1% Fixmilch Instant (Maresi Austria GmbH®) in PBS	0.1% Fixmilch Instant (Maresi Austria GmbH®) in PBS

As depicted below (Figure 30), Standard 1 (blue curve) – using our classic blocking solution - showed the most satisfying outcomes with the highest signals and the broadest detection range, covering almost all concentrations.

To further investigate if a less expensive BSA alternative would have the same effect on these non-specific interactions as the MDS® Blocker A Kit, we compared them in a separate experiment.

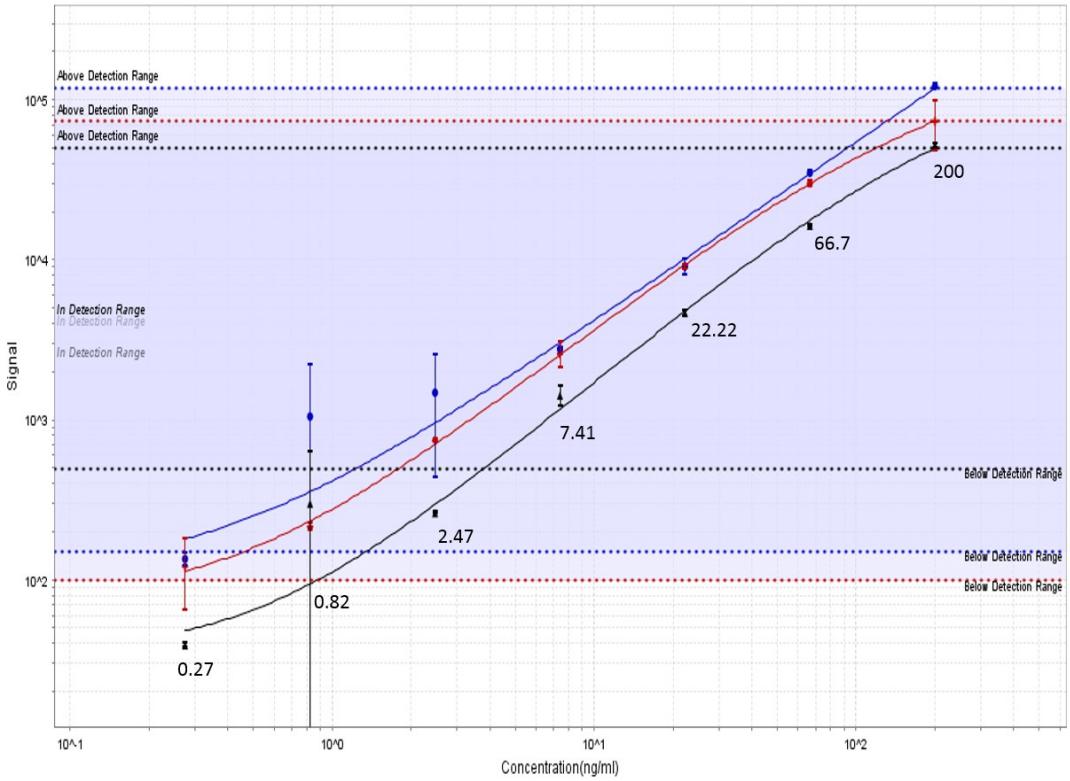

Figure 30: Standard curves of TAT-MeCP2 using different blocking solutions: MSD Blocker A Kit (Meso Scale Diagnostics®) (blue), Fixmilch Instant (Maresi Austria GmbH®) (red), Blocker Casein (Thermo Fisher Scientific Inc. ®) (black). Error bars show standard error at each dilution (n=2) and were partly smaller than the symbols. 5-Parameter-Logistic curves in a range from 3.8 ng/ml to 200 ng/ml were generated using Discovery Workbench 4.0 software from Meso Scale Discovery.

10. Experimental set-up:

Standard	Protein	Standard serial dilution (n=8)	Blocking solution	Detection ab dilution (1:6000)	Sulfo-tag™-ab dilution (1:666.67)
1	TAT-MeCP2	three-fold, starting at 200ng/ml plus blank value	3% BSA (Sigma-Aldrich®) in PBS	1% BSA (Sigma-Aldrich®) in PBS	1% BSA (Sigma-Aldrich®) in PBS
2	TAT-MeCP2	three-fold, starting at 200ng/ml plus blank value	3% MSD Blocker A Kit (Meso Scale Diagnostics®) in PBS	1% MSD Blocker A Kit (Meso Scale Diagnostics®) in PBS	1% MSD Blocker A Kit (Meso Scale Diagnostics®) in PBS

Herein, a huge difference was notable between the two different BSA blocking solutions (Figure 31 a&b). Whereas the detection limits for Standard 1 (BSA of Sigma-Aldrich®) ranged from 2.31ng/ml to 200ng/ml, the ones of Standard 2 (BSA of Meso Scale Diagnostics®) were more expanded, compromising 0.362ng/ml and 200ng/ml. Furthermore, the concentration CVs were less than 20% for Standard 2 - indicating good precision and acceptable experimental errors – whereas Standard 1 showed concentration CVs over 60%. Insofar as the recovery rate is concerned, again Standard 2 performed better than Standard 1, leading to a superior

dilution linearity. Most importantly, the reduction of the background interference was much more effective with MSD® BSA than with Sigma-Aldrich® BSA (mean signals at 0ng/ml: 76 vs. 365), resulting in higher different signal-to-noise-ratios of 901.4 (Standard 2) and 150.8 (Standard 1) for the highest standard concentration (200ng/ml).

Due to these results, we retained our original blocking solution *MSD Blocker A Kit (Meso Scale Diagnostics®)* and fixed it in our final protocol.

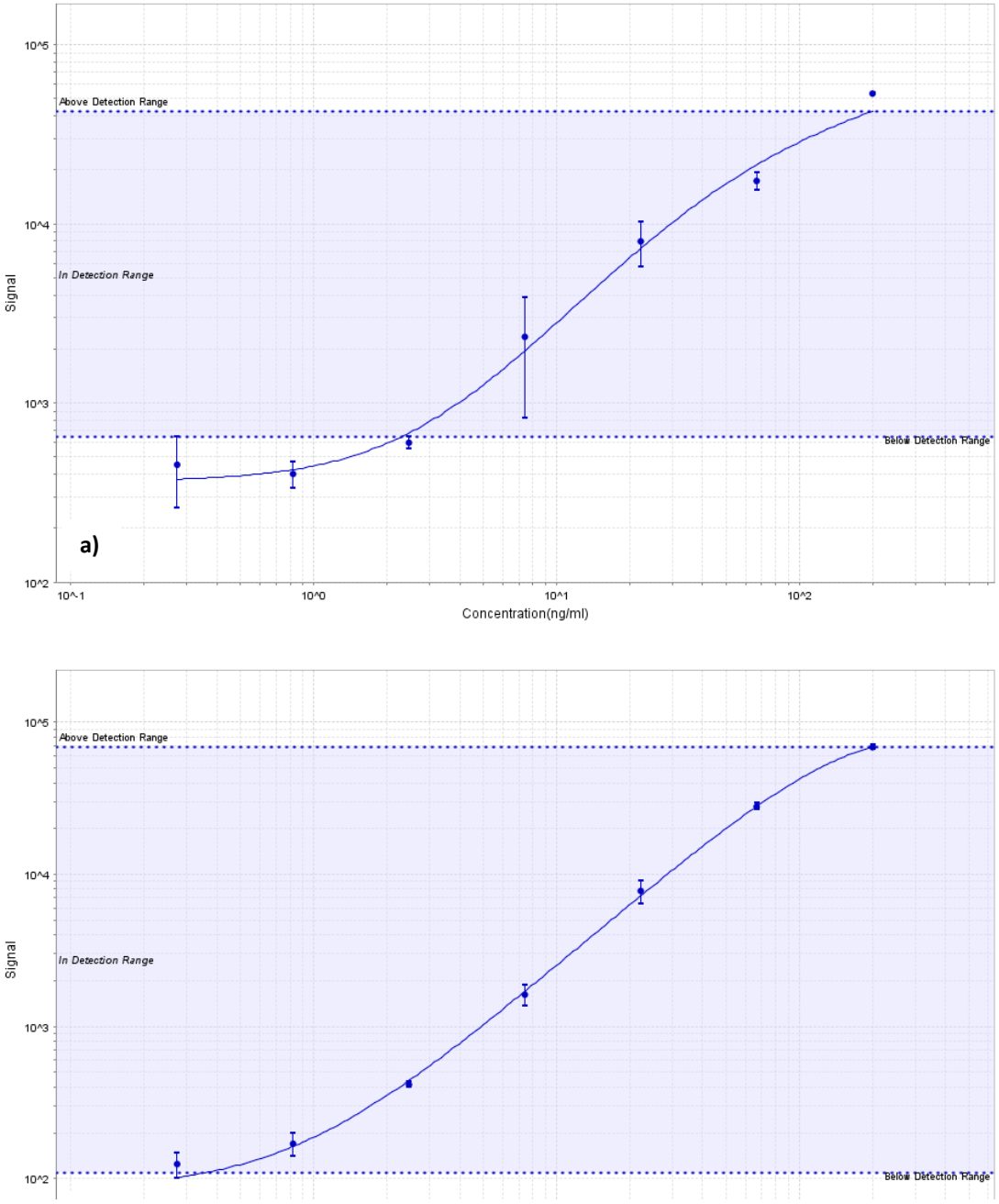

Figure 31: Standard curves of TAT-MeCP2 using different blocking solutions. a): Standard 1, using BSA of Sigma-Aldrich®. b): Standard 2, using MSD Blocker A Kit of Meso Scale Diagnostics®. Error bars show standard error at each dilution (n=2) and were partly smaller than the symbols. 5-Parameter-Logistic curves in a range from 2.31 ng/ml to 200 ng/ml (Standard 1) respectively from 0.36 ng/ml to 200 ng/ml (Standard 2) were generated using Discovery Workbench 4.0 software from Meso Scale Discovery.

3.1.3. Final protocol

To sum up the results of our developmental research, we set up a final protocol to work with, before validating the assay as well as starting the measurements of MeCP2 in different sample types.

<table>
<tr><td>Coat Plate</td><td>Capture antibody: monoclonal, anti-MeCP2, clone Mec-168, produced in mouse (Sigma-Aldrich®)</td></tr>
<tr><td></td><td>Dilution: 1:6000 in 1x PBS (pH=7.4)</td></tr>
<tr><td></td><td>Coating volume: 25µl/well, solution coating method, change pipette tips after every well</td></tr>
<tr><td></td><td>Tap plate gently</td></tr>
<tr><td></td><td>Incubation: seal the plate and incubate overnight (4°C)</td></tr>
<tr><td>Prepare Washing and Blocking Solution</td><td>Washing solution: 1x PBS (pH=7.4) + 0.05% Tween 20</td></tr>
<tr><td></td><td>Blocking solution: 3% MSD Blocker A Kit (Meso Scale Diagnostics®) in 1x PBS (pH=7.4)</td></tr>
<tr><td>Block</td><td>Remove liquid from the wells (absorbent paper)</td></tr>
<tr><td></td><td>Pipetting Volume: 125µl/well, solution coating method with dead volume, multichannel-pipette</td></tr>
<tr><td></td><td>Tap plate gently</td></tr>
<tr><td></td><td>Incubation: seal the plate, incubate for 1.5 hours on a high-speed microplate shaker (Grant Instruments®) at 850rpm, room temperature</td></tr>
<tr><td>Prepare Standard Solution</td><td>Standard stock solution: TAT-MeCP2 fusion protein [200ng/ml]</td></tr>
<tr><td></td><td>Serial dilution: 1:3 with 1x PBS (pH= 7.4)
<table>
<tr><th colspan="2">Protein concentration [ng/ml]</th><th>MeCP2 (200ng/ml)</th><th>PBS (1x)</th></tr>
<tr><td>Standard 1</td><td>200</td><td>180 µl</td><td>0 µl</td></tr>
<tr><td>Standard 2</td><td>66.67</td><td>60 µl</td><td>120 µl</td></tr>
<tr><td>Standard 3</td><td>22.22</td><td>60 µl</td><td>120 µl</td></tr>
<tr><td>Standard 4</td><td>7.41</td><td>60 µl</td><td>120 µl</td></tr>
<tr><td>Standard 5</td><td>2.47</td><td>60 µl</td><td>120 µl</td></tr>
<tr><td>Standard 6</td><td>0.82</td><td>60 µl</td><td>120 µl</td></tr>
<tr><td>Standard 7</td><td>0.27</td><td>60 µl</td><td>120 µl</td></tr>
<tr><td>Standard 8</td><td>0</td><td>0 µl</td><td>120 µl</td></tr>
</table></td></tr>
<tr><td>Prepare Samples</td><td>Samples: different sample types (cell lines & mouse tissues)</td></tr>
<tr><td></td><td>Lysis: nuclear or total protein extraction (2.2.3.)</td></tr>
<tr><td></td><td>Protein determination: according to Bradford (2.2.2.)</td></tr>
<tr><td></td><td>Adjustment of required protein concentration: dilute in respective lysis buffers (2.2.3.)</td></tr>
</table>

Wash	Remove liquid from the wells (absorbent paper)
	Washing volume: 150µl/well, solution coating method with dead volume, multichannel-pipette
	Frequency: 3 times
Add Standard & Sample	Coating volume: 27µl/well, spot coating method, changing pipette tips after every well
	Tap plate gently
	Incubation: seal the plate, incubate for 4 hours on a high-speed microplate shaker (Grant Instruments®) at 850rpm, room temperature
	Remove liquid from the wells (absorbent paper)
Wash	Washing volume: 150µl/well, solution coating method with dead volume, multichannel-pipette
	Frequency: 3 times
	Primary detection antibody: polyclonal, anti-MeCP2, produced in rabbit (Eurogentec S.A.®)
Add Primary Detection Reagent	Dilution: 1:6000 in 1% MSD Blocker A Kit (Meso Scale Diagnostics®) in 1x PBS (pH=7.4)
	Coating volume: 25µl/well, solution coating method with dead volume, multichannel-pipette
	Tap plate gently
	Incubation: seal the plate, incubate for 1 hours on a high-speed microplate shaker (Grant Instruments®) at 850rpm, room temperature
	Remove liquid from the wells (absorbent paper)
Wash	Washing volume: 150µl/well, solution coating method with dead volume, multichannel-pipette
	Frequency: 3 times
	Secondary detection antibody: SULFO-TAG™ labeled anti-rabbit antibody, produced in goat (Meso Scale Diagnostics®)
Add Secondary Detection Reagent	Dilution: 1:666.67 in 1% MSD Blocker A Kit (Meso Scale Diagnostics®) in 1x PBS (pH=7.4)
	Coating volume: 25µl/well, solution coating method with dead volume, multichannel-pipette
	Tap plate gently
	Incubation: seal the plate, incubate for 1 hours on a high-speed microplate shaker (Grant Instruments®) at 850rpm, room temperature, avoid sun exposure
	Remove liquid from the wells (absorbent paper)
Wash	Washing volume: 150µl/well, solution coating method with dead volume, multichannel-pipette
	Frequency: 3 times
	Reading buffer: Read Buffer T (4x) With Surfactant (Meso Scale Diagnostics®)

Add Read Buffer	Dilution: 1:4 in ddH_2O
	Coating volume: 150µl/well, solution coating method with dead volume, multichannel-pipette
Measure	Instrument: MSD SECTOR® Imager 2400 (Meso Scale Diagnostics®), measure quickly

3.2. Validation of the assay

Validating the assay is essential if an appropriate establishment of the method is to be achieved. Herein, parameters like the sensitivity, accuracy and precision, matrix effects, specificity as well as assay robustness and stability have to be evaluated. As depicted in the previous chapter (Figure 30), our assays' sensitivity for MeCP2 was about 30 pg/ml. To determine our assays' accuracy and precision we conducted an inter- as well as intra-assay, measuring different samples on three ensuing days in a triplicate mode. In doing so, we obtained an intraday precision of coefficient of variation (CV) ≤1.21% as well as an interday precision of CV ≤12.50% (Table 5).

	ng MeCP2/µg Protein						
	Well 1	Well 2	Well 3	Mean	SD	SEM	%CV
Intra-assay	0.49	0.46	0.47	0.47	0.01	0.01	**3.14**
Inter-assay				0.48	0.06	0.02	**12.5**

Table 5: Intra-assay and inter-assay precision of MeCP2 electrochemiluminescence immunoassay. Intra-assay precision (n=3 wells per day) and inter-assay precision (n=3 separate days) of different isolated lysates from wild-type mouse brain. SD, standard deviation; SEM, standard error mean; CV, coefficient of variation.

3.3. Measurements of MeCP2 in different sample types

3.3.1. Sample type: cells lines

3.3.1.1. Testing different lysis protocols

In the course of measuring MeCP2 in different cell lines, we tested various protocols for preparing cell lysates – total protein extractions (Protocol for cell lysis using MeCP2 complete lysis buffer, Protocol for cell lysates of LifeSpan BioScience®) as well as a nuclear protein extraction method (Nuclear protein extraction without the use of detergent from adherent cells of Sigma-Aldrich®). Keeping the ECLIA-protocol as described in 3.1.3., we determined the MeCP2 concentration in human wild-type fibroblasts, using these three different lysis strategies. Comparing the protocols, the highest protein concentration was observed by nuclear protein extraction (Figure 32), reflecting the localisation of MeCP2 in the nucleus.

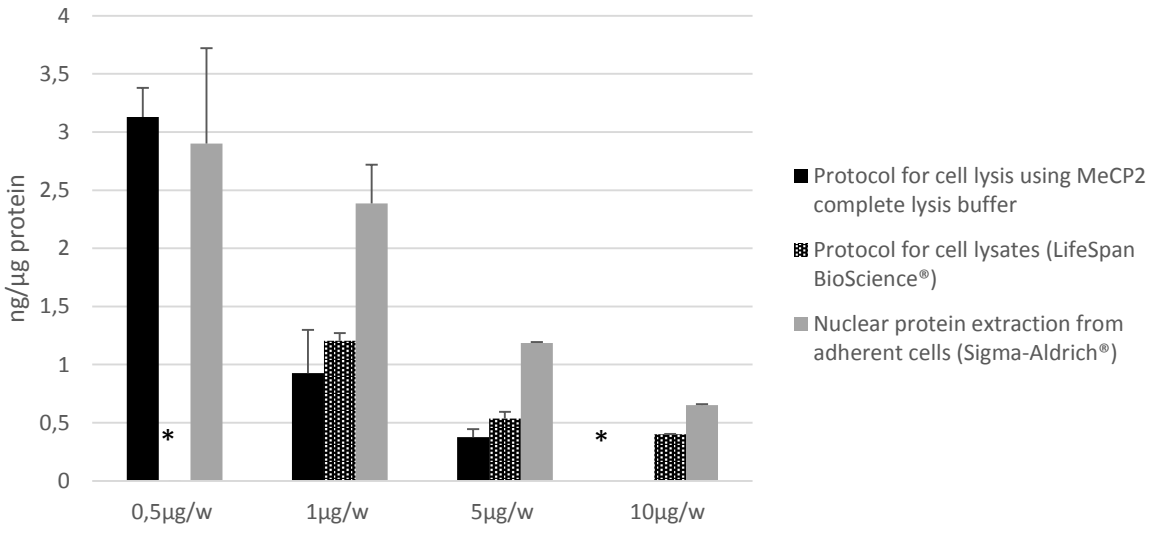

Figure 32: MeCP2 protein levels in human wild-type fibroblasts after different cell lysis protocols. Used protein concentrations were ranging from 0.5µg protein/well to 10µg protein/well. Error bars show standard error at each concentration (n=2) and were partly too small to be visible. *****Missing columns indicate that there was no signal available.

3.3.1.2. Different cell lines and their calculated working ranges

Defining the nuclear protein extraction as our standard lysis protocol, we measured MeCP2 in different cell lines next, including the calculation of respective working ranges.

Human fibroblasts

For the first experiments we examined human wild-type fibroblasts as well as fibroblasts from Rett patients, a widely used in-vitro model for investigating the underlying mechanisms of the disease. Starting with human wild-type fibroblasts we could measure an increase in MeCP2 concentration between 0.5µg protein/well and 10µg protein/well with our assay. In this range the assay remained sensitive and in a relatively linear range (Figure 33). Comparing wild-type fibroblasts with Rett patients' fibroblasts, we could further show a marked difference in MeCP2 concentration, as we found marginal MeCP2 levels in the patients' fibroblasts (Figure 34).

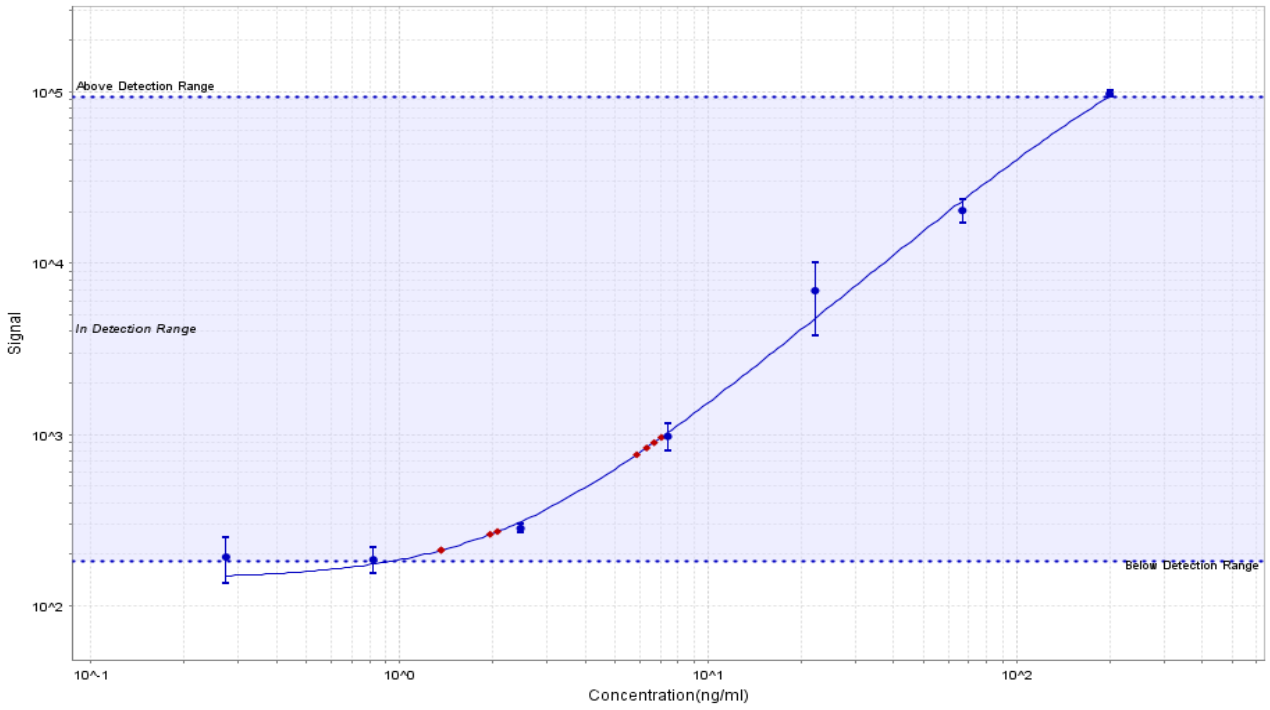

Figure 33: Standard curve of TAT-MeCP2 (blue) and the measured MeCP2 concentration in wild-type fibroblasts (red) using nuclear protein extraction for cell lysis, ranging from 0.5µg/well to 10µg/well. Error bars show standard error at each dilution (n=2) and were partly smaller than the symbols. 5-Parameter-Logistic curves in a range from 0.48 ng/ml to 200 ng/ml were generated using Discovery Workbench 4.0 software from Meso Scale Discovery.

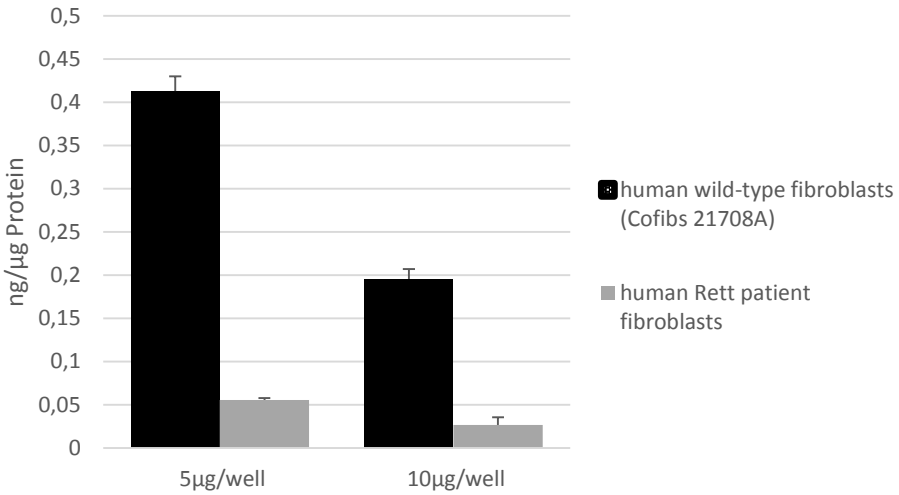

Figure 34: MeCP2 protein levels in human wild-type fibroblasts and Rett patient fibroblasts using nuclear protein extraction for cell lysis. Error bars show standard error at each concentration (n=2) and were partly too small to be visible.

Human hepatocellular carcinoma cells

Further on, we investigated the human hepatocellular carcinoma cell line HepG2. Herein, we obtained two noteworthy results. On the one hand we could show that our antibodies were able to detect endogenous MeCP2, by the use of Western Blot (Figure 35) and on the other hand we could measure an increase in MeCP2 concentration in a sample range of 1-40µg protein/well with our ECLIA (Figure 36).

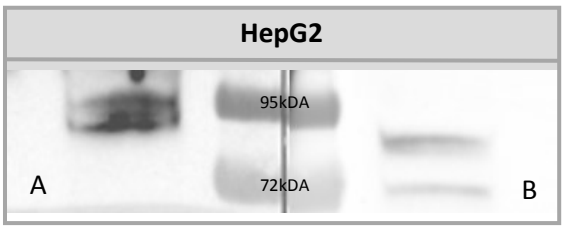

Figure 35: Specificity of the antibodies. Western Blot using cell extracts from HepG2 cells. 50µg of protein were loaded onto a 10% SDS-gel using the polyclonal primary detection antibody (Eurogentec S.A.®) on the left side (A) as well as the monoclonal capture antibody, clone Mec-168 (Sigma-Aldrich®) on the right side (B).

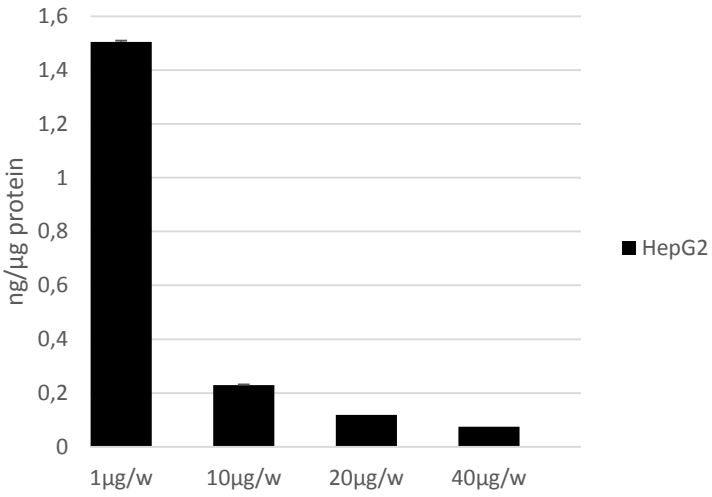

Figure 36: MeCP2 protein levels in human hepatocellular carcinoma cell line HepG2 using nuclear protein extraction for cell lysis. Error bars show standard error at each concentration (n=2) and were partly too small to be visible.

Human Schwann cells

For human Schwann cells, which were kindly provided for our research by Prof. Ahmet Höke of the John Hopkins University in Baltimore, the calculated concentration of MeCP2 at 1µg protein per well was about 0.7ng MeCP2 per µg protein (Figure 37), not even half as much as we found in HepG2 cells (1.5ng MeCP2 per µg protein) and just less than 30% of the concentration found in human wild-type fibroblasts (2.4ng MeCP2 per µg protein).

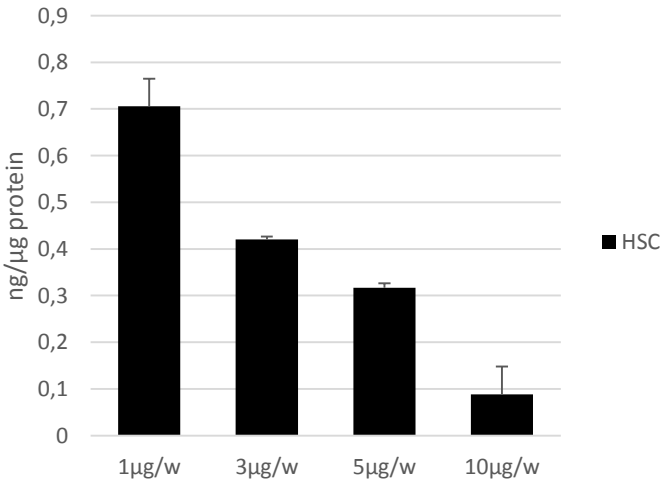

Figure 37: MeCP2 protein levels in human Schwann cells using nuclear protein extraction for cell lysis. Error bars show standard error at each concentration (n=2) and were partly too small to be visible.

3.3.2. Sample type: tissues

3.3.1.1. Testing different lysis protocols

Even in terms of measuring MeCP2 in various tissues, testing different lysis protocols was the entering wedge entering wedge. Herein, we compared a total protein extraction (Protocol for tissue homogenates of LifeSpan BioScience®) with a nuclear protein extraction (Nuclear protein extraction without the use of detergent from tissues of Sigma-Aldrich®), using three different wild-type mouse organs (heart, kidney and brain) in a range of 1-80µg protein per well (Figure 38). In doing so, the experiment yielded the expected results as we could again achieve higher MeCP2 concentrations with the nuclear extraction method. This effect was and well-marked in the wild-type mouse's brain, where we could not even register a signal in the wells with low protein concentrations, using the total protein extraction.

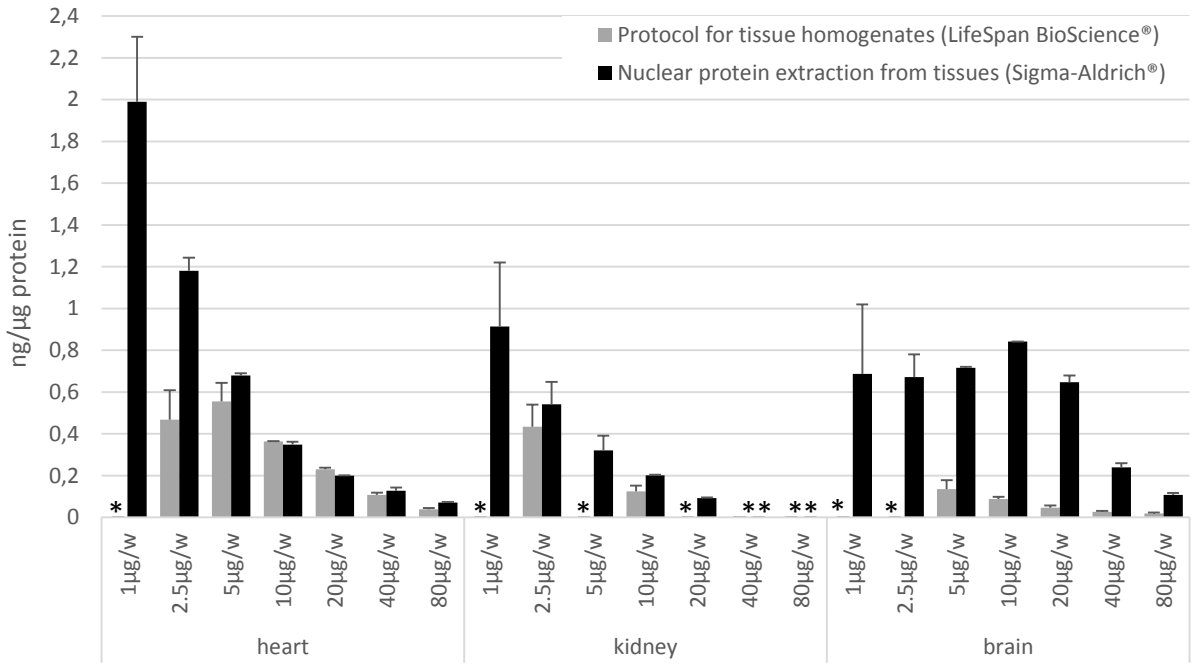

Figure 38: MeCP2 protein levels in various mouse organs after different tissue lysis protocols. Used protein concentrations ranged from 1µg protein per well to 80µg protein per well. Error bars show standard error at each concentration (n=2) and were partly too small to be visible. *Missing columns indicate that there was no signal available.

5.2.1.2. Tested mouse tissues and their calculated working ranges

From here on, we used the previously tested nuclear protein extraction as the standard method for preparing our tissue lysates and conducted MeCP2 determinations in different mouse organs next. Pursuing the target of calculating respective working ranges with our MeCP2-assay, we used protein concentrations from 1-80µg protein per well for each tested organ. Herein, we observed differences concerning the MeCP2 concentration in diverse organs as well as in their associated working ranges (Figure 39 a-e). Commonly in all organs, the highest signals, i.e. the highest MeCP2 concentrations, were achieved using a protein concentration of 1µg per well. However, the liver and especially the spleen just showed marginal MeCP2 concentrations or even no registered signal. Considering the high standard deviation at 1µg per well in the liver, the MeCP2 expression in these two organs remained questionable. Nevertheless, we were able to detect endogenous MeCP2 in heart, kidney and brain tissue. Herein, we achieved the best results – even if not the highest MeCP2 concentrations - in brain tissue as our assay remained sensitive and in a linear range from 1-20µg protein of brain cell lysate per well.

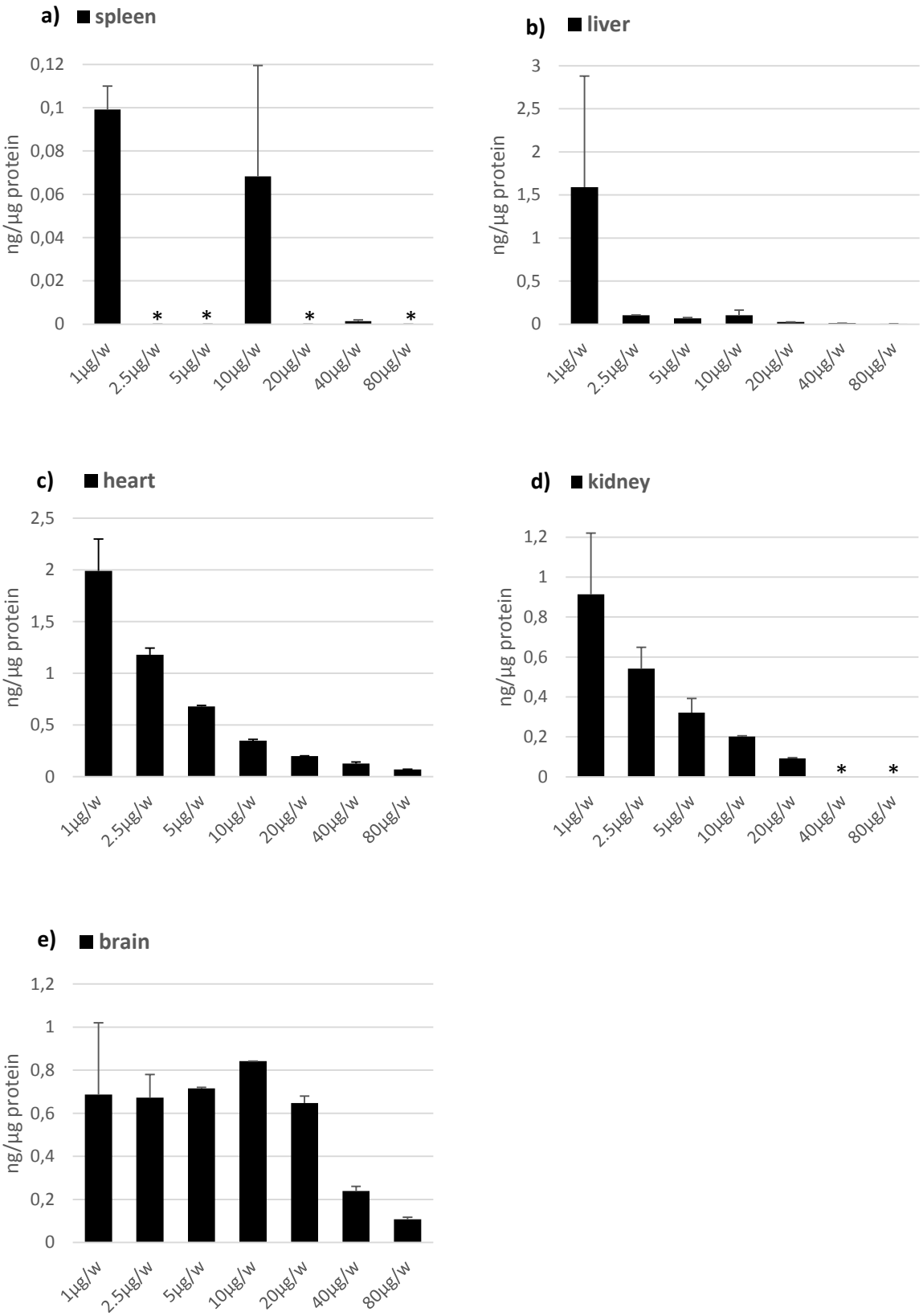

Figure 39: MeCP2 protein levels in various mouse organs after nuclear protein extraction from tissues lysis: spleen (a), liver (b), heart (c), kidney (d), brain (e). Used protein concentrations ranged from 1µg protein per well to 80µg protein per well. Error bars show standard error at each concentration (n=2) and were partly too small to be visible. *Missing columns indicate that there was no signal available.

In addition to these findings, we further investigated the hypothesis of a possible age-dependent MeCP2-expression in the mices' nervous system. Therefore, we prepared brain lysates of wild-type mice at different ages (postnatal day 4, 10, 14 and 60). Using a protein concentration of 20µg per well of the respective brain lysates, we observed MeCP2 levels that remained quite constant during this period of maturation (Figure 40).

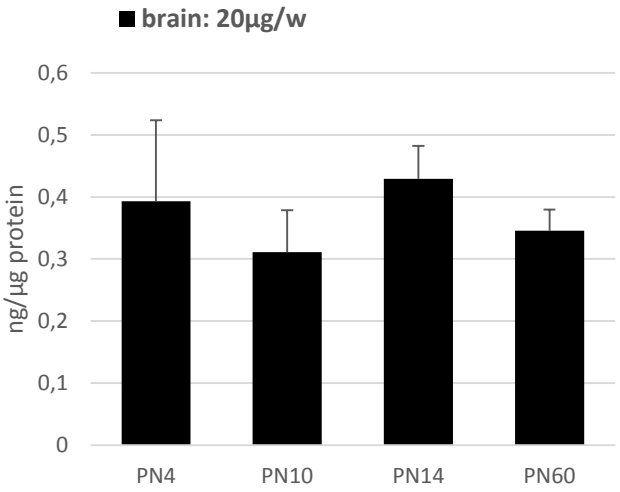

Figure 40: MeCP2 protein levels in brain lysates of wild-type mice at different age (postnatal day 4, 10, 14 and 60) after nuclear protein extraction from tissues lysis. Measuring brain lysates from 16 different mice, 4 at each postnatal day. Using a protein concentration of 20µg per well. Error bars show standard error at each time point (n=4).

On a final note, and very essential for the establishment of our assay, we could observe clear differences in the MeCP2 concentrations of brain lysates from wild-type, heterozygote and MeCP2-knock-out mice (Figure 41). Herein, the wild-type brain lysates showed the highest MeCP2 concentrations, which were about 50% higher than those found in the heterozygote mice brains. In the same experiment we could not detect any MeCP2 protein in the knock-out mice with our assay.

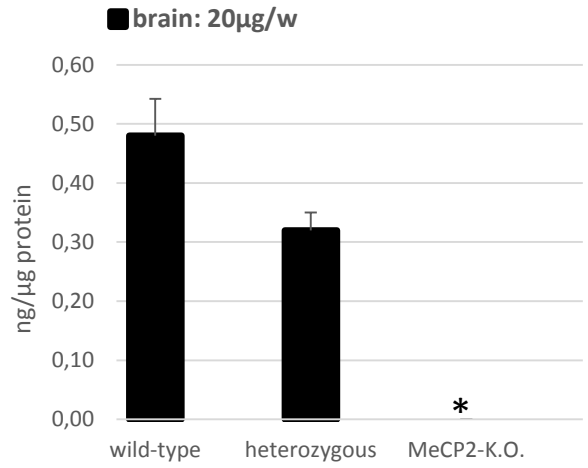

Figure 41: MeCP2 protein levels in wild-type, heterozygous and MeCP2-knock out mouse brains after nuclear protein extraction from tissues lysis. Using a protein concentration of 20µg per well. Measuring brain lysates from 6 different mice, 2 of each genotype. *****Missing column indicates that there was no signal available. Error bars show standard error in each group (n=2).

3.3.1.3. Comparison of our ECLIA with a commercially available ELISA

Finally, we were interested in comparing our ECLIA with a commercially available ELISA. Here, parameters such as the detection range, sensitivity, reactivity, linearity regarding a rise in concentration as well as the price and the assay duration are of scientific or economic consequences respectively. Therefore, we lysed the brain of a wild-type mouse in two different ways and prepared samples with an increasing protein concentration (1µg/well, 2.5µg/well, 5µg/well, 10µg/well, 20µg/well, 40µg/well, 80µg/well) for both lysis strategies. Preparing the ECLIA samples, we lysed the brain according to the previously used nuclear protein extraction protocol (Sigma-Aldrich®). As recommended by the manufacturer, the ELISA samples were prepared according to the total protein extraction protocol (LifeSpan BioScience®). In a parallel design, we measured the associated MeCP2 concentrations with our ECLIA as well as the ELISA Kit for Methyl CpG Binding Protein 2 (MECP2) (Cloud-Clone-Corp.®). The results showed a discrepancy between the two sets of data (Figure 42). On the one hand, the commercial ELISA measured 10-fold higher MeCP2 concentrations (ng/µg protein) than our ECLIA. On the other hand, we observed a positive linear correlation between the MeCP2 concentration and the utilized protein concentration in our ECLIA. This effect was noticeable between 1µg protein per well and 20µg protein per well. In contrast, the commercial ELISA failed in regards of linearity.

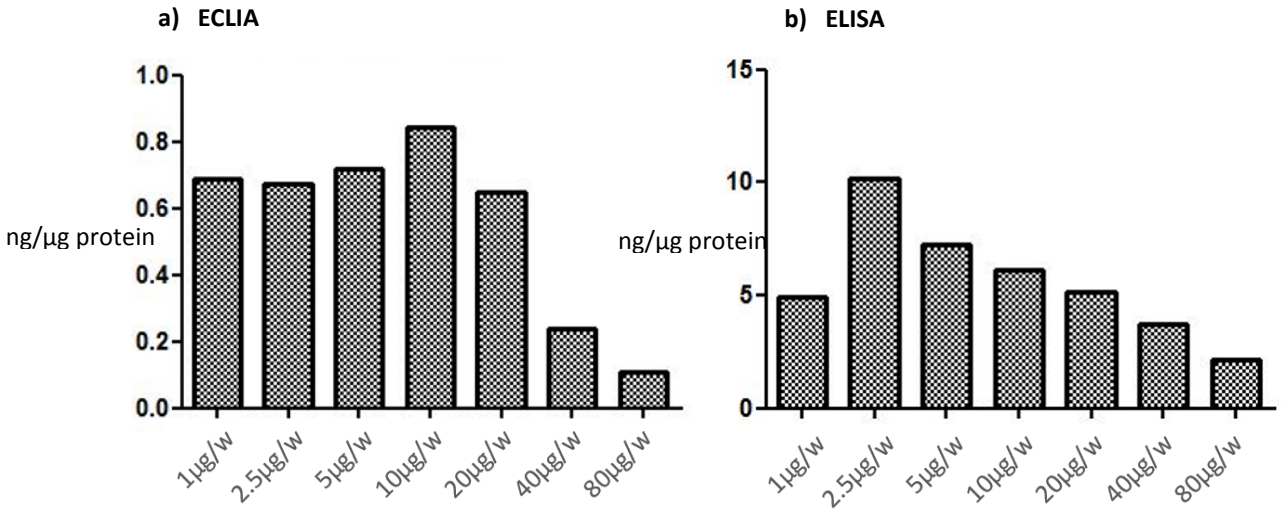

Figure 42: Comparison of two different assays measuring MeCP2 protein levels in wild-type mouse brain: ECLIA (a), commercial ELISA Kit (b). Used protein concentrations ranged from 1µg protein per well to 80µg protein per well. Presented data are the mean of duplicates (n=2).

4. DISCUSSION

4.1. Aspects of development and validation

In this study, we developed an ECLIA based assay for MeCP2 that fulfills several essential quality specifications, which are necessary for the establishment of a highly quantitative, accurate and reproducible assay. Furthermore, we use this discussion as an opportunity to compare the verification data of our ECLIA with those of the tested, commercially available ELISA (Cloud-Clone-Corp.®) (Table 6).

a) Sensitivity

Starting with *"the smallest amount of substance in a sample that can accurately be measured by an assay"* [Saah et al., 1997], the sensitivity of our ECLIA is characterized by a lower limit of detection (LLOD) of 28.5pg/ml. This value is calculated as 2.5 standard deviations above the blank. In comparison with the commercially available ELISA for MeCP2 quantification, which showed a minimum detectable dose of 127pg/mL [Cloud-Clone-Corp.®, 2009-2016], our ECLIA was 4 times more sensitive than the ELISA kit. Furthermore, our ECLIA showed a broad dynamic range from 0.029ng/ml to 200ng/ml, whereas the stated working range of the ELISA was much smaller with 0.312ng/ml to 20ng/ml [Cloud-Clone-Corp.®, 2009-2016]. In course of our research we found several further providers for commercial MeCP2-ELISA Kits, Cloud-Clone-Corp.®, antibodies-online® GmbH, Abbexa Ldt.®, Biorbyt Ltd®, Biocompare® and Aviva Systems Biology Corporation®. However, none of them stated a wider detection range nor a lower LLOD than our assay. Herein the usual detection ranges were 0.156-10ng/mL (human) and 0.312ng-20ng/ml (mouse).

b) Specificity

In terms of specificity - *"the ability of an assay to measure one particular organism or substance, rather than others, in a sample"* [Saah et al., 1997] - we calculated several signal-to-noise ratios, especially during the period of antibody testing. Dividing the signal of the calibrator, respectively the sample, by the signal of the blank value, acted as useful measure for the specificity of various antibody combinations as well as their optimal dilution ranges. The antibodies, which were adapted for our ECLIA by showing the highest tested specificity,

were a mouse monoclonal capture antibody of Sigma-Aldrich® and a rabbit polyclonal primary detection antibody of Eurogentec S.A.®. The former monoclonal one is of mouse IgG1 isotype and derived from the Mec-168 hybridoma. *"This hybridoma was produced by the fusion of mouse myeloma cells (NS1) and splenocytes from BALB/c mice immunized with a synthetic peptide corresponding to the C- terminus (amino acids 471- 486) of human MeCP2"* [Sigma-Aldrich®, 2012]. According to the manufacturer, this antibody recognizes human, rat and mouse MeCP2 and has already been used successfully for several studies [Liang et al., 2015, Brown et al., 2016]. To optimise its specificity, we diluted the antibody in a 1: 6000 regime, receiving a working concentration of 333.34pg/ml. In terms of the primary detection antibody, again a dilution regime of 1:6000 fitted our system best.

Besides the calculation of signal-to-noise ratios, we further performed a Western Blot, measuring human cell lysates, to test our antibody's specificity. The manufacturer MSD® recommends expressing the specificity in the percentage of non-specificity, which is calculated through a particular run [Meso Scale Discovery®, 2014]. However, the given data of the commercial ELISA concerning their specificity was still less satisfying, as they just described it as *"excellent"* without any further information [Cloud-Clone-Corp.®, 2009-2016].

c) Accuracy and Precision

Reference to accuracy, calculating the intra-assay precision as well as the inter-assay precision is of statistical relevance. Our ECLIA showed an intra-assay precision, i.e. the precision within an assay (n=3), of CV≤ 3.14 % and an inter-assay precision, i.e. the precision between assays (n=3), of CV≤12.5%. According to the manufacturer (MSD®), accuracy and precision is ensured if the intra-run CVs stay below 7% and the inter-run CVs below 15%, assuming these issues as accomplished [Meso Scale Discovery®, 2013-2014]. Herein, our tested ELISA kit showed a similar inter-day precision of CV<12% as our ECLIA, but a higher intra-assay precision of CV<10% [Cloud-Clone-Corp.®, 2009-2016].

d) Reactivity

All of the commercially available ELISAs mentioned above showed either human or mouse reactivity, meaning none of them offers the possibility to combine samples from different origins in one assay. We demonstrated successfully that our ECLIA is able to measure both mouse and human samples, including tissue homogenates as well as cell lysates.

e) Stability

As the ELISA kits show an expiration date, the validation of stability is an essential tool here. The manufacturer [Cloud-Clone-Corp.®, 2009-2016] defined the stability of their assay by the rate of activity loss, which was less than 5% within the expiration date. In course of our research we observed a limited freeze-thaw stability of our ECLIA (data not shown). Reconstituted calibrators, controls and samples should not go through more than 3 freeze-thaw cycles if good assay performance is to be ensured. Therefore dipping diluted antibodies and calibrators in smaller volumes is a helpful step. Calibrators, controls and samples can be stored frozen for several months at -80°C. To further minimize factors that might influence the assay's performance, lab conditions (e.g. room temperature, air humidity, light conditions) should be kept constant.

f) Costs and Assay Duration

Another advantage of our ECLIA lies in the economical view. As the commercial ELISAs cost about 600-900$ exclusive of shipping charges, our self-made ECLIA is a much cheaper option. However, the assay duration of our ECLIA is much longer (19.5h) than the one of the ELISA (3h). This is mainly due to the ECLIAs' overnight incubation step with the capture antibody. As opposed to this, the kit arrives already pre-coated.

	ECLIA	**ELISA**
Sensitivity	0.030 ng/ml	<0.127ng/ml
Detection range	0.030-200ng/ml	0.312-20ng/ml
Specificity	-	excellent
Matrix effects	not yet clear	-
Precision		
Intra-assay	CV≤1.21%	CV<10%
Inter-assay	CV≤12.5%	CV<12%
Reactivity	human, mouse	mouse
Sample type	tissue homogenates, cell lysates	tissue homogenates, cell lysates, other biological fluids
Stability	-	<5% (loss rate of activity)
Prize	<300$	720$
Assay time	19h	3h

Table 6: Overview of the main differences in verification parameters of our ECLIA and the tested ELISA kit (Cloud-Clone-Corp.®). Any information regarding the ELISA kit was published by the manufacturer. [Cloud-Clone-Corp.®, 2009-2016; http://www.cloud-clone.com/products/SEC616Mu.html]

g) Further influencing factors

Except for the lab conditions mentioned before, we found out that shaking the plate during the particular incubation steps has a considerable impact on the signal strength. Additionally, the signal strength increases with shaking speed. This might be due to the fact that shaking leads to a boost of diffusion rates, resulting in better binding kinetics and therefore reducing the period of time in which the binding equilibrium is reached [Meso Scale Discovery®, 2013-2014]. Besides the shaking and its speed, the incubation time is of equal importance regarding the achievement of the binding equilibrium. Therefore, especially the incubation of the samples should be prolonged as long as possible.

4.2. MeCP2 in cell and tissue lysates

In the second part of our study we were interested in measuring MeCP2 in different samples with our high-throughput assay. As a result, we were able to quantify MeCP2 in diverse cell lines from both human and mouse origin as well as in mouse tissues, focusing on the brain.

a) Lysis strategies

As the MeCP2 protein is localised in the nucleus, it was not surprising that the nuclear extraction strategies yielded significantly higher MeCP2 concentrations than the total protein extraction methods. This effect was supported by the circumstance that the chemical lysis of the cells showed a superior efficacy in comparison with the physical ones.

b) MeCP2 in different cell lines

Fibroblast cell lines are a widely used in-vitro model for investigating the underlying mechanisms of Rett Syndrome [Segatto et al., 2014; Signorini et al., 2014; Traynor et al., 2002]. Hence, we first analysed MeCP2 concentrations in those cell lines. Thereby, our ECLIA enabled us to demonstrate a difference in MeCP2 levels between human wild-type fibroblasts and Rett patients' fibroblasts. The concentration of MeCP2 protein was about 10 times higher in the control than in the patients' cells. Wild-type fibroblasts showed the highest MeCP2 concentrations in our study with 2.4ng MeCP2/µg protein, using 1µg protein per well. Furthermore, we were able to measure an increase in MeCP2 concentration between 0.5µg protein/well and 10µg protein/well in a relatively linear range.

In keeping with the literature, also human hepatocellular carcinoma cell lines such as HepG2 are known for their considerably high expression of MeCP2. Using real-time PCR and Western Blot, Zhao et al. showed that the level of MeCP2 mRNA in human HCC HepG2 cells significantly exceeded the MeCP2 concentration of normal hepatocellular tissue. The authors drew their conclusion from the promoting effect of MeCP2 in the proliferation of human HCC HepG2 cells via the activation of ERK1/2 signalling pathways [Zhao et al., 2013]. Regarding the MeCP2 content in HepG2 cells, our results were consistent with those of Zhao et al. As a result, we found the second highest MeCP2 concentration of our study with 1.5ng MeCP2/µg protein, using 1µg protein per well in those cells.

Quite different were our measurements in human Schwann cells, which are, however, known for their missing MeCP2 expression. For instance, Tochiki et al. found that there is MeCP2 expression in neurons, oligodendrocytes and astrocytes, but by means of immunohistochemistry they could not find any positive staining in microglia, oligodendrocyte precursor as well as Schwann cells [Tochiki et al., 2012]. When we measured the MeCP2 level in these cells with our ECLIA, the calculated concentration of MeCP2 was not even half as much as we found in HepG2 cells and even less than 30% of the concentration found in human wild-type fibroblasts.

c) MeCP2 in different mouse tissues

Data concerning the MeCP2 expression in mouse tissue is very limited and inconsistent. Song et al., for instance, used immunostaining on cryosections to determine the MeCP2 expression in mouse tissues and in different cell types respectively. They concluded that the overwhelming part of the 64 cell types studied from 12 non-neuronal adult mouse tissues expresses the MeCP2 protein. Solely the epithelial cells of intestine and colon, hair matrix keratinocytes, mature gonads and the cells of the erythropoietic lineage showed no detectable MeCP2 signals [Song et al., 2014]. In terms of cells of the erythropoietic lineage such as late erythroblasts, myeloblasts and megakaryocytes, these authors' findings were consistent with our ECLIA results as we could just measure a marginal or even no signal in the splenic tissue. However, according to Song et al. we should have been able to measure a certain MeCP2 level in the hepatic tissue, as the authors were successful in detecting the protein in cells of the myeloid lineage such as Kupffer cells as well as hepatocytes by immunostaining (Figure 43).

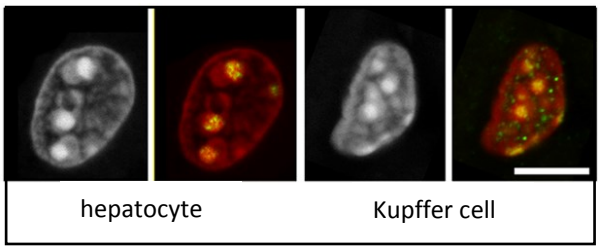

Figure 43: Immunostaining of MeCP2 (green) in different hepatic cells of adult mouse tissue. Scale bar: 5µm [Song et al., 2013].

On the contrary, Shahbazian et al. demonstrated by immunoblot analysis that MeCP2 was present at high concentrations in the brain, spleen and lung. In comparison with the brain, they found a moderate, actually a 2 to 4 fold lower, MeCP2 expression in heart and kidney. Herein, the data concerning a marked MeCP2 content in heart and kidney confirm our results, as we measured concentrations between 0.9 and 2 ng MeCP2/µg protein, using 1µg protein per well in heart and kidney tissues. However, the authors noticed just a marginal signal in the liver, stomach and small intestine, which was reduced up to 19 fold (Figure 44). Interestingly they could not find any correlation between the protein and RNA levels of MeCP2 in the investigated tissues, concluding that MeCP2 transcripts underlie post-translational regulation in a tissue-specific way [Shahbazian et al., 2002].

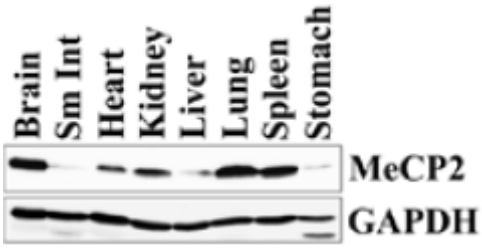

Figure 44: Immunoblot analysis showing MeCP2 levels in tissues of a 9 week old mouse. Observing high concentrations in the brain, lung and spleen, moderate concentrations in the heart and kidney as well as marginal concentrations in the small intestine, liver and stomach [Shahbazian et al., 2002].

What both publications had in common was their data concerning the brain tissue, including the knowledge that microglia are the only neuronal cells which do not express MeCP2. Our study also achieved the best results – even if not the highest MeCP2 concentrations - in brain tissue as our assay remained sensitive and in a linear range from 1-20µg protein of brain cell lysate per well. Noteworthy, the commercially tested ELISA kit (Cloud-Clone-Corp.®) failed here in showing such a linearity. This effect was absent in all the other analysed mouse tissues.

Furthermore, we could measure with our assay a difference between the MeCP2 content in the brain of wild-type mice and the brain of MeCP2 knock-out mice. In the latter, MeCP2 was not detectable, confirming the specificity of our test. In the heterozygous female mice our ECLIA detected 40% lower MeCP2 concentration as expected.

In addition to that, both Song et al. and Shahbazian et al. showed that the MeCP2 expression in the nervous system is age-dependent and correlates with its maturation. This effect was observable in mice as well as humans [Shahbazian et al., 2002; Song et al., 2014]. Concerning the pattern of the MeCP2 expression, the two species resemble each other, which means that in humans as well as in mice a correlation between the ontogeny of the central nervous system and the time course of MeCP2 abundance was observable. Similar to the developmental stages of the central nervous system, MeCP2 was found to be expressed in the spinal cord and brainstem first, followed by a later expression in other brain regions, such as hippocampus and cerebral cortex. However, the authors noticed some species-specific differences. Although a "*gradual increase in the percentage of MeCP2-positive neurons"* was observable in both species, they significantly differed concerning the developmental period of this increase. Whereas in mice the majority of the neuronal MeCP2 abundance is limited to the embryonic development (around embryonic day 18.5), in humans this process even persists after birth and might last up to 10 years of age. The authors hypothesized "*the extended period of developmental plasticity in humans*" to be the reason for this phenomenon. Thus Shahbazian et al. did not find differences in the MeCP2 levels of mouse brain lysates between postnatal day 0 and 28 weeks after birth (Figure 45) [Shahbazian et al., 2002]. In view of this finding we could confirm this hypothesis with our ECLIA, as our measured MeCP2 levels also stayed uniform between day 4 and day 60 of the postnatal period.

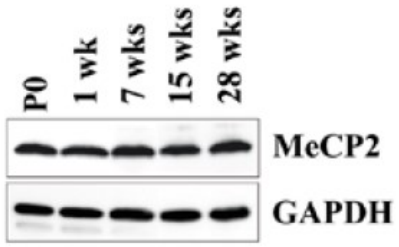

Figure 45: Immunoblot analysis showing MeCP2 levels in brain lysates of mice with different age (postnatal day 0 to 28 weeks after birth). Observing high and quite consistent MeCP2 concentrations. [Shahbazian et al., 2002].

5. CONCLUSION

Here we report on the investigation to measure endogenous MeCP2 and TAT-MeCP2 fusion protein concentrations, in cellular as well as animal models, through a electrochemiluminescence immunoassay (ECLIA). The system used was a $Ru(bpy)_3^{2+/}$TPA-ECL-one together with a carbon coated 96-well high-bind microplate.

The assay showed high sensitivity and specificity with a lower limit of detection (LLOD) of 28.5pg/ml and a recovery rate of 88.2%. Accuracy assumptions were successfully met by displaying intra-assay precision of CV≤1.21% as well as inter-assay precision of CV≤12.5%. Comparing the ECLIA with a commercially available ELISA, our assay shows economic advantages, but also superiority in regards of detection range, reactivity, and variety of sample types.

Furthermore, our ECLIA reflected marked differences in MeCP2 levels between wild-type fibroblasts and male Rett patients' fibroblasts. When measuring MeCP2-levels in wild-type and MeCP2-knock out mice brains, the latter did not show any MeCP2 signal. Heterozygote ones took an intermediate position, showing a 40% lower MeCP2 concentration than the wild-type mice brain. In accordance with the literature, we could further confirm the hypothesis of uniform MeCP2 concentrations between day 4 and day 60 of the postnatal period in mice, indicating that MeCP2 accumulation is already completed during embryonic development. Methodically essential for all these experiments and findings was the implementation of nuclear extraction strategies as well as the usage of very small amounts of protein (1µg/well) per well.

The results constitute the successful establishment of a new tool for quantifying endogenous MeCP2 as well as TAT-MeCP2 fusion protein. It therefore represents a promising diagnostic agent in terms of MeCP2 replacement strategies for RTT. The easy handling of the assay, requirement of a very small amount of samples and high-throughput system confers great value even in investigating other potential treatments for neurological disease involving MeCP2 dysfunction.

6. REFERENCES

6.1. Internet figures

[1] http://www.medscape.com/viewarticle/515577_3 (accessed on: 18/03/2017).

[2] https://www.google.at/search?q=microplate+well&biw=1301&bih=592&source=lnms&tbm=isch&sa=X&ved=0ahUKEwjh9sXGpZnQAhVElxoKHT2oC_MQ_AUIBigB#imgrc=Qy7XM5pCvKGz_M%3A (accessed on: 08/11/2016).

[3] https://www.mesoscale.com/~/media/files/product%20inserts/msd%20sulfo%20tag%20nhs%20ester.pdf (accessed on: 11/11/2016).

[4] https://www.google.at/search?q=tripropylamin&biw=1301&bih=592&source=lnms&tbm=isch&sa=X&ved=0ahUKEwi8uLfHy6DQAhXHSRoKHchXDtoQ_AUIBygC#imgrc=xoN9SnmMi71I-M%3A (accessed on: 11/11/2016).

[5] https://www.mesoscale.com/en/technical_resources/our_technology/ecl (accessed on: 08/11/2016).

6.2. Literature

Adler DA, Quaderi NA, Brown SD, Chapman VM, Moore J, Tate P, Disteche CM. The X-linked methylated DNA binding protein, MeCP2 is subject to X inactivation in the mouse. Mammalian Genome 6:491–92 (1995).

Amir RE, Van den Veyver IB, Wan M, Tran CQ, Francke U, Zoghbi, HY. Rett syndrome is caused by mutations in X-linked MECP2, encoding methyl-CpG-binding protein 2. Nat.Genet. 23, 185–188 (1999).

Ariani F, Hayek G, Rondinella D, et al. FOXG1 is responsible for the congenital variant of Rett syndrome. Am J Hum Genet. 83:89–93 (2008).

Arruda VR, Stedman HH, Nichols TC, Haskins ME, Nicholson M, Herzog RW, Couto LB, High KA. Regional intravascular delivery of AAV-2-F.IX to skeletal muscle achieves long-term correction of hemophilia B in a large animal model. Blood 105, 3458–3464 (2005).

Bahi-Buisson N, Nectoux J, Rosas-Vargas H, Milh M, Boddaert N, Girard B, Cances C, Ville D, Afenjar A, Rio M, Héron D, N'guyen Morel MA, Arzimanoglou A, Philippe C, Jonveaux P, Chelly J, Bienvenu T. Key clinical features to identify girls with CDKL5 mutations. Brain 131(Pt 10):2647-61 (2008).

Bio-Rad. Bio-Rad Protein Assay. Bio-Rad Life Science Group (1994). Internet: http://www.bio-rad.com/LifeScience/pdf/Bulletin9004.pdf (accessed on: 16/11/2016)

Bradford M.M. A rapid and sensitive method for the quantitation of microgram quantities of protein utilizing the principle of protein-dye binding. Anal Biochem. 72:248-54 (1976).

Brown K, Selfridge J, Lagger S, Connelly J, De Sousa D, Kerr A, Webb S, Guy J, Merusi C, Koerner MV, Bird A. The molecular basis of variable phenotypic severity among common missense mutations causing Rett syndrome. Human Molecular Genetics 25:3 558–570 (2016).

Chahrour M, Zoghbi HY. The story of Rett syndrome: from clinic to neurobiology. Neuron 56(3):422-37 (2007).

Chang Q, Khare G, Dani V, Nelson S, Jaenisch R. The disease progression of Mecp2 mutant mice is affected by the level of BDNF expression. Neuron 49(3):341-8 (2006).

Cloud-Clone-Corp.®. ELISA Kit for Methyl CpG Binding Protein 2 (MECP2). Cloud-Clone-Corp.®, 2009-2016. Internet: http://www.cloudclone.com/products/SEC616Mu.html (accessed on: 02/02/2017)

Cooper RA, Kerr AM, Amos PM. Rett syndrome: critical examination of clinical features, serial EEG and video-monitoring in understanding and management. Eur J Paediatr Neurol 2:127–135 (1998).

Dani VS, Chang Q, Maffei A, Turrigiano GG, Jaenisch R, Nelson SB. Reduced cortical activity due to a shift in the balance between excitation and inhibition in a mouse model of Rett syndrome. Proc. Natl. Acad. Sci. USA 102:12560–12565 (2005).

Darwish IA. Immunoassay Methods and their Applications in Pharmaceutical Analysis: Basic Methodology and Recent Advances. International Journal of Biomedical Science 2:3 217-235 (2006).

Duan D, Sharma P, Yang J, Yue Y, Dudus L, Zhang Y, Fisher KJ, Engelhardt JF. Circular intermediates of recombinant adeno-associated virus have defined structural characteristics responsible for long-term episomal persistence in muscle tissue. J. Virol. 72:8568–8577 (1998).

Ellaway C, Christodoulou J. Rett syndrome: clinical characteristics and recent genetic advances. Disabil Rehabil 23: 98–106 (2001).

Engvall E, Perlmann P. Enzyme-linked immunosorbent assay (ELISA). Quantitative assay of immunoglobulin G. Immunochemistry 8:9 871-4 (1971).

Fehr S, Bebbington A, Nassar N, Downs J, Ronen GM, et al: Trends in the diagnosis of Rett syndrome in Australia. Pediatr Res 70: 313–319 (2011).

Gadalla KKE, Bailey MES, Cobb SR. MeCP2 and Rett syndrome: reversibility and potential avenues for therapy. Biochem. J. 439, 1–14 (2011).

GE Healthcare®. Western Blotting – Principles and Methods. GE Healthcare Bio-Sciences AB (2011). Internet: https://www.sigmaaldrich.com/content/dam/sigma-aldrich/docs/Sigma-Aldrich/General_Information/1/ge-western-blotting.pdf (accessed on: 14/11/2016)

Goldsby RA, Kindt TJ, Osborne BA. Antigen-Antibody Interactions. In: Immunology 4th Edition. W.H. Freeman and Company (2001).

Guy J, Cheval H, Selfridge J, Bird A. The Role of MeCP2 in the Brain. Annu. Rev. Cell Dev. Biol. 27:631–52 (2011).

Guy J, Gan J, Selfridge J, Cobb S, Bird A. Reversal of neurological defects in a mouse model of Rett syndrome. Science 315:1143–1147 (2007).

Hagberg B, Aicardi J, Dias K, Ramos O. A progressive syndrome of autism, dementia, ataxia, and loss of purposeful hand use in girls: Rett's syndrome: report of 35 cases. Ann Neurol. 14(4):471–9 (1983).

Hagberg B, Witt-Engerstrom I. Rett syndrome: a suggested staging system for describing impairment profile with increasing age towards adolescence. Am J Med Genet Suppl. 1:47–59 (1986).

Hagberg B. Clinical manifestations and stages of Rett syndrome. Mental retardation and developmental disabilities research reviews 8: 61-65 (2002).

Hagberg BA, Skjeldal OH. Rett variants: a suggested model for inclusion criteria. Pediatr Neurol. 11(1):5–11 (1994).

Hanefeld F. The clinical pattern of the Rett syndrome. Brain Dev. 7:320–325 (1985).

Helen Leonard, Stuart Cobb, Jenny Downs. Clinical and biological progress over 50 years in Rett syndrome. Nat Rev Neurol 13:37–51 (2016).

Herzog, RW, Hagstrom JN, Kung SH, Tai SJ, Wilson JM, Fisher KJ, High KA. Stable gene transfer and expression of human blood coagulation factor IX after intramuscular injection of recombinant adeno-associated virus. Proc. Natl. Acad. Sci. U.S.A. 94:5804–5809 (1997).

Huppke P, Laccone F, Kramer N, Engel W, Hanefeld F: Rett syndrome: analysis of MECP2 and clinical characterization of 31 patients. Hum Mol Genet 9: 1369–1375 (2000).

Ishii T, Makita Y, Ogawa A, Amamiya S, Yamamoto M, Miyamoto A, Oki J. The role of different X-inactivation pattern on the variable clinical phenotype with Rett syndrome. Brain Dev 23 (suppl 1):S161–S164 (2001).

Jiang H, Lillicrap D, Patarroyo-White S, Liu T, Qian X, Scallan CD, Powell S, Keller T, McMurray M, Labelle A, Nagy D, Vargas JA, Zhou S, Couto LB, Pierce GF. Multiyear therapeutic benefit of AAV serotypes 2, 6, and 8 delivering factor VIII to hemophilia A mice and dogs. Blood 108:107–115 (2006).

Julu PO, Kerr AM, Apartopoulos F, Al-Rawas S, Engerström IW, Engerström L, Jamal GA, Hansen S. Characterisation of breathing and associated central autonomic dysfunction in the Rett disorder. Arch Dis Child 85:29–37 (2001).

Julu PO, Witt Engerström I. Assessment of the maturity-related brainstem functions reveals the heterogeneous phenotypes and facilitates clinical management of Rett syndrome. Brain Dev 27 (suppl 1):S43–S53 (2005).

Katz DM, Bird A, Coenraads M, Gray SJ, Menon DU, Philpot BD, Tarquinio DC. Rett syndrome: crossing the threshold to clinical translation. Trends Neurosci. 39, 100–113 (2016).

Soultanis KC, Payatakes AH, Chouliaras VT, Mandellos GC, Pyrovolou NE, Pliarchopoulou FM Soucacos PN. Rare causes of scoliosis and spine deformity: experience and particular features. Scoliosis, 2:15 (2007).

Laccone F, inventor. Georg-August Universität Göttingen Stiftung öffentlichen Rechts, Laccone F., assignee. Synthetic mecp2 sequence for protein substitution therapy. Patent Pub. No.: WO/2007/115578. 2007 Oct 18 (internet: https://patentscope.wipo.int/search/en/ detail.jsf?

docId=WO2007115578&recNum=1&maxRec=&office=&prevFilter=&sortOption=&query String =&tab=PCT+Biblio (assessed on 21/03/2017)

Laccone F. Das Rett-Syndrom. Medgen 18 (2006).

Leonard H, Silberstein J, Falk R, Houwink-Manville I, Ellaway C, Raffaele LS, Engerström IW, Schanen C. Occurrence of Rett syndrome in boys. J Child Neurol 16: 333–338 (2001).

Liang Z, Ye T, Zhou X, Lai KO, Fu AK, Ip NY. Cdk5 Regulates Activity-Dependent Gene Expression and Dendrite Development. The Journal of Neuroscience 35(45):15127–15134 (2015).

LifeSpan BioScience®. Mouse MECP2 ELISA Kit (Sandwich ELISA) - User Manual. Catalog No. LS-F8426. LifeSpan BioScience, Inc (2016). Internet: https://www.lsbio.com/elisakits/ manual pdf/ls-f8426.pdf (accessed on: 17/11/2016)

Luikenhuis S, Giacometti E, Beard CF, Jaenisch R. Expression of MeCP2 in postmitotic neurons rescues Rett syndrome in mice. Proc. Natl. Acad. Sci. U.S.A. 101, 6033–6038 (2004).

Martin R, Mogg AE, Heywood LA, Nitschke L, Burke JF. Aminoglycoside suppression at UAG, UAA and UGA codons in Escherichia coli and human tissue culture cells. Mol Gen Genet 217: 411–418 (1989).

Martinowich K, Hattori D, Wu H, Fouse S, He F, Hu Y, Fan G, Sun YE. DNA methylation-related chromatin remodeling in activity-dependent BDNF gene regulation. Science 302: 890 (2003).

Meso Scale Discovery®. MSD Multi Spot Assay System – Proinflammatory Panel 1 (human) Kits. Meso Scale Diagnostics (2014). Internet: https://www.mesoscale.com/~/media/files/ product%20inserts/proinflammatory%20panel%201%20human%20insert.pdf (accessed on: 01/02/2017)

Meso Scale Discovery®. MSD Plates – Standard and High Bind Plates. Meso Scale Diagnostics (2013-2014). Internet: https://www.mesoscale.com/~/media/files/ technical%20notes/ assay %20development%20plates%20uncoated.pdf (accessed on: 08/11/2016)

Meso Scale Discovery®. MSD Plates – Standard and High Bind Plates. Meso Scale Diagnostics (2013-2014). Internet: https://www.mesoscale.com/~/media/files/technical%20notes/ assay %20development%20plates%20uncoated.pdf (accessed on: 11/10/2016)

Namba Y, Usami M, Suzuki O. Highly sensitive electrochemiluminescence immunoassays using the ruthenium chelate-labeled antibody bound on the magnetic micro beads. Analytical Science 15, 1087-1092 (1999).

Nan X, Hou J, Maclean A, Nasir J, Lafuente MJ, Shu X, Kriaucionis S, Bird A. Interaction between chromatin proteins MECP2 and ATRX is disrupted by mutations that cause inherited mental retardation. Proc. Natl. Acad. Sci. USA 104, 2709–2714 (2007).

Nan X, Ng HH, Johnson CA, Laherty CD, Turner BM, Eisenman RN, Bird A. Transcriptional repression by the methyl-CpG-binding protein MeCP2 involves a histone deacetylase complex. Nature 393, 386–389 (1998).

Nectoux J, Bahi-Buisson N, Guellec I, Coste J, De Roux N, Rosas H, Tardieu M, Chelly J, Bienvenu T. The p.Val66Met polymorphism in the BDNF gene protects against early seizures in Rett syndrome. Neurology 70(22 Pt 2):2145–2151 (2008).

Neul JL, Kaufmann WE, Glaze DG, Christodoulou J, Clarke AJ, Bahi-Buisson N, Leonard H, Bailey ME, Schanen NC, Zappella M, Renieri A, Huppke P, Percy AK; RettSearch Consortium. Rett syndrome: revised diagnostic criteria and nomenclature. Ann Neurol 68: 944–950 (2010).

Ogier M, Wang H, Hong E, Wang Q, Greenberg ME, Katz DM. Brain-derived neurotrophic factor expression and respiratory function improve after ampakine treatment in a mouse model of Rett syndrome. J. Neurosci. 27:10912–10917 (2007).

Percy AK. Progress in Rett Syndrome: from discovery to clinical trials. Wien Med Wochenschr (2016).

Philippe C, Villard L, De Roux N, Raynaud M, Bonnefond JP, Pasquier L, Lesca G, Mancini J, Jonveaux P, Moncla A, Chelly J, Bienvenu T. Spectrum and distribution of MECP2 mutations in 424 Rett syndrome patients: a molecular update. Eur. J. Med. Genet. 49, 9–18 (2006).

Pyati R, Richter MM. ECL—Electrochemical luminescence. Annu. Rep. Prog. Chem., Sect. C, 103, 12–78 (2007).

Renieri A, Meloni I, Longo I, Ariani F, Mari F, Pescucci C, Cambi F. Rett syndrome: the complex nature of a monogenic disease. J Mol Med 81: 346–354 (2003).

Rett A. Cerebral atrophy associated with hyperammonemia. In: Vinken PJ, Bruyn GW, editors. Handbook of clinical neurology. Amsterdam: North-Holland Publishing Company 305–29 (1977).

Rett A. On an unusual brain atrophy syndrome in hyperammonemia in childhood. Wien Med Wochenschr. 116(37):723–6 (1966).

Roche Diagnostics Ltd. Elecsys® HE4 Electro-chemiluminescence immunoassay (ECLIA) for the quantitative determination of human epididymal protein 4 (HE4) in serum and plasma. Roche (2011).

Rolando S. Rett syndrome: report of eight cases. Brain Dev. 7:290–296 (1985).

Saah AJ, Hoover DR. "Sensitivity" and "specificity" reconsidered: the meaning of these terms in analytical and diagnostic settings. Ann Intern Med 126(1):91-4 (1997).

Schule B, Armstrong DD, Vogel H, Oviedo A, Francke U. Severe congenital encephalopathy caused by MECP2 null mutations in males: central hypoxia and reduced neuronal dendritic structure. Clin. Genet. 74:116–26 (2008).

Schwarze SR, Ho A, Vocero-Akbani A, Dowdy SF. In vivo protein transduction: delivery of a biologically active protein into the mouse. Science 285(5433):1569-72 (1999).

Segatto et al. Cholesterol Metabolism Is Altered in Rett Syndrome: A Study on Plasma and Primary Cultured Fibroblasts Derived from Patients. PLoS ONE (2014) 9(8): e104834.

Shahbazian MD, Antalffy B, Armstrong D, Zoghbi HY. Insight into Rett-Syndrome: MeCP2 levels display tissue-and cell-specific differences and correlate with neuronal maturation. Human Molecular Genetics 11:2 115-124 (2002).

Shahbazian MD, Antalffy B, Armstrong D, Zoghbi HY. Insight into Rett-Syndrome: MeCP2 levels display tissue-and cell-specific differences and correlate with neuronal maturation. Human Molecular Genetics 11:2 115-124 (2002).

Sigma-Aldrich®. Nuclear protein extraction without the use of detergent. Sigma-Aldrich Co.LLC (2016). Internet: http://www.sigmaaldrich.com/technical-documents/protocols/ biology/ nuclear-protein-extraction.html (accessed on: 17/11/2016)

Sigma-Aldrich®. Product information - Monoclonal Anti-MeCP2, clone Mec-168. Sigma-Aldrich Co.LLC (2012). Internet: http://www.sigmaaldrich.com/content/dam/sigma-aldrich/docs/ Sigma/Datasheet/4/m6818dat.pdf (accessed on: 02/02/2017)

Signorini C, Leoncini S, De Felice C, Pecorelli A, Meloni I, Ariani F, Mari F, Amabile S, Paccagnini E, Gentile M, Belmonte G, Zollo G, Valacchi G, Durand T, Galano JM, Ciccoli L, Renieri A, Hayek J. Redox Imbalance and Morphological Changes in Skin Fibroblasts in Typical Rett Syndrome. Hindawi Publishing Corporation Oxidative Medicine and Cellular Longevity (2014).

Smeets E, Terhal P, Casaer P, Peters A, Midro A, Schollen E, van Roozendaal K, Moog U, Matthijs G, Herbergs J, Smeets H, Curfs L, Schrander-Stumpel C, Fryns JP. Rett syndrome in females with CTS hot spot deletions: a disorder profile. Am J Med Genet A 132A:117–120 (2005).

Smeets E, Pelc K, Dan B. Rett Syndrome. Mol Syndromol 2:113-127 (2011).

Song C, Feodorova J, Guy J, Peichl L, Jost KL, Kimura H, Cardoso MC, Bird A, Leonhardt H, Joffe H, Solovei I. DNA methylation reader MECP2: cell type- and differentiation stage-specific protein distribution. Epigenetics & Chromatin 7:17 (2014).

Steffenburg U, Hagberg G, Hagberg B. Epilepsy in a representative series of Rett syndrome. Acta Paediatr 90:34–39 (2001).

Tarquinio DC, Hou W, Neul JL, Lane JB, Barnes KV, O'Leary HM, Bruck NM, Kaufmann WE, Motil KJ, Glaze DG, Skinner SA, Annese F, Baggett L, Barrish JO, Geerts SP, Percy AK. Age of diagnosis in Rett syndrome: patterns of recognition among diagnosticians and risk factors for late diagnosis. Pediatr Neurol. 52(6):585–591.e2 (2015).

Thermo Scientific™. ELISA technical guide and protocols. Thermo Fisher Scientific Inc. (2010). Internet: https://tools.thermofisher.com/content/sfs/brochures/TR0065-ELISA-guide.pdf (accessed on: 08/11/2016)

Thermo Scientific™. Spike-and-recovery and linearity-of-dilution assessment. Thermo Fisher Scientific Inc. (2007). Internet: https://tools.thermofisher.com/content/sfs/brochures/ TR0058-Spike-and-Recovery.pdf (accessed on: 01/02/2017)

Thermo Scientific™. Thermo Scientific Pierce Assay Development Technical Handbook. Thermo Fisher Scientific Inc. (2011). Internet: https://www.thermofisher.com/content/dam/ LifeTech/Images/integration/1602127_Assay_Dev_HB_v2_INTL.pdf (accessed on: 08/11/2016).

Tochiki KK, Cunningham J, Hunt SP, Géranton SM. The expression of spinal methyl-CpG binding protein 2, DNA methyltransferases and histone deacetylases is modulated in persistent pain states. Molecular Pain 8:14 (2012).

Towbin H, Staehelin T, Gordon J. Electrophoretic transfer of proteins from polyacrylamide gels to nitrocellulose sheets: procedure and some applications. Proc Natl Acad Sci U S A. 76:9, 4350-4 (1979).

Traynor J, Agarwal P, Lazzeroni L, Francke U. Gene expression patterns vary in clonal cell cultures from Rett syndrome females with eight different MECP2 mutations. BMC Medical Genetics 3:12 (2002).

Tudor M, Akbarian S, Chen RZ, Jaenisch R. Transcriptional profiling of a mouse model for Rett syndrome reveals subtle transcriptional changes in the brain. Proceedings of the National Academy of Sciences of the United States of America 99(24): 15536-41 (2002).

Van Esch H, Bauters M, Ignatius J, Jansen M, Raynaud M, Hollanders K, Lugtenberg D, Bienvenu T, Jensen LR, Gecz J, Moraine C, Marynen P, Fryns JP, Froyen G. Duplication of the MECP2 region is a frequent cause of severe mental retardation and progressive neurological symptoms in males. Am. J. Hum. Genet. 77, 442–453 (2005).

Williams CA, Driscoll DJ, Dagli AI. Clinical and genetic aspects of Angelman syndrome. Genet Med 12: 385–395 (2010).

Young, JI, Hong EP, Castle JC, Crespo-Barreto J, Bowman AB, Rose MF, Kang D, Richman R, Johnson JM, Berget S, Zoghbi HY. Regulation of RNA splicing by the methylation-dependent transcriptional repressor methyl-CpG binding protein 2. Proc. Natl. Acad. Sci. USA 102, 17551–17558 (2005).

Zahorakova D. Rett syndrome. In: Radzioch D. Chromatin Remodelling. InTech (2013). Available from: http://www.intechopen.com/books/chromatin-remodelling/rett-syndrome (accessed on: 01/02/2017)

Zappella M. The Rett girls with preserved speech. Brain Dev. 14:98–101 (1992).

Zhao LY, Zhang J, Guo B, Yang J, Han J, Zhao X.G, Wang XF, Liu LIY, Li ZF, Song TS, Huang C. MeCP2 promotes cell proliferation by activating ERK1/2 and inhibiting p38 activity in human hepatocellular carcinoma HepG2 cells. Cell. Mol. Biol. 59 OL1876-OL1881 (2013).

Zhou Z, Hong EJ, Cohen S, Zhao WN, Ho HY, Schmidt L, Chen WG, Lin Y, Savner E, Griffith EC, Hu L, Steen JA, Weitz CJ, Greenberg ME. Brain-specific phosphorylation of MeCP2 regulates activity-dependent Bdnf transcription, dendritic growth, and spine maturation. Neuron 52, 255–269 (2006).